



Universitat Autònoma de Barcelona

**ADVERTIMENT.** L'accés als continguts d'aquesta tesi queda condicionat a l'acceptació de les condicions d'ús establertes per la següent llicència Creative Commons:  [http://cat.creativecommons.org/?page\\_id=184](http://cat.creativecommons.org/?page_id=184)

**ADVERTENCIA.** El acceso a los contenidos de esta tesis queda condicionado a la aceptación de las condiciones de uso establecidas por la siguiente licencia Creative Commons:  <http://es.creativecommons.org/blog/licencias/>

**WARNING.** The access to the contents of this doctoral thesis it is limited to the acceptance of the use conditions set by the following Creative Commons license:  <https://creativecommons.org/licenses/?lang=en>

**Uptake and metabolism of the antiepileptic drug carbamazepine  
in plants and role of endophytic bacteria**

Andrés Sauvêtre

PhD Thesis

Doctoral Program in Plant Biology and Biotechnology

Directors:

Prof. Dr. Peter Schröder

Prof. Dr. Charlotte Poschenrieder Wiens

**Co-director**

**Co-director**

**PhD candidate**

Prof. Dr. Peter Schröder

Prof. Dr. Charlotte Poschenrieder Wiens

Andrés Sauvêtre

Barcelona, May 2017

“Every kid starts out as a natural-born scientist, and then we beat it out of them. A few trickle through the system with their wonder and enthusiasm for science intact.”

Carl Sagan

A mis padres.

Gracias por haber mantenido intacto y alimentado el espíritu científico en mí.

# Acknowledgements

I want to express my gratitude to Professor Dr. Charlotte Poschenrieder who had confidence in me and gave me the opportunity to do this thesis. Thank you for your support and your positive attitude, always encouraging me and making things easier.

I will be always grateful to Professor Dr. Peter Schröder for accepting me in his working group and giving me the chance to take part in such a thrilling research field. Thank you for your supervision, and for recognising my personal enthusiasm in the project, pushing me to go further. You were always there for scientific and personal discussions and I always felt supported.

Besides my directors, I want to thank Prof. Dr. Anton Hartmann and Prof. Dr. Michael Schloter for the opportunity to work in their research units and for the scientific feedback and good advices during our seminars.

A very special gratitude goes out to Dr. Robert May for his tuition and training in mass spectrometry and his positive and enthusiastic attitude towards the difficulties encountered along the road. Thank you for animating me, it was very nice to cooperate with you.

I want to give my warm thanks to all members of AMP and COMI (former EGEN) for the nice time spent together and the altruistic help. With a special mention to Dr. Michael Rothballe, Dr. Soumitra Paul-Chowdhury for their assistance and tips for the isolation and characterization of endophytes and Dr. Christian Huber for his help during HPLC and MS analyses. I am very grateful to Rudi for his precious help with hairy root experiments and in general with all the lab work. Many thanks to Sivan for her help during my last experiments. Thanks to Angelo for his altruistic help in technical questions and to Tobias, Christopher, Nik, Sandrine and Marlene for their engagement during their internships.

Special thanks to my working group colleagues Vivi, Michi, Simone, Feiran, Hao, Christoph, Helga and former colleagues Lyudmila, and Max, for the good moments at work and outside of work

and for creating always a great and diverting work atmosphere during my thesis. A special mention to Miquel Llimós, thank you for your help and the coordination between Spain and Germany.

I thank Dr. Barbro Winkler, Peter Kary, Monika Kugelmann and Ulrich Junghans for their inestimable help in the greenhouse.

To Prof. Dr. Eckart Priesack, Dr. Christian Biernath, Dr. Nastasia Wanat, Christian Klein, Christoph Thieme, Dr. Rainer Hentschel and, Dr. Sebastian Bittner, many thanks for the nice conversations around the institute and the nice excursion into the Alps.

I want to express my sincere gratitude to the NEREUS COST Action ES1403 for the opportunity to present my work in several occasions and to all its members for the fantastic atmosphere and scientific networking.

Finally, I want to thank my family, my parents and my brother for supporting me spiritually during this work and in my life. Many thanks to Burkhard, Geli, Kai and Anne for the help and support in this last years. Stephie, thank you for your patience and unconditional support during these years. It is my joy to share this life with you, Leo and Émile. Leo, thank you for showing me through your eyes all the amazing things that are hidden in our daily routine.

# Table of contents

Abstract .....	viii
i. List of abbreviations.....	xi
ii. List of figures .....	xiii
iii. List of tables .....	xv
1. Introduction.....	1
1.1. Emerging contaminants and pharmaceuticals in our environment.....	1
1.2. Carbamazepine .....	3
1.3. Phytoremediation and xenobiotic detoxification in plants.....	4
1.4. Endophytic bacteria and their role in plant growth promotion.....	6
1.5. Interactions plant-endophytic bacteria for xenobiotic removal.....	9
1.6. Hairy roots to study plant-bacteria interactions .....	10
2. Objectives .....	13
3. Material and methods.....	14
3.1. Plant material and experimental setup.....	14
3.1.1. Common reed ( <i>Phragmites australis</i> (Cav.) Trin. ex Steud.).....	14
3.1.2. Horseradish hairy root cultures ( <i>Armoracia rusticana</i> Gaertn. Mey. et Scherb.)	16
3.2. Isolation of endophytic bacteria from <i>Phragmites australis</i> .....	19
3.2.1. Isolation from plants treated with carbamazepine.....	19
3.2.2. Enrichment cultures.....	20
3.2.3. Characterization of endophytic bacteria.....	22
3.3. Biochemical techniques .....	27
3.3.1. Protein extraction from plant tissues .....	27
3.3.2. Determination of total protein concentration .....	28
3.3.3. Determination of enzymatic activities .....	29

---

3.4. Analytical techniques .....	35
3.4.1. Chemicals .....	35
3.4.2. In vitro synthesis of glutathione related metabolites.....	35
3.4.3. Extraction of carbamazepine and transformation products from plant tissues .	35
3.4.4. Sample preparation for HPLC and LC-QTOF-MS/MS analysis.....	36
3.4.5. Quantification of CBZ by HPLC.....	36
3.4.6. LC-QTOF-MS/MS analysis for TPs identification.....	37
3.4.7. Identification of carbamazepine transformation products.....	38
3.5. Statistical treatment of data.....	38
4. Results.....	39
4.1. Carbamazepine removal by reed plants and its endophytic bacteria from nutrient solutions: a view on close-to-real conditions in CWs.....	39
4.1.1. Carbamazepine removal from nutrient media by <i>Phragmites australis</i> .....	39
4.1.2. Oxidative stress and enzymatic defence responses in <i>Phragmites australis</i> .....	40
4.2. Microbial communities associated to <i>Phragmites australis</i> .....	43
4.2.1. Rhizome-associated microbial communities.....	44
4.2.2. Isolation of endophytic bacteria.....	46
4.2.3. Carbamazepine removal from liquid medium by endophytic bacteria .....	52
4.2.4. Plant growth promoting characteristics .....	53
4.2.5. Enrichment cultures.....	54
4.3. Metabolism of carbamazepine in <i>Armoracia rusticana</i> hairy roots and interactions with endophytic bacteria.....	55
4.3.1. Carbamazepine removal from nutrient media by hairy roots and endophytic bacteria	55
4.3.2. Oxidative stress and antioxidant responses in HRs .....	57
4.3.3. Metabolism of carbamazepine in hairy roots and endophytic bacteria.....	60
4.3.4. Proteomics analyses in hairy root cultures.....	72

---

5. Discussion .....	84
5.1. Phytoremediation of carbamazepine: plant uptake and oxidative stress .....	85
5.1.1. Carbamazepine uptake in <i>Armoracia rusticana</i> hairy roots.....	85
5.1.2. Carbamazepine uptake in <i>Phragmites australis</i> .....	86
5.1.3. Antioxidants responses in <i>Phragmites australis</i> and role of GSTs.....	87
5.2. Isolation of endophytic bacteria from reed to improve phytoremediation.....	89
5.2.1. Rhizome associated microbial communities .....	89
5.2.2. Endophytic bacteria from plants exposed to carbamazepine .....	90
5.3. Interactions between plant roots and endophytic bacteria: carbamazepine metabolism .....	95
5.3.1. Carbamazepine removal from nutrient media.....	95
5.3.2. Metabolism of carbamazepine in hairy roots and endophytic bacteria.....	96
5.3.1. Analyses of proteins and antioxidant enzymatic activities in HRs.....	103
5.4. Practical applications.....	105
6. Conclusions .....	108
7. References .....	109



## Abstract

Our environment and our freshwater reserves suffer from increasing inputs of personal care products and pharmaceuticals. Despite partial degradation, some of these compounds have very low removal efficiency in conventional wastewater treatment facilities. The antiepileptic drug carbamazepine (CBZ) is one of the most recalcitrant compounds in this context. It is frequently found in wastewater, but also in the effluents of waste water treatment facilities after the treatment, reaches surface water and in some cases even drinking water reserves. With a growing urban population, forecasts are such that many of us will have to use reclaimed, treated wastewater instead of ground water. Hence, proper removal of recalcitrant compounds will be a necessity in the future to alleviate the stress put on the water cycle, the environment, and on consumers.

Phytoremediation is the biological treatment of wastewater with plants in constructed wetlands and represents a cheap and environmental friendly alternative to retrofit existing waste water treatment facilities. With this technology it might be possible to remove these contaminants from treated wastewater before its release into the environment . Efforts have been put on the design of constructed wetlands to improve removal efficiencies of hazardous compounds, including the selection of best suited plant species or water flow regimes. Other studies have considered the role of microbial communities found in water or sediments, but little attention has been put into plant-associated and endophytic communities. However, the importance of the microbiome in plant fitness and resistance to biotic and abiotic stresses has been demonstrated recently.

In this work, the uptake and metabolism of CBZ in plants is studied using a holobiontic conceptual approach in which plant and selected endophytic bacteria interact for mutual benefit. Common reed plants (*Phragmites australis*) were grown in liquid Hoagland solution under control conditions. After treatment with CBZ (5 mg/L) for nine days, up to 90% of the compound was removed. Endophytic bacteria were extracted from roots and rhizomes of these exposed plants, identified by 16S rRNA sequencing, and further characterized for their plant growth promoting traits and CBZ removal.

*Rhizobium radiobacter* and *Diaphorobacter nitroreducens* were selected among the isolates for a comprehensive study of CBZ uptake and metabolism in interaction with plant roots. An axenic horseradish (*Armoracia rusticana*) hairy root (HR) culture was used as plant model to unravel which metabolic pathways are used for CBZ transformation by plants in the absence and presence of their endophytic partners. Inoculation with *D. nitroreducens* and *R. radiobacter* led to a 2-fold and 4-fold increase in the removal capacity of HRs alone, respectively.

In total, thirteen transformation products in the liquid media were identified by LC-QTOF-MS/MS. These metabolites were classified in four distinct metabolic pathways. For the first time, a CBZ-glutathione conjugate was detected in plants. Glutathione and 10,11-diol pathways were preferred by horseradish HRs while inoculation with *R. radiobacter* and *D. nitroreducens* favour the 2,3-diol and the acridine pathway respectively.

The activity of the reactive oxygen species (ROS) scavenging enzymes glutathione reductase (GR), peroxidases (POX) and ascorbate peroxidase (APOX) and the detoxification enzymes glutathione-S-transferases (GSTs) were determined in cytosolic extracts of *P. australis* plants exposed to 100  $\mu$ M CBZ to characterize oxidative stress and defence mechanisms induced by the pharmaceutical. These enzymes play a major role in the detoxification and degradation of xenobiotics in plants. A slight increase of ROS scavenging enzymes observed only in leaves tissues suggests that active metabolites formed in the root system by endophytic strains and plant cells are rapidly transported into the aerial part, inducing an antioxidant response in leaves followed by an increase in metabolic capacity of CBZ and its metabolites. GSTs were induced in rhizomes as well, indicating that the 10,11-diol and subsequent GSH pathways are the main metabolic pathways for CBZ degradation in *P. australis*.

Antioxidant responses in HRs were induced by CBZ treatment but also after inoculation with endophytic bacteria. Similar observations were made on GST activities. The hypothesized protective role of endophytic bacteria when plants are confronted to abiotic stress by enhancing their antioxidant responses and detoxification mechanisms was evidenced by proteomics analyses. Superoxide dismutase, GR, monodehydroascorbate reductase, ascorbate peroxidase, all from the Halliwell-Asada cycle, were indeed identified in the growth media of inoculated

roots. Additionally, proteomics results revealed a shift on HR metabolism from primary metabolism to structural and chemical defence processes after CBZ treatment.

It can be concluded that *P. australis* is a species well-suited to remove CBZ at relevant environmental concentrations and that removal and degradation of the compound can be improved by enhancing the presence and functionality of selected beneficial strains among the endophytic bacterial community.

## **i. List of abbreviations**

Å	Ångström
APOX	Ascorbate peroxidase
bp	Base pairs
BSA	Bovine serum albumin
°C	Celsius degree
CFU	Colony-forming unit
cm	Centimetre
CBZ	Carbamazepine
CBZE	Carbamazepine-10,11-epoxide
CW	Constructed wetland
DNA	Deoxyribonucleic acid
dNTP	Deoxyribonucleotide triphosphate
DTT	Dithiothreitol
ESI	Electrospray ionization
g	Gram
GR	Glutathione reductase
GSH	Glutathione
GSSG	Glutathione disulfide
GST	Glutathione-S-transferase
h	hour
HPLC	High-performance liquid chromatography
HR	Hairy root
IAA	Indole-3-acetic acid
L	Litre
LB	Lysogeny broth
LC	Liquid chromatography
M	Molar (mol/L)
m/z	Mass-to-charge ratio
min	Minute
MS	Murashige and Skoog medium

---

NADPH	Nicotinamide adenine dinucleotide phosphate
PBS	Phosphate-buffered saline
PCR	Polymerase chain reaction
POX	Peroxidase
ppm	Parts per Million
PVK	Pikovskaya (agar medium)
QTOF-MS	Quadrupole time-of-flight mass spectrometry
RNA	Ribonucleic acid
RH	Relative humidity
RF	Radio frequency
RP	Reversed phase
rpm	Revolutions per minute
rRNA	Ribosomal ribonucleic acid
s	Second
SI	Solubilization index
SPI	Siderophore production index
TFA	Trifluoroacetic acid
TP	Transformation product
V	Volt
V <sub>pp</sub>	Peak-to-peak voltage
v/v	Volume to volume ratio
WWTP	Wastewater treatment plant
x g	Times gravity

## ii. List of figures

Figure 1: Main sources and fates of pharmaceuticals in the environment.....	2
Figure 2: Mean removal efficiency for pharmaceuticals and personal care products in WWTPs with activated sludge processes.....	3
Figure 3: Beneficial properties of endophytes.....	8
Figure 4: Layout of phenotypic assays included in the Biolog GEN III Microplate™ .....	26
Figure 5: Enzymatic conjugation of substrates used in this study by GSTs .....	30
Figure 6: Oxidation of guaiacol to tetraguaiacol by the enzyme POX in presence of H <sub>2</sub> O <sub>2</sub> .....	31
Figure 7: Reduction of GSSG to the sulfhydryl form GSH by the enzyme GR.....	32
Figure 8: Standard curve for the quantification of CBZ in nutrient media and plant extracts....	37
Figure 9: CBZ removal from the nutrient solution by <i>P. australis</i> .....	40
Figure 10: Antioxidant enzyme activities in <i>P. australis</i> exposed to 100 μM CBZ.....	41
Figure 11: Specific GST activity in <i>P. australis</i> exposed to 100 μM CBZ.....	43
Figure 12: Total cultivable endophytic bacterial community composition isolated from <i>P. australis</i> plants exposed to 21 μM CBZ .....	48
Figure 13: Evolutionary relationships of isolates from <i>P. australis</i> plants exposed to 21 μM CBZ .....	49
Figure 14: Genotypic characterization of the cultivable bacterial population of <i>P. australis</i> exposed to 21 μM CBZ grown in two different agar media: PDA and R2A.....	50
Figure 15: Community composition of total (A) and rhizomes (B) endophytic bacteria isolated from <i>P. australis</i> plants exposed to 21 μM CBZ .....	51
Figure 16: CBZ removal from liquid cultures by endophytic bacteria associated to <i>P. australis</i> and plant growth promoting traits.....	52
Figure 17: CBZ removal in <i>A. rusticana</i> HR cultures and effect of inoculation with the endophytic bacteria <i>R. radiobacter</i> and <i>D. nitroreducens</i> isolated from <i>P. australis</i> .....	56
Figure 18: Relationship between the initial concentration of CBZ in the growth medium and the removal by HR cultures after 6 days of incubation.....	57
Figure 19: Antioxidant enzyme activities in <i>A. rusticana</i> HRs and endophytic bacteria exposed to 250 μM CBZ.....	58
Figure 20: Specific GST activity in <i>A. rusticana</i> HRs and endophytic bacteria exposed to 250 μM CBZ .....	59

---

Figure 21: CBZ metabolism in <i>A. rusticana</i> HRs assisted by endophytic bacteria: the 10,11-diol pathway.....	60
Figure 22: CBZ transformation products in <i>A. rusticana</i> HR cultures I.....	63
Figure 23: CBZ transformation products in control <i>A. rusticana</i> HR cultures I.....	64
Figure 24: CBZ metabolism in <i>A. rusticana</i> HRs assisted by endophytic bacteria: the 2,3-diol pathway.....	63
Figure 25: CBZ metabolism in <i>A. rusticana</i> HRs assisted by endophytic bacteria: the GSH pathway.....	65
Figure 26: CBZE-GSH chromatograms after chemical synthesis (A) and in biological samples (B) .....	66
Figure 27: CBZE-CYS chromatograms after chemical synthesis (A) and in biological samples (B) .....	67
Figure 28: CBZ metabolism in <i>A. rusticana</i> HRs assisted by endophytic bacteria: the acridine pathway.....	68
Figure 29: CBZ transformation products in <i>A. rusticana</i> HR cultures II.....	69
Figure 30: CBZ transformation products in control <i>A. rusticana</i> HR cultures II .....	70
Figure 31: CBZ transformation products in root extracts .....	72
Figure 32: Functional classification of proteins identified in the nutrient media of <i>A. rusticana</i> HR cultures (A) and HR cultures exposed to 250 $\mu$ M CBZ (B).....	77
Figure 33: Number of plant proteins identified in nutrient media from <i>A. rusticana</i> HR cultures void of or inoculated with endophytic bacteria and exposed to 250 $\mu$ M CBZ.....	78

### iii. List of tables

Table 1: Structure and important chemical properties. of CBZ.....	4
Table 2: Application of HRs to phytoremediation of organic and inorganic pollutants.....	12
Table 3: Composition of the Hoagland solution used to grow <i>P. australis</i> plants in semi-hydroponic conditions in the greenhouse. ....	15
Table 4: Composition of the MS medium used to grow <i>A. rusticana</i> HR cultures.....	17
Table 5: Conditions for experiments with <i>A. rusticana</i> HR cultures exposed to CBZ.....	18
Table 6: Composition of the different media used for isolation and growth of endophytic bacteria from <i>P. australis</i> . ....	20
Table 7: Composition of different nutrient media for the isolation of bacteria associated to <i>P. australis</i> from enrichment cultures.....	21
Table 8: Primers used for the amplification of the 16S rRNA bacterial encoding gene.....	22
Table 9: Pikosvkaya agar medium composition for the quantification of phosphate solubilization.....	24
Table 10: Composition and preparation of the Chrome Azurol S agar medium for the determination of siderophore production in plant associated bacteria.....	25
Table 11: Substrates used for the determination of GST activities in plant cytosolic extracts....	29
Table 12: Collision cell operating parameters during proteomics experiments.....	34
Table 13: HPLC solvent gradient used for quantification of CBZ.....	36
Table 14: LC solvent gradient used for LC-QTOF-MS/MS analysis of CBZ and its transformation products.....	38
Table 15: Differential biochemical characteristics of rizoplane and endosphere rhizome-associated microbial communities in <i>P. australis</i> .....	44
Table 16: Biochemical characteristics conserved in endophytitic and rhizoplane rhizome-associated microbial communities of <i>P. australis</i> .....	45
Table 17: Taxonomic identification of endophytic bacteria isolated from <i>P. australis</i> plants exposed to 21 $\mu$ M CBZ.....	47
Table 18: Taxonomic identification of root and rhizome associated bacteria from <i>P. australis</i> plants isolated using enrichment cultures with CBZ as sole carbon source.....	54
Table 19: CBZ structure and transformation products identified in the liquid media during degradation by <i>A. rusticana</i> HR cultures and the endophytic bacteria <i>R. radiobacter</i> and <i>D. nitroreducens</i> .....	61



---

Table 20: Proteins identified in the nutrient medium of <i>A. rusticana</i> HR cultures after 4 days.	74
Table 21: Proteins identified in the nutrient medium of <i>A. rusticana</i> HR cultures exposed to 250 $\mu$ M CBZ after 4 days. ....	75
Table 22: Proteins identified in the nutrient medium of <i>A. rusticana</i> HR cultures inoculated with <i>R. radiobacter</i> and exposed to 250 $\mu$ M CBZ.....	79
Table 23: Proteins identified in the nutrient medium of <i>A. rusticana</i> HR cultures inoculated with <i>D. nitroreducens</i> and exposed to 250 $\mu$ M CBZ.....	83

# 1. Introduction

## 1.1. Emerging contaminants and pharmaceuticals in our environment

The term emerging contaminants is used to designate pollutants of emerging concern in our days. They are of anthropogenic origin, although not necessarily synthetic. From the massive lead contamination during the Roman Empire, through the irruption of pesticides after the second agricultural revolution, to the inclusion of nanoparticles or microplastics in the last years, and medical products of today, emerging contaminants are in constant change. The public became warned by the book “Silent spring” (Rachel Carson, 1962) who showed the negative impact of DDT in the food chain, settling the bases of environmentalism. With the development of analytical methods, the group of detectable emerging contaminants has expanded in the last years and today includes pharmaceuticals and personal care products (PPCPs), endocrine disruptors (EDCs), industrial additives, surfactants, flame retardants and many others.

Daughton and Ternes were among the first scientists observing the occurrence and significance of pharmaceuticals in our environment and urging the scientific community to develop environmental risk assessment strategies for these compounds in addition to the traditional priority pollutants (Daughton and Ternes, 1999). Since then, pharmaceuticals in aquatic environment have become a problem of increasing attention as is reflected in the increasing number of publications (Fatta-Kassinos et al., 2011). Detected normally in low concentrations, their persistence and bioaccumulation may pose an increasing problem for drinking water quality in the future.

Pharmaceutical pollutants are derived from human activities and enter the environment via different routes (Fig. 1). Whereas residues from the production process seem to play a minor role, parent compounds from medical use and prescription are transformed to secondary metabolites mainly in human and animal livers, and excreted via the urinary

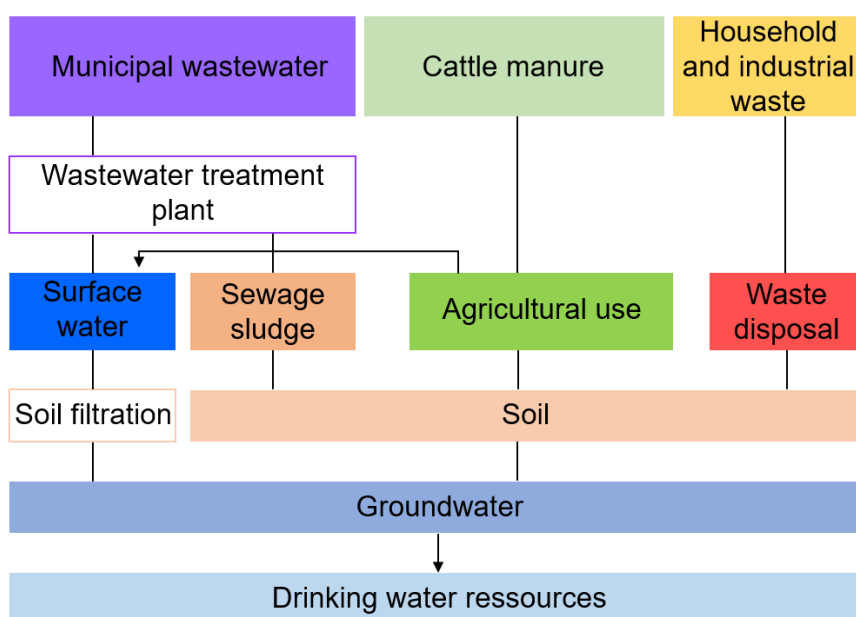


Figure 1: The main sources and fates of pharmaceuticals in the environment (adapted from Ternes, 1998).

system. Some of these transformation products (TPs) are still pharmacologically relevant and toxic for our ecosystems. After excretion via urine and faeces in households and hospitals, parent compounds and their TPs attain wastewater treatment facilities. Topical skin pharmaceuticals are washed off during body hygiene and flow with the water directly to the wastewater without even entering the human body. In addition, many drugs enter the wastewater directly as people flush them down the toilet instead of ensuring proper disposal. Veterinary medicines mainly enter the terrestrial environment via manure and slurries and pharmaceuticals used in fish farming (mostly antibiotics) enter the aquatic environment directly.

In wastewater treatment plants (WWTPs), several processes are applied to degrade and eliminate these compounds. However, conventional systems (primary and secondary treatments and disinfection by chlorine or chlorine dioxide), are unable to completely remove the utmost amount of the pharmaceutical micropollutants present in urban wastewaters (Rivera-Utrilla et al., 2013, Schröder et al. 2016). More effective treatments are required and improvements are currently under research (e.g., adsorption/bioadsorption on activated carbon, advanced oxidation processes by means of ozonation, photooxidation, radiolysis, and electrochemical processes). Still, some compounds remain recalcitrant to transformation during wastewater treatment

(Fig. 2, Miège et al., 2009), ending up in surface and groundwater or in the worst of the cases in drinking water (Mompelat et al., 2009). Because treated wastewater is often used in agriculture as irrigation water, pharmaceuticals can also enter the food chain via plant uptake from soil (Boxall et al., 2006). This may represent a serious problem in countries where even untreated wastewater is used for irrigation and leads to a direct exposure of soil to the pollutants (Kinney et al., 2006).

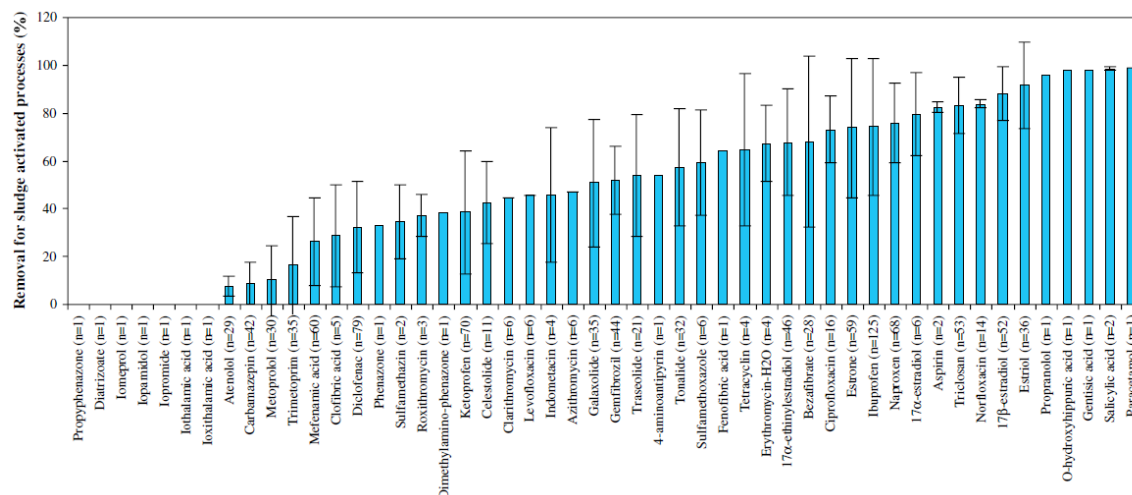


Figure 2: Mean removal efficiency (%) and relative standard deviation for pharmaceuticals and personal care products in wastewater treatment plants with activated sludge processes (Miège et al., 2009).

## 1.2. Carbamazepine

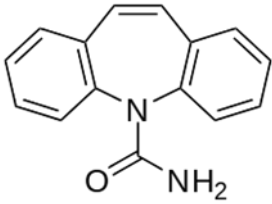
Carbamazepine (CBZ) was discovered by the Swiss chemist Walter Schindler in 1953. It was first marketed as a drug to treat trigeminal neuralgia in 1962 and has been used as an anticonvulsant and antiepileptic in the UK since 1965. At present, CBZ is predominantly used as an anticonvulsant and mood-stabilizing drug, prescribed mainly in the management of epilepsy, bipolar disorder, attention-deficit hyperactivity disorder (ADHD), schizophrenia, phantom limb syndrome, complex regional pain syndrome, paroxysmal extreme pain disorder, neuromyotonia, disorder, borderline, and post-traumatic stress disorder such as postcerebrovascular accident thalamic pain (Tolou-Ghamari et al., 2013).

CBZ and its metabolites are frequently detected in sewage and surface waters, in concentrations generally ranging from few ng/L to 6  $\mu$ g/L (Ternes, 1998; Heberer et

al., 2002; Tixier et al., 2003; Wiegel et al., 2004). The presence of CBZ has been reported also in groundwater (Lapworth et al., 2012) as well as in drinking water (Huerta-Fontela et al., 2011). In fact, CBZ can pass the soil-aquifer passage to groundwater without degradation (Ternes et al., 2007). Exhaustive studies have listed CBZ as one of the most recalcitrant PPCPs to removal via traditional wastewater treatment (Miège et al., 2009; Oulton et al., 2010). In none of the reported cases, removal efficiency exceeded 30%. CBZ is only prescribed to humans and because of its persistence in the environment it has been suggested as an indicator of human influence on water systems (Strauch et al., 2008).

Chemically, it belongs to the group of the dibenzazepines. These are compounds with two benzene rings connected by an azepine ring. Azepine is an unsaturated seven-member heterocycle with one nitrogen atom replacing a carbon atom. CBZ consists of two benzene rings and one azepine ring with a simple amide group attached to the N atom (Table. 1).

Table 1: Structure and important chemical properties of carbamazepine.

<b>Carbamazepine</b>	<b>Commercial names:</b>	<b>Carbatrol, Epitol, Tegretol XR</b>
	IUPAC name	benzo[b][1]benzazepine-11-
	Molecular weight	236.26858 g/mol
	Molecular formula	C <sub>15</sub> H <sub>12</sub> N <sub>2</sub> O
	Water solubility	170 mg/L
	pKa	13,9
	Log K <sub>ow</sub>	2,45
	UV absorption peaks	210 nm, 285 nm
	MS intense peaks	165 m/z, 193 m/z, 236 m/z

### 1.3. Phytoremediation and xenobiotic detoxification in plants

The presence of pharmaceuticals in surface waters has increased in the last years, and the aging of the population will lead to an increase of pharmaceuticals prescription resulting in a higher discharge of the parent compounds and their metabolites in

sewage water. Efficient cleaning systems are needed to avoid or reduce the intrusion of these compounds in our surface and groundwater systems, thus providing us with drinking water of good quality.

Phytoremediation, a novel green technology, is the use of plants to reduce or eliminate a given pollutant from contaminated soil, water or air. The use of constructed wetlands (CWs) as final polishing step in WWTPs or as a restricted treatment in small communities can constitute a good solution for recalcitrant compounds (Verlicchi and Zambello, 2014).

CWs are engineered systems that have been designed and constructed to utilize the natural processes but do so within a more controlled environment (Vymazal, 2011). Natural wetlands have been used to treat wastewater since centuries. However, under the uncontrolled conditions that prevailed at most of these sites, those wetlands were rather systems for wastewater discharge than for efficient treatments. CWs try to mimic the conditions of natural wetlands by using macrophytes plant species emerged, submerged or free-floating and controlling water supply and regime. Natural wetlands are still used for wastewater treatment under controlled conditions (Mander and Jenssen, 2002) but the use of CWs is now preferred.

Macrophytes are good tools for water cleaning because of their ability to grow in water saturated conditions and are therefore generally used in CWs in water treatment facilities. In 1998, the COST action 837 "Plant biotechnology for the removal of organic pollutants and toxic metals from wastewaters and contaminated sites" was run to develop phytoremediation-based processes to remove organic pollutants and metals from wastewater. The pioneering work of COST action 837 has led to the identification of the most promising helophytes for constructed wetlands, amongst them *Phragmites*, *Typha* and *Brassica* species, but also fast growing trees (Schröder et al., 2007). *Phragmites australis* had shown at this time a great potential for the removal of herbicides (Schröder et al., 2005). More recently, this species has been successfully utilized for phytoextraction of various xenobiotics including pharmaceuticals (Matamoros et al., 2005; Hijosa-Valsero et al., 2010; Carvalho et al., 2012). If not

completely, these systems have shown to reduce significantly the concentration of CBZ in the final effluent (Conkle et al., 2008; Matamoros et al., 2008; Matamoros et al., 2009; Park et al., 2009).

Xenobiotic uptake and transport in plants may occur by simple diffusion because there are no transporters specific for these man-made compounds (Schröder and Collins, 2011). Uptake into and distribution within plant tissues are affected mainly by the chemical properties of the compound where their octanol-water partition coefficient ( $\log K_{ow}$ ) plays the most important role, but also environmental factors (pH, T, organic matter, soil composition), and plant and tissue characteristics. Plants have developed specific mechanisms to reduce the toxicity of xenobiotics that enter their tissues. Similar to drug metabolism occurring in animals, plants possess specific enzymes that intervene to detoxify xenobiotics. Because of the resemblance with the process of drug detoxification in humans, a “green liver” model was proposed for detoxification of xenobiotics by plants (Sandermann, 1994). This concept is based on ground-breaking observations of Shimabukuro, who divided xenobiotic plant metabolism into three distinct phases ((I) activation of the xenobiotic, (II) detoxification and (III) sequestration) in analogy to drug human hepatic metabolism (Shimabukuro, 1976). In a first phase, the xenobiotic is transformed to prepare it for the next phases. Cytochrome P450 monooxygenases and peroxidases are usually the enzymes with major functions during this phase, activating the parent compound to yield a more polar and reactive molecule. During the second phase, the detoxification of the modified metabolites is driven mainly by glutathione- and glycosyl-transferases, resulting in less or non-toxic molecules after conjugation to sugars or glutathione respectively. In the last phase, a set of further reactions result in the compartmentation, or excretion of the conjugate or in the formation of bound residues (Sandermann, 1994).

#### **1.4. Endophytic bacteria and their role in plant growth promotion**

The German botanist Heinrich Friedrich Link was the first to describe endophytes, in 1809 (Link, 1809, cited in Hardoim et al., 2015) At that time, they were termed “Entophytæ” and were described as a distinct group of partly parasitic fungi living in

plants. Influenced by the discoveries of Koch and Pasteur establishing a link between microbes and disease, the belief in the 19th century was that healthy or normally growing plants are free of microorganisms. However, Galippe reported the occurrence of bacteria and fungi in the interior of vegetable plants and suggested that these microorganisms colonize plant tissues from the surrounding soil and might play a beneficial role for the host plant (Galippe, 1887). After the discovery of symbiotic *Rhizobium* nitrogen fixing bacteria in nodules of Leguminosae plants by the Dutch microbiologist Martinus Willem Beijerinck (Beijerinck, 1888) and the German agronomist Hermann Hellriegel (Hellriegel and Wilfarth, 1888) the mutualistic character of the relationships between endophytes and their hosts became evident.

The most common definition of endophytic bacteria was given by Hallmann and coauthors, who stated that those are “bacteria that can be isolated from surface disinfected plant tissue or extracted within the plant, and that do not visibly harm the plant” (Hallmann et al., 1997). This definition has been valid for culturable species and is the one used in this work. However, this definition may be incomplete when studying non-cultured endophytes with molecular techniques because surface sterilization does not guarantee the elimination of nucleic acids from non-endophytic dead bacteria.

Endophytic bacteria reside mostly in the intercellular apoplast and in dead or dying cells. They are also often found in the xylem vessels, within which they may be translocated from the roots to the aerial parts (Turner et al., 2013). Many bacterial endophytes originate from the rhizosphere and are attracted by root exudates. Various colonization routes have been described involving specific interactions (Hallmann, 2001). Endophytic bacteria migrate from the rhizoplane to the cortical cell layer by passive or active mechanisms and encounter the plant endodermis which represents a barrier for further colonization (Compant et al., 2010).

Commensal endophytes have no apparent effect on plant performance. On the contrary, a group of endophytes confer beneficial effects to the host such as protection against pathogens and insects, protection against abiotic stress and plant growth promotion (Fig. 3). Protection against pathogens can be via antibiotics production or



via induced resistance. In this last case, various bacterial structures, such as flagella, pili, secretion system machineries (e.g., TIV SS and SEC), and lipopolysaccharides, as well as bacterium-derived proteins and molecules, such as effectors (EF), autoinducers, and antibiotics, are detected by the host cells and trigger the induced systemic resistance (ISR) response. Protection against abiotic stress is mainly conferred by the sequestration of ACC, the direct precursor of ethylene (ET). ACC is metabolized by bacteria via the enzyme ACC deaminase (ACCd), thus lowering abiotic stress. Additionally, a range of reactive oxygen species detoxification (ROS detox) enzymes might also ameliorate the plant-induced stress. Diazotrophic bacterial endophytes can fix atmospheric nitrogen ( $N_2$ ) and might actively transport ammonium ( $NH_4^+$ ) and nitrate ( $NO_3^-$ ) to the host. Siderophore production (Sid) and iron uptake (Fe) are bacterial processes involved in plant growth promotion, biocontrol, and phytoremediation. Plant growth endophytic bacteria can promote growth of their hosts by synthesizing and secreting phytohormones such as auxin (IAA), gibberellins (GAs) or cytokinins (CKs) or other molecules like volatile organic compounds (VOC) or polyamines (poly- $NH_2$ ). Communications and interactions between cells of microorganisms inside the plant tissues are promoted by growth factors (GF), antibiotics (A), and autoinducer molecules. (Fig. 3, from Hardoim et al., 2015).

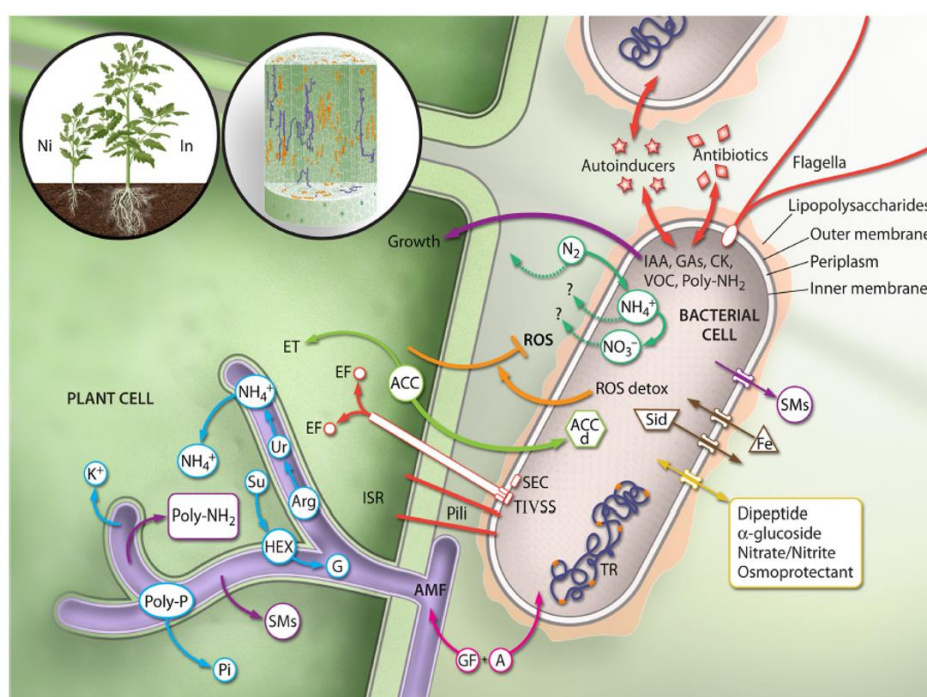


Figure 3: Beneficial properties of endophytes. The left panel shows plants inoculated (In) with beneficial microorganisms that significantly improve plant growth compared to noninoculated (Ni) plants. From Hardoim et al., 2015.

## 1.5. Interactions plant-endophytic bacteria for xenobiotic removal.

Interactions between rhizosphere-inhabiting bacteria and plants were first studied by Lorenz Hiltner. As early as in 1904, Hiltner defined the concept of the rhizosphere and established the foundations of rhizosphere microbial ecology (Hartmann et al., 2008). Since then, researchers have demonstrated that root associated microbial communities play an important role in plant health and nutrition (Mendes et al., 2013).

Besides the impact on human health through the diet, one of the most promising applications of beneficial microbe-plant interactions is the removal of pollutants. Plant-associated bacteria can directly mediate the degradation of organic pollutants by activating specific catabolic genes (Segura and Ramos, 2013). In addition, they can aid plants to cope with stress resulting from exposure to xenobiotics even though they might be devoid of enzymes involved in appropriate catabolic routes.

Endophytic bacteria harbouring both qualities (catabolic genes and plant growth promoting traits) can establish successful and durable mutualistic relationships with their hosts, certainly because they do not have to compete with the dense populations of microorganisms present in the different soil compartments (Rosenblueth and Martínez-Romero, 2006). Endophytes capable of degrading xenobiotics have been isolated in the last years. Most of the studies focus on organic pollutants such as petroleum derivatives, PAHs, TCE, organochlorines, naphthalene, pyrene, or phenolic compounds (Siciliano et al., 2001; Aken et al., 2004; Germaine et al., 2006; Sheng et al., 2008; Germaine et al., 2009; Weyens et al., 2009; Weyens et al., 2010; Yousaf et al., 2011; Ho et al., 2012; Kang et al., 2012; Peng et al., 2013). In re-inoculation experiments, some of these strains have improved remediation, favouring the metabolism of these compounds as well as the fitness of the plant (Afzal et al., 2014). However, research on the degradation of pharmaceuticals by endophytic microorganisms is scarce and the available research addresses mainly *in vitro* degradation without the host, usually in synthetic culture media. Only bacteria from activated sludge in a municipal or ligninolytic fungi have been tested for CBZ degradation (Santos et al., 2012; Li et al., 2013a).

## 1.6. Hairy roots to study plant-bacteria interactions

The first studies of hairy roots (HRs) date from the early 1900s, when Riker identified a bacterium, *Phytomonas rhizogenes* (later on reclassified as *Agrobacterium rhizogenes*) as causative agent of the hairy root (HR) disease in apple trees (Riker et al., 1930). This disease is characterized by the induction of abnormal growth of adventitious HRs in affected plants. *A. rhizogenes* has molecular mechanisms analogous to those of *Agrobacterium tumefaciens* to induce HRs formation by transfer of T-DNA to plant cells. The T-DNA of the Ri (root inducing) plasmid contains several virulent genes causing rhizogenic growth to the transformed cells (Păcurar et al., 2011; Chandra, 2012). As it occurs with *A. tumefaciens*, the transformed plant tissues by *A. rhizogenes* are also directed by T-DNA genes to produce opines, that serve as specific nutrients for the bacteria (Chilton et al., 1982; Chilton, 2001). Nevertheless, the physiologic basis of the tumorigenesis disease is different. Alteration of auxin metabolism has been proposed to play an important role in the expression of the HR phenotype (Zambryski et al., 1989; Gelvin, 1990). These findings have constituted the basis for the development of HR cultures with different valuable biotechnological applications such as secondary metabolites production, biotransformation processes or phytoremediation studies (Sevón and Oksman-Caldentey, 2002; Agostini et al., 2013).

HRs possess several characteristics making them a valuable tool for research studies. They have a stable genotype and phenotype, a fast *in vitro* growth with no need of additional phytohormones and a high production of secondary metabolites, a reason for which they are often called “phytochemical factories” (Georgiev et al., 2007). Furthermore, they are easy to subculture in sterile media, characteristic for which they constitute a good tool to study interactions with other microorganisms, especially rhizospheric and endophytic bacteria or fungi. HR cultures have been obtained from a large number of plant species (to date, more than 500), predominantly dicotyledonous. It has been shown that monocotyledonous species remain recalcitrant to the transformation by *A. rhizogenes*. Nonetheless, in the last years advances in

transformation techniques have permitted to obtain HR cultures from several monocotyledonous species (Georgiev et al., 2011).

As mentioned before, plants can be used to reduce or eliminate pollutants from contaminated water. Since plants have evolved different detoxification systems against xenobiotics, the selection of the plant species is crucial for a good remediation of the compound in question (Schröder et al., 2008). In this sense, HRs can be used as a model to elucidate xenobiotic uptake and transformation mechanisms such as conjugation, and compartmentation into vacuoles or cell walls, in different plant species. Because plant roots are the first organs to have contact with pollutants, they have developed specific mechanisms of detoxification. For these reasons, the use of HRs has been consolidated in the last two decades as study model for degradation and metabolism of organic pollutants, heavy metals, radionuclides and more recently of pharmaceuticals and personal care products (Huber et al., 2009; Chen et al., 2016) (Table 2). Additionally, they can be used for production of enzymes involved in detoxification such as peroxidases and laccases (González et al., 2008; Telke et al., 2011).

Table 2: Application of hairy roots to phytoremediation of organic and inorganic pollutants. Examples of assisted hairy root phytoremediation with mycorrhizae and/or bacteria are included, as well as transgenic hairy roots obtained for the improvement of phytoremediation process (modified from Agostini et al., 2013).

<b>Pollutant</b>	<b>Plant species</b>	<b>Studies involving microorganisms</b>
PPCPs		
- Paracetamol	<i>Armoracia rusticana</i>	-
- Tetracycline	<i>Helianthus annuus</i>	-
- Oxybenzone	<i>Armoracia rusticana</i>	-
Phenols	<i>Brassica napus</i>	Rhizobacteria
	<i>Brassica juncea</i>	-
	<i>Daucus carota</i>	-
	<i>Ipomoea batatas</i>	-
	<i>Solanum aviculare</i>	-
	<i>Solanum lycopersicum</i>	-
	<i>Nicotiana tabacum</i>	Arbuscular mycorrhizal fungus
PCB	<i>Solanum nigrum</i>	-
	<i>Atropa belladonna</i>	-
	<i>Brassica juncea</i>	-
TNT	<i>Catharanthus roseus</i>	-
	<i>Armoracia rusticana</i>	-
DDT	<i>Cichorium intybus</i>	-
	<i>Brassica juncea</i>	-
Dyes	<i>Tagetes patula</i> L.	-
	<i>Brassica juncea</i>	-
	<i>Blumea malcolmii</i> Hook.	-
	<i>Typhonium flagelliforme</i>	-
TCE	<i>Atropa belladonna</i>	-
Cadmium	<i>Thlaspi caerulescens</i>	-
	<i>Alyssum bertolonii</i>	-
	<i>Daucus carota</i>	<i>Glomus intraradices</i> and <i>Gigaspora margarita</i> (mycorrhiza)
Nickel	<i>Alyssum murale</i>	-
Zink	<i>Solanum nigrum</i>	-
Uranium	<i>Brassica juncea</i>	-
	<i>Chenopodium amaranticolor</i>	-
	<i>Armoracia rusticana</i>	-
	<i>Daucus carot</i>	-

## 2. Objectives

The general objective of this work was to characterize uptake and metabolism processes of CBZ in plants with emphasis on the role of endophytic bacteria to improve the removal efficiency of the compound in CWs under real conditions. The specific objectives of this study are:

- to characterize uptake and metabolism of CBZ in plants.
- to isolate endophytic bacteria from *Phragmites australis* exposed to CBZ and to characterize their plant growth promoting traits during CBZ removal.
- to study the interactions between isolated strains and plant roots using a horseradish HR culture as model system.
- to describe the metabolism of CBZ in plant roots assisted by endophytic bacteria.

## 3. Material and methods

### 3.1. Plant material and experimental setup

#### 3.1.1. Common reed (*Phragmites australis* (Cav.) Trin. ex Steud.)

Common reed was used to investigate CBZ removal and to explore the potential of its endophytic community. *Phragmites australis* (Cav.) Trin. ex Steud., known best as common reed, may be considered as the most widely distributed angiosperm, with populations found on every single continent except Antarctica (Ridley, 1930). Due to its capacities to exploit anthropogenic habitats, this plant has a great potential for phytoremediation. This perennial grass species grows in inland and estuary wetland areas. *P. australis* belongs to the *Poaceae* family of and can reproduce vegetatively through horizontal rhizomes or sexually via seeds. Adult *P. australis* plants were supplied from a local grower (Jörg Petrowski, Eschede, Germany). Shoots were cut in the mesocotyl region. Attached soil was carefully removed with a brush and tap water from the root systems. Those containing primary and secondary roots and rhizomes were transferred to single pots containing perlite and acclimated to the greenhouse at the Helmholtz Zentrum München.

##### 3.1.1.1. Nutrient solution and greenhouse conditions

Plants were regenerated in semi-hydroponic conditions under long days, at 25 °C and RH 60%. Pots were placed in groups of 6 in trays containing a modified Hoagland solution (Table 3). The nutrient solution was changed every week. Plants that had developed enough biomass to conduct experiments were selected for the study after 8 weeks.

Table 3: Composition of the Hoagland solution used to grow *Phragmites australis* plants in semi-hydroponic conditions in the greenhouse.

Components	Chemical formula	Stock solution (g/L)	Final concentration (mg/L)
<b>Macronutrients</b>			
Calcium nitrate tetrahydrate	Ca(NO <sub>3</sub> ) <sub>2</sub> ·4H <sub>2</sub> O	236.15	472.30
Potassium nitrate	KNO <sub>3</sub>	101.11	202.22
Magnesium sulphate heptahydrate	MgSO <sub>4</sub> ·7H <sub>2</sub> O	246.48	492.96
Monopotassium phosphate	KH <sub>2</sub> PO <sub>4</sub>	34.02	68.04
Ammonium nitrate	NH <sub>4</sub> NO <sub>3</sub>	80.04	80.04
<b>Micronutrients</b>			
Boric acid	H <sub>3</sub> BO <sub>3</sub>	2.8	2.8
Manganese chloride tetrahydrate	MnCl <sub>2</sub> ·4H <sub>2</sub> O	1.8	1.8
Zinc sulphate heptahydrate	ZnSO <sub>4</sub> ·7H <sub>2</sub> O	0.2	0.2
Copper sulphate pentahydrate	CuSO <sub>4</sub> ·5H <sub>2</sub> O	0.1	0.1
Sodium molybdate	NaMoO <sub>4</sub>	0.025	0.025
Ethylenediaminetetraacetic acid ferric sodium salt	FeNa-EDTA	1.835	3.67

### 3.1.1.2. Treatment for carbamazepine uptake and isolation of endophytic bacteria

Plants with sufficient biomass and of uniform size (approximately 80 cm) were selected and placed into individual pots containing 2 L of Hoagland solution. The nutrient medium was then spiked with CBZ from a stock solution to a final concentration of 5 mg/L (21.16 µM). Control pots containing only perlite but no plants were used to investigate non-biological effects such as photodegradation, volatilization and adsorption to the plastic pot walls or hydrolysis. Three pots were set up for every of the four exposure times (0, 1, 4 and 9 days). Each assay consisted of three replicates arranged in the greenhouse following a randomized design. To compensate water losses by evapotranspiration, distilled water was added daily to the pots to a final volume of 2 L. Samples from the nutrient solution were taken at 0, 1, 4 and 9 days of exposure, immediately frozen and stored at -20 °C until further analysis.

### 3.1.1.3. Carbamazepine treatment for enzyme stress

Pots containing plants of uniform size (height around 120 cm) were placed in individual reservoirs containing 4 L of nutrient solution. A stock solution of CBZ in ethanol was spiked to



the nutrient media to yield a final concentration of 23,64 mg/L (100  $\mu$ M). Controls containing nutrient solution without CBZ were spiked with the same volume of ethanol. Three plants were set up for each of the treatments (CBZ 100  $\mu$ M or no CBZ) and each of the exposure times (0, 24 and 48 h). Plants were exposed in the greenhouse following a complete randomized design. The first five leaves from each stem were collected after 24 and 48 h and were frozen immediately in liquid nitrogen. Root systems were washed carefully with tap water. Roots and rhizomes were separated, dried using absorbent paper, frozen immediately in liquid nitrogen and stored at -80 °C until preparation.

### **3.1.2. Horseradish hairy root cultures (*Armoracia rusticana* Gaertn. Mey. et Scherb.)**

#### **3.1.3.1. Description**

The use of a HR culture for research studies has several advantages. They develop a stable genotype and phenotype, are easy to grow in vitro and can produce secondary metabolites in high amounts. For this reason, HR cultures are often called “phytochemical factories” (Georgiev et al., 2007). Horseradish (*Armoracia rusticana* Gaertn. Mey. et Scherb.) is a perennial plant belonging to the *Brassicaceae* family. This species is known to produce peroxidases in high amounts. This enzyme family plays an important role in the first oxidation of xenobiotics and in abiotic and biotic stress defence (Knaak et al., 1962; Sasaki et al., 2004). Therefore, *A. rusticana* is indeed a well-suited species for xenobiotic metabolism studies.

HR cultures of horseradish (*A. rusticana*) had been obtained previously by transformation of nodal segments by *Agrobacterium rhizogenes* strain A4 (Nepovím et al., 2004). Briefly, seeds of horseradish plants were sterilized and grown in a sterile Murashige and Skoog (MS) medium hormone-free at 28 °C with a dark/light period of 6/18 h. After the emergence of the second pair of leaves, nodal segments were cut and transferred onto fresh medium. Wounded nodal segments were inoculated with a suspension of *A. rhizogenes* strain A4 ( $10^7$  cells/mL) for 24 h. When nodal segments started to produce callus and transformed roots, those were excised and first cultured on MS medium supplemented with phytohormones 0.6  $\mu$ M naphthalene acetic acid (NAA) and 4.4  $\mu$ M 6-benzylam-inopurine (BAP) and 500 mg/L ticarcillin. Ticarcillin was added for three subcultivation periods. At this point, HR cultures free of bacteria were obtained. The MS medium used in the second and third subcultivation period was hormone-free.

### 3.1.3.2. Nutrient media and growing conditions

*A. rusticana* HRs were grown in Erlenmeyer flasks containing 100 mL of full-strength Murashige and Skoog (MS) medium (Duchefa Biochemie bv.) (Table 4) supplemented with sucrose 3%, inositol, 0.1 g/L and thiamine, 0.32 mg/L. Cultures were grown at 23 +/- 2 °C under slow rotation in the dark and sub cultured every two weeks. A new generation was established when old tissue was cut into small pieces and transferred to fresh medium. Usually, from an old culture, four new fresh cultures were obtained. All the work was done carefully under sterile conditions in a laminar flow bench. When fresh material was needed for experiments, HRs were obtained from the same generation and grown in 50 mL Erlenmeyer flasks.

Table 4: Composition of the MS medium used to grow *Armoracia rusticana* hairy root cultures.

Components	Chemical formula	Final concentration mg/L
<b>Macro elements</b>		
Calcium chloride	CaCl <sub>2</sub>	332.02
Monopotassium phosphate	KH <sub>2</sub> PO <sub>4</sub>	170.00
Potassium nitrate	KNO <sub>3</sub>	1900.00
Magnesium sulphate	MgSO <sub>4</sub>	180.54
Ammonium nitrate	NH <sub>4</sub> NO <sub>3</sub>	1650.00
<b>Micro elements</b>		
Cobalt chloride hexahydrate	CoCl <sub>2</sub> ·6H <sub>2</sub> O	0.025
Copper sulphate pentahydrate	CuSO <sub>4</sub> ·5H <sub>2</sub> O	0.025
Ethylenediaminetetraacetic acid ferric sodium salt	FeNa-EDTA	36.70
Boric acid	H <sub>3</sub> BO <sub>3</sub>	6.20
Potassium iodide	KI	0.83
Manganese sulphate	MnSO <sub>4</sub>	16.90
Sodium molybdate dihydrate	Na <sub>2</sub> MoO <sub>4</sub> ·2H <sub>2</sub> O	0.25
Zinc sulphate heptahydrate	ZnSO <sub>4</sub> ·7H <sub>2</sub> O	8.60

### 3.1.3.3. Bacteria inoculation

Endophytic bacteria isolated from *P. australis* (*Rhizobium radiobacter* and *Diaphorobacter nitroreducens*) were grown in sterile lysogeny broth LB-Lennox medium at 24 °C in an orbital shaker (150 rpm) for one to two days. Bacterial cultures in logarithmic phase were then centrifuged at 7,000 rpm for 10 min, washed twice PBS and resuspended in a convenient volume of PBS to reach a final OD<sub>600nm</sub> of 0.5. HRs were subsequently incubated in those bacterial suspensions for one hour in an orbital shaker under slow rotation (75 rpm).

### 3.1.3.4. Carbamazepine treatment

Inoculated HRs were individually washed twice with sterile PBS and transferred to new Erlenmeyer flasks containing 100 mL of full-strength MS medium supplemented with CBZ 10, 25 or 250 µM. Following the same protocol, non-inoculated HRs were washed twice in PBS before incubation with CBZ. Autoclaved HRs, void of or inoculated with endophytic bacteria, were used as controls. Three biological replicates were set for each condition (three individual HR cultures inoculated with three individual bacterial cultures). HR cultures were incubated at 23 ± 2 °C under slow rotation in the dark for 6 to 21 days. One mL of the nutrient media was sampled under sterile conditions at different time points and stored at -20 °C until further analysis. HRs were washed in sterile PBS at the end of the experiment, dried in lint tissue paper, immediately frozen in liquid nitrogen and stored at -80 °C until sample processing. All concentrations and sampling time points used during exposure experiments are resumed in Table 5.

Table 5: Experimental design for exposure of *Armoracia rusticana* hairy root cultures to carbamazepine.

[CBZ]	Sampling time points in nutrient media (days)	Sampling time points in root tissues (days)
<i>Short-term exposure</i>		
10 µM		
25 µM	0, 1, 3, 6	6
50 µM		
<i>Long-term exposure</i>		
250 µM	0, 1, 4, 8, 14, 21	21

### 3.1.3.5. Sample preparation for identification of CBZ and TPs

For the analysis of CBZ, acridine and its metabolites, samples from the growing media of HR cultures were centrifuged at 13,000 g for 10 min. The pellet containing cell residues and debris was discarded. A protein precipitation was carried out before LC-QTOF-MS/MS analysis. Samples were mixed with 45 mg/mL 5-sulfosalicylic acid (1:10, v:v), vortexed briefly, and centrifuged 5 min at 13,000 g. The protein-free supernatant was filtered using a 0.22 µm polyvinylidene difluoride (PVDF) filter and used for metabolite identification. Supernatants were then stored at – 20 °C for further analyses.

## 3.2. Isolation of endophytic bacteria from *Phragmites australis*

### 3.2.1. Isolation from plants treated with carbamazepine

Segments of 2 to 3 cm from roots and rhizomes were collected from three different plants exposed to 5 mg/L CBZ for 9 days (see section 2.1.1.2, p 24). Root and rhizome segments were washed with tap water to remove attached perlite and soil particles, and pooled to constitute two independent sample sets (roots and rhizomes) for isolation of endophytic bacteria. Samples were surface sterilized in a 2% hypochlorite sodium (NaClO) solution for 20 min in a rotary shaker at 150 rpm and rinsed subsequently with sterile water three times for one min. Plant samples were then ground with a glass mortar in two mL of sterile water. One mL from the extract was ten-fold diluted to render 6 different dilutions ( $10^{-1}$  to  $10^{-6}$ ). One hundred µL of every dilution were spread in duplicate onto R2A and PDA agar plates containing 10 µM CBZ. Additionally, 100 µL from the last rinsing water were plated in order to check for efficiency of surface sterilization. Plates were incubated at room temperature for 14 days. Distinct colony morphotypes were identified and sub-cultured three times to ensure purity. Each morphotype was cryopreserved in 20% glycerol for further characterization.

Endophytic isolates were maintained in R2A and PDA agar plates. For removal experiments or when pre-cultures were needed, isolates were grown in liquid LB-Lennox. Composition of these media are detailed in Table 6.

Table 6: Composition of the different media used for isolation and growth of endophytic bacteria from *Phragmites australis*.

Components	Chemical formula	Amount (g/L)
<b>LB-Lennox</b>		
Tryptone	-	10
Yeast extract	-	5
Sodium chloride	NaCl	5
<b>R2A agar (pH 7.2)</b>		
Casein acid hydrolysate	-	0.5
Dextrose	C <sub>6</sub> H <sub>12</sub> O <sub>6</sub>	0.5
Dipotassium phosphate	K <sub>2</sub> HPO <sub>4</sub>	0.3
Magnesium sulphate	MgSO <sub>4</sub>	0.024
Proteose peptone	-	0.5
Sodium pyruvate	C <sub>3</sub> H <sub>3</sub> NaO <sub>3</sub>	0.3
Starch, soluble	(C <sub>6</sub> H <sub>10</sub> O <sub>5</sub> ) <sub>n</sub>	0.5
Yeast extract	-	0.5
Agar		15
<b>PDA agar</b>		
Dextrose	C <sub>6</sub> H <sub>12</sub> O <sub>6</sub>	20
Potato extract	-	4
Agar		15

### 3.2.2. Enrichment cultures

Roots and rhizomes from adult reed plants were cut and washed shortly with tap water to remove perlite and attached soil particles. Explants of 3 cm were excised and kept in PBS. An enrichment culture was performed using three root segments and three rhizome segments from three different plants. Explants were incubated in 50 mL of sterile minimal medium AB (Table 7) supplemented with 0.4 mM CBZ as sole carbon source for three days at 24 °C and 150 rpm in an orbital shaker. Explants were then removed and 0.5 mL of the homogenised culture was transferred to a new flask containing 50 mL fresh medium. Every two weeks, 0.5 mL of the old culture was transferred to a new flask containing fresh medium. After three sub-cultures, one mL of the last culture was used to make serial dilutions up to 10<sup>-4</sup>. From each dilution, 100 µL were spread onto agar plates containing different growth media (MB/10, TSAII, PDA and R2A) (Table 7). A second enrichment culture was set up after surface sterilizing root and rhizomes explants. For the sterilization, plant tissues were incubated in a sodium hypochlorite 2% solution for 20 min in an orbital shaker (150 rpm). Explants were then washed three times

with sterile PBS and crushed in a mortar under axenic conditions. The resulting material was used for the enrichment culture as described for non-sterilized explants.

Table 7: Composition of different nutrient media for the isolation of bacteria associated to *Phragmites australis* from enrichment cultures.

Components	Chemical formula	Final concentration (g/L)
<b>AB</b>		
Ammonium sulphate	(NH <sub>4</sub> ) <sub>2</sub> SO <sub>4</sub>	2
Sodium phosphate dibasic	Na <sub>2</sub> HPO <sub>4</sub>	6
Monopotassium phosphate	KH <sub>2</sub> PO <sub>4</sub>	3
Sodium chloride	NaCl	3
Magnesium sulphate	MgSO <sub>4</sub>	241 x 10 <sup>-3</sup>
Calcium chloride	CaCl <sub>2</sub>	11 x 10 <sup>-3</sup>
Iron (III) chloride	FeCl <sub>3</sub>	487 x 10 <sup>-6</sup>
<b>MB agar (Difco)</b>		
Peptone	-	5
Yeast extract	-	1
Ferric citrate	C <sub>6</sub> H <sub>5</sub> FeO <sub>7</sub>	0.1
Sodium chloride	NaCl	19.45
Magnesium chloride	MgCl <sub>2</sub>	8.8
Sodium sulphate	Na <sub>2</sub> SO <sub>4</sub>	3.24
Calcium chloride	CaCl <sub>2</sub>	1.8
Potassium chloride	KCl	0.55
Sodium bicarbonate	NaHCO <sub>3</sub>	0.16
Potassium bromide	KBr	0.08
Strontium chloride	SrCl <sub>2</sub>	34 x 10 <sup>-3</sup>
Boric acid	H <sub>3</sub> BO <sub>3</sub>	22 x 10 <sup>-3</sup>
Sodium silicate	Na <sub>2</sub> SiO <sub>3</sub>	4 x 10 <sup>-3</sup>
Sodium fluoride	NaF	2.4 x 10 <sup>-3</sup>
Ammonium nitrate	NH <sub>4</sub> NO <sub>3</sub>	1.6 x 10 <sup>-3</sup>
Disodium diphosphate	Na <sub>2</sub> H <sub>2</sub> P <sub>2</sub> O <sub>7</sub>	8 x 10 <sup>-3</sup>
Agar	(C <sub>12</sub> H <sub>18</sub> O <sub>9</sub> ) <sub>n</sub>	15
<b>TSII (Fisher Scientific)</b>		
Pancreatic digest of casein	-	14.5
Papaic digest of soybean meal	-	5
Sodium chloride	NaCl	5
Growth factors	-	1.5
Defibrinated sheep blood	-	5
Agar	(C <sub>12</sub> H <sub>18</sub> O <sub>9</sub> ) <sub>n</sub>	14
<b>PDA Agar (Sigma)</b>	-	see Table 6
<b>RZA agar (Difco)</b>	-	see Table 6

### 3.2.3. Characterization of endophytic bacteria

#### 3.2.6.1. Sequencing of the bacterial 16S rRNA encoding gene

Endophytic bacteria isolated from *P. australis* were identified by sequencing the gene coding for the smaller subunit 30S of the prokaryotic ribosome (16S rRNA).

Genomic DNA was extracted from fresh bacterial cultures using the FastDNA™ SPIN Kit for Soil (MP Biomedicals) following the recommendations of the manufacturer. Depending on the cell density, two to three mL of fresh cultures were used. Typically, 30 µL containing 0.5 µg to 1 µg of genomic DNA were obtained from each strain. DNA purity and concentration were determined by measuring the absorbance at 230, 260 and 280 nm using a Nanodrop™ spectrophotometer.

Universal primers 16S-27f and 16S-1492R (Table 8) were used to partially amplify the 16S rRNA encoding gene from the endophytic bacteria by the polymerase chain reaction (PCR). The 50 µL PCR reaction mixture contained 100 to 200 ng of extracted DNA, 1x Top Taq buffer, 200 µM of each dNTP, 200 pM of each primer and 1.25 U of Top Taq polymerase (Qiagen). After initial denaturation at 94 °C for 5 min, each thermal cycling consisted of 60 s denaturation at 94 °C, 60 s annealing at 52 °C and 90 s elongation at 72 °C. After 35 cycles, a final extension step at 72 °C for 10 min was added. PCR products were separated by electrophoresis in a 1% agarose gel. Bands corresponding to approx. 1450 bp were excised from the agarose gel and purified using the NucleoSpin® Gel and PCR Clean-up kit (Macherey-Nagel) according to the manufacturer's protocol. The purified PCR products were sequenced using the primers 16S-27f, 16S-609f, 16S-907R and 16S-1492R in an ABI 3730 48-capillary sequencer. PCR reactions for the sequencing were performed using the BigDye® Terminator v3.1 Cycle Sequencing Kit (Life Technologies) following the instructions of the supplier.

Table 8: Primers used for the amplification of the 16S rRNA bacterial encoding gene.

Primer	Sequence (5'- 3')	Region	Reference
16S-27f	AGAGTTTGATCCTGGCTCAG	27-47	(Lane, 1991)
16S-609f	TTAGATACC CCDGTAGT	609-629	-
16S-907R	CCGTC AATTCMTTTRAGTTT	888-907	(Lane et al., 1985)
16S-1492R	GGTTACCTTGTTACGACTT	1473-1492	(Lane, 1991)

### 3.2.6.2. Phylogenetic analysis

The identification of phylogenetic neighbours was initially carried out by the BLASTN (Altschul et al., 1997) program against the database containing type strains with validly published prokaryotic names and representatives of uncultured phylotypes (Kim et al., 2012). The top thirty sequences with the highest scores were then selected for the calculation of pairwise sequence similarity using a global alignment algorithm (Myers and Miller, 1988), which was implemented at the EzTaxon server (<http://www.ezbiocloud.net/eztaxon>; Kim et al., 2012).

The evolutionary history was inferred using the Neighbour-Joining method (Saitou and Nei, 1987). A phylogeny test was conducted using the Bootstrap method (2000 replicates) (Felsenstein, 2009). The evolutionary distances were computed using the Maximum Composite Likelihood method (Tamura et al., 2004). Evolutionary analyses were conducted in MEGA6 (Tamura et al., 2013).

### 3.2.6.3. Plant growth promoting traits

#### a. Phosphate solubilization

The potential for phosphate solubilization was determined by the appearance of a clear halo on Pikovskaya's (PVK) agar medium (Pikovskaya, 1948). Bacterial strains were first grown overnight in 5 mL LB-Lennox liquid media at 28 °C and 150 rpm until a cell density of approx. 10<sup>6</sup> CFU/mL. Bacterial cells were then washed twice with Phosphate-buffered saline (PBS) and resuspended in 5 mL PBS. After homogenization, a 10 µL drop from this last suspension was placed onto PVK agar medium (Table 9). PVK agar plates were incubated at 28 °C for 72 h. Strains inducing a clear zone around the colonies were considered as positive. Phosphate solubilization was quantified by the determination of the solubilization index (SI) as follows:

$$SI = \frac{\text{colony diameter} + \text{halo zone diameter}}{\text{colony diameter}}$$

Isolates were classified in three groups according to their solubilization index: (+) for a SI lower than 1.3, (++) for a SI between 1.3 and 1.7, and (+++) for a SI higher than 1.7.



Table 9: Pikosvkaya agar medium composition for the quantification of phosphate solubilization.

Constituents	Chemical formula	Amount (g/L)
Yeast extract	-	0.5
Glucose	C <sub>6</sub> H <sub>12</sub> O <sub>6</sub>	10
Calcium phosphate	Ca <sub>3</sub> (PO <sub>4</sub> ) <sub>2</sub>	5
Ammonium sulphate	(NH <sub>4</sub> ) <sub>2</sub> SO <sub>4</sub>	0.5
Potassium chloride	KCl	0.2
Magnesium sulphate	MgSO <sub>4</sub> ·7H <sub>2</sub> O	0.1
Manganese sulphate	MnSO <sub>4</sub> ·H <sub>2</sub> O	0.0001
Ferrous sulphate	FeSO <sub>4</sub> ·7H <sub>2</sub> O	0.0001
Agar	(C <sub>12</sub> H <sub>18</sub> O <sub>9</sub> ) <sub>n</sub>	15

### b. Siderophore production

Bacterial isolates were assayed for potential siderophore production on the Chrome azurol S agar medium as described by (Alexander and Zuberer, 1991). The preparation of the medium is described in Table 10.

Bacterial strains were grown overnight in 5mL LB-Lennox liquid media at 28 °C in a rotary shaker (150 rpm) until a cell density of approx. 10<sup>6</sup> CFU/mL. Bacterial cells were then washed twice with PBS and resuspended in 5 mL PBS. After homogenization, a drop containing 10 µL of this last suspension was placed on Chrome azurol S agar medium. Cells were incubated at 28 ± 2 °C for 72 h. Development of a yellow–orange halo around the colonies was considered as positive for siderophore production. Siderophore production was quantified by the determination of the siderophore production index (SPI):

$$SPI = \frac{\text{colony diameter} + \text{halo zone diameter}}{\text{colony diameter}}$$

Isolates were classified in three groups according to their siderophore production potential as follows: + for a SPI lower than 1.8, ++ for a SPI between 1.8 and 2.7, and +++ for a SPI higher than 2.7.

Table 10: Composition and preparation of the Chrome Azurol S agar medium for the determination of siderophore production in plant associated bacteria

Constituents	Amount
<b>Solution 1 (indicator):</b> <i>mix A and B first and add to C with continuous stirring</i>	
A. FeCl <sub>3</sub> ·6H <sub>2</sub> O (1 mM in 10 mM HCl)	10 mL
B. Chrome azurol S (1.21 mg/mL)	50 mL
C. Hexadecyltrimethylammonium (1.82 mg/mL)	40 mL
<i>Autoclave and cool to 50 °C</i>	
<b>Solution 2 (buffer):</b> <i>dissolve in H<sub>2</sub>O to a final volume of 800 mL</i>	
PIPES	30.24 g
KH <sub>2</sub> PO <sub>4</sub>	0.3 g
NaCl	0.5 g
NH <sub>4</sub> Cl	1 g
Agar	15 g
<i>Autoclave and cool down to 50 °C</i>	
<b>Solution 3:</b> <i>dissolve in H<sub>2</sub>O to a final volume of 70 mL</i>	
Glucose	2 g
Mannitol	2 g
MgSO <sub>4</sub> ·7H <sub>2</sub> O	493 mg
CaCl <sub>2</sub>	11 mg
MnSO <sub>4</sub> ·H <sub>2</sub> O	1.17 mg
H <sub>3</sub> BO <sub>3</sub>	1.4 mg
CuSO <sub>4</sub> ·5H <sub>2</sub> O	0.04 mg
ZnSO <sub>4</sub> ·7H <sub>2</sub> O	1.2 mg
Na <sub>2</sub> MoO <sub>4</sub> ·2H <sub>2</sub> O	1 mg
<i>Autoclave and cool down to 50 °C</i>	
<b>Solution 4</b>	
Casaminoacids 10% (w/v)	30 mL
<i>Sterilize by filtration</i>	

### c. Indole-3-acetic acid production

Indole-3-acetic acid (IAA) production was quantified according to (Bano and Musarrat, 2003). Isolates were inoculated in 5 mL LB-Lennox liquid medium supplemented with 0.5% glucose and 500 µg/mL tryptophan and incubated at 28 °C and 150 rpm for 48 h. Cultures were centrifuged at 10,000 rpm for 15 min and 2 mL of the supernatant were transferred to a fresh tube to which 100 µL of 10 mM orthophosphoric acid and 4 mL of the Salkowski reagent (1 mL of 0.5 M FeCl<sub>3</sub> in 50 mL of 35% HClO<sub>4</sub>) were added. The mixture was incubated at room temperature for 25 min and the absorbance of pink color developed was read at 530 nm. The

IAA concentration in culture was calculated from a calibration curve of pure IAA (Biochemica) ranging from 10-50 µg/mL.

### 3.2.6.4. Analysis of rhizome-associated microbial communities

Phenotypic patterns of microbial communities associated with the rhizomes of common reed were performed using the Biolog GEN III microplate™. The test panel included 94 biochemical tests such as utilization of 71 different carbon sources (Fig. 4, columns 1-9) and 23 chemical sensitivity assays (Fig. 4, columns 10-12). Rhizomes were carefully harvested from adult plants and without being washed or altered, they were transferred as fast as possible to the incubation flasks. The rhizosphere community was studied by incubating 5 pieces of fresh rhizomes (3 to 4 cm) in 50 mL liquid R2A medium overnight at 28 °C under slight rotation. The rhizome endophytic community was studied sterilizing 5 pieces of fresh rhizomes (3 to 4 cm) previously in 2% sodium hypochlorite for 20 min in a rotary shaker at 150 rpm. Rhizomes were then washed three times with sterile PBS and crushed in a mortar containing 2 mL of sterile PBS. The material obtained was transferred to a flask containing 50 mL of R2A medium and incubated overnight at 28 °C and 150 rpm. In both cases, the liquid R2A was supplemented with 10 µM CBZ.

GEN III MicroPlate™											
A1 Negative Control	A2 Dextrin	A3 D-Maltose	A4 D-Trehalose	A5 D-Cellobiose	A6 Gentiobiose	A7 Sucrose	A8 D-Turanose	A9 Stachyose	A10 Positive Control	A11 pH 6	A12 pH 5
B1 D-Raffinose	B2 α-D-Lactose	B3 D-Melibiose	B4 β-Methyl-D-Glucoside	B5 D-Salicin	B6 N-Acetyl-D-Glucosamine	B7 N-Acetyl-β-D-Mannosamine	B8 N-Acetyl-D-Galactosamine	B9 N-Acetyl-Neuraminic Acid	B10 1% NaCl	B11 4% NaCl	B12 8% NaCl
C1 α-D-Glucose	C2 D-Mannose	C3 D-Fructose	C4 D-Galactose	C5 3-Methyl Glucose	C6 D-Fucose	C7 L-Fucose	C8 L-Rhamnose	C9 Inosine	C10 1% Sodium Lactate	C11 Fusidic Acid	C12 D-Serine
D1 D-Sorbitol	D2 D-Mannitol	D3 D-Arabitol	D4 myo-Inositol	D5 Glycerol	D6 D-Glucose-6-PO4	D7 D-Fructose-6-PO4	D8 D-Aspartic Acid	D9 D-Serine	D10 Troleandomycin	D11 Rifamycin SV	D12 Minocycline
E1 Gelatin	E2 Glycyl-L-Proline	E3 L-Alanine	E4 L-Arginine	E5 L-Aspartic Acid	E6 L-Glutamic Acid	E7 L-Histidine	E8 L-Pyroglytamic Acid	E9 L-Serine	E10 Lincomycin	E11 Guanidine HCl	E12 Niaproof 4
F1 Pectin	F2 D-Galacturonic Acid	F3 L-Galactonic Acid Lactone	F4 D-Gluconic Acid	F5 D-Glucuronic Acid	F6 Glucuronamide	F7 Mucic Acid	F8 Quinic Acid	F9 D-Saccharic Acid	F10 Vancomycin	F11 Tetrazolium Violet	F12 Tetrazolium Blue
G1 p-Hydroxy-Phenylacetic Acid	G2 Methyl Pyruvate	G3 D-Lactic Acid Methyl Ester	G4 L-Lactic Acid	G5 Citric Acid	G6 α-Keto-Glutaric Acid	G7 D-Malic Acid	G8 L-Malic Acid	G9 Bromo-Succinic Acid	G10 Nalidixic Acid	G11 Lithium Chloride	G12 Potassium Tellurite
H1 Tween 40	H2 γ-Amino-Butyric Acid	H3 α-Hydroxy-Butyric Acid	H4 β-Hydroxy-D,L-Butyric Acid	H5 α-Keto-Butyric Acid	H6 Acetoacetic Acid	H7 Propionic Acid	H8 Acetic Acid	H9 Formic Acid	H10 Aztreonam	H11 Sodium Butyrate	H12 Sodium Bromate

Figure 4: Layout of phenotypic assays included in the Biolog GEN III Microplate™

After incubation, cultures were filtered using sterile lint-free tissue paper and the clear culture was homogenized and diluted in inoculating fluid A (IF-A) to give a final transmittance of 97% ( $\pm 0.5$ ). Each well of the plate was loaded carefully with 100  $\mu$ L of the homogenized inoculum and the plate was incubated at 28 °C for 24 h. All the wells were colorless when inoculated. After the incubation, wells where purple color had developed were considered as positive wells. Negative wells remained colorless, as did the negative control well.

### **3.2.6.5. Carbamazepine removal from liquid cultures**

Endophytic isolates were tested for CBZ removal. Cells were initially grown in 5 mL of LB-Lennox medium until saturation. One hundred  $\mu$ L were then transferred to 5 mL of fresh LB-Lennox/10 medium containing 50  $\mu$ M of CBZ. Cells were incubated at 28 °C in a rotary shaker (150 rpm) for three days. Cultures containing different final cell numbers were then centrifuged and one mL of the supernatant was frozen at -20 °C until analysis. CBZ concentration in the growing media was determined by HPLC.

In a second experiment, the capacity of the isolates to use CBZ as sole carbon source was investigated. Cells were initially grown in 5 mL of LB-Lennox medium until saturation and then, 100  $\mu$ L were transferred to 5 mL of fresh AB minimal medium containing CBZ as sole carbon source (400  $\mu$ M). Cells were incubated at 28 °C in an orbital shaker (150 rpm) for three weeks. Cell growth was followed by measuring the optical density at 600 nm every seven days. CBZ concentration in the media was determined by HPLC.

## **3.3. Biochemical techniques**

### **3.3.1. Protein extraction from plant tissues**

Cytosolic enzymes were extracted from plant tissues as described by Schröder and co-workers (Schröder et al., 2005) with some modifications. For the cytosolic extract, 3 g of frozen plant tissue were homogenised to obtain a fine powder on a mortar under liquid nitrogen. The resulting material was extracted in 0.1 M sodium phosphate buffer pH 6.5 containing 10 mM DTE, 2 mM MgCl<sub>2</sub>, 1 mM EDTA, 1 mM PMSF and 1% PVP K90 (w/v) for 30 min on ice, under constant agitation using a magnetic stirrer. The suspensions were filtered through Miracloth and

centrifuged at 15,000 x g and 4 °C for 30 min. The supernatants were collected and precipitated by stepwise addition of ammonium sulphate ((NH<sub>4</sub>)<sub>2</sub>SO<sub>4</sub>) (Sigma-Aldrich, Taufkirchen, Germany). In a first step, ammonium sulphate was added slowly to a final concentration of 40%. Samples were then stirred on ice for 30 min using a magnetic stirrer and centrifuged at 20,000 x g and 4 °C for 30 min. In a second step, supernatants were collected and ammonium sulphate was added to a final concentration of 80%. Samples were then stirred on ice for 30 min and centrifuged again at 20,000 x g and 4 °C for 30 min. The supernatants were then discarded and the pellets were carefully resuspended in 2.5 mL of 200 mM Tris-HCl buffer pH 7.3 containing 1 mM DTE and 2 mM MgCl<sub>2</sub> with the help of the pipette. Excess of ammonium sulphate salts were removed from the protein extracts using PD-10 gel filtration columns (Pharmacia, Freiburg, Germany) and following the recommendations of the manufacturer. Samples were finally eluted in 3.5 mL 25 mM Tris-HCl buffer (pH 7.8) and stored at -83 °C in aliquots. The amount of ammonium sulphate to add in each of the two steps of the protein precipitation was calculated according to Jaenicke, 1984, using the following formula:

$$\text{Ammonium sulphate amount (g)} = \frac{V * 1.77 * (S - s)}{3.5 - S}$$

V: volume in mL

S: desired final ammonium sulphate saturation expressed as decimal equivalent of percentage

s: initial ammonium sulphate amount in the sample expressed as decimal equivalent of percentage

### 3.3.2. Determination of total protein concentration

Protein contents in cytosolic extracts were determined following the method of Bradford (1976) using the dye Coomassie Blue G250. This dye change its colour after binding to proteins. This change in colour from red to blue can be measured spectroscopically, determining the absorbance of the samples at 595nm (its bound form). For the measurements, 10 µL of enzyme extracts were added to 200 µL ten-fold diluted Coomassie Blue dye and incubated for 10 min at room temperature. The absorbance was then measured at 595 nm. The protein content was calculated using a calibration curve performed with a standard of bovine serum albumin (BSA) purchased from Sigma-Aldrich (Taufkirchen, Germany).

### 3.3.3. Determination of enzymatic activities

Enzymatic activities were determined carrying out spectrophotometric enzyme assays in a 96-well plate reader SPECTRAMax PLUS 384 (Molecular Devices, Ismaning, Germany) using the data analyser software SOFTmax PRO 4.6 (Molecular Devices Corporation, Sunnyvale, CA). Measurements in the visible light spectrum (390 to 750 nm) were performed using 96-well BRANDplates® (Brand, Wertheim, Germany). Changes in the OD were measured in time intervals of 15 sec for 5 min at room temperature. Measurements were performed using three biological replicates comprising three technical replicates each. A reaction mixture without enzyme extract was used as blank. Enzyme activities are expressed in  $\mu\text{kat}$  ( $\mu\text{mol}/\text{sec}$ ).

#### 3.3.6.1. Glutathione-S-transferases, GSTs (EC 2.5.1.18)

GST activity was determined using different substrates covering the activity of different isoforms of the enzyme (Fig. 5). The test consisted in following the formation of a glutathione-substrate conjugate by measuring the absorbance at its specific wavelength. The reaction was started by adding 10  $\mu\text{L}$  of the enzyme extract to 190  $\mu\text{L}$  of the reaction buffer containing fresh glutathione. Buffer composition, GSH and substrate concentrations, substrate specific extinction coefficients and specific wavelength used to measure the absorbance of the conjugate with each substrate are summarized in Table 11.

Table 11: Substrates used for the determination of GST activities in plant cytosolic extracts. Substrate names, abbreviations, extinction coefficients and wavelengths ( $\lambda$ ) used for the photometric enzyme assays are shown. Conditions for the enzyme assay (buffers, substrate and glutathione concentrations) depending on the substrate used are indicated.

Substrate	Abbv.	$\epsilon$ ( $\text{mM}^{-1} \text{cm}^{-1}$ )	$\lambda$ (nm)	Buffer	[substrate] (mM)	[GSH] (mM)
1-Chloro-2,4-dinitrobenzene	CDNB	9.6	340	Tris-HCl 0.1M pH 6.4	1	1
1,2-Dichloro-4-nitrobenzene	DCNB	8.5	345	Tris-HCl 0.1M pH 7.5	1	1
p-Nitrobenzylchloride	pNBC	1.8	310	Tris-HCl 0.1M pH 6.4	0.5	1
p-Nitrobenzoylchloride	pNBoC	1.9	310	Tris-HCl 0.1M pH 6.4	0.5	1
Fluorodifen		3.1	400	Tris-HCl 0.1M pH 7.5	0.3	1.2

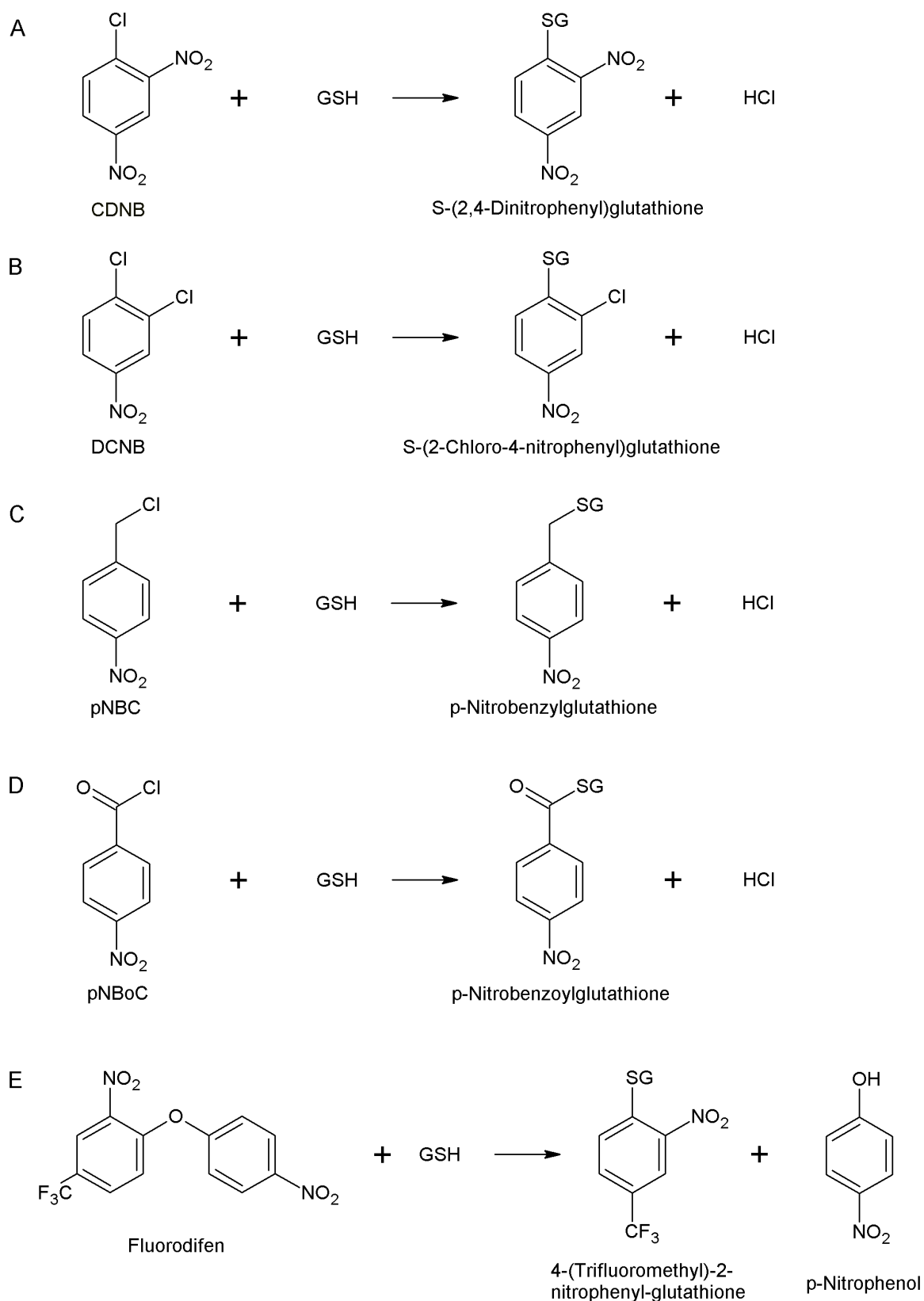


Figure 5: Enzymatic conjugation of substrates used in this study by GSTs in the presence of GSH. (A) 1-Chloro-2,4-dinitrobenzene (CDNB), (B) 1,2-Dichloro-4-nitrobenzene (DCNB), (C) p-Nitrobenzylchloride (pNBC), (D) p-Nitrobenzoylchloride (pNBoc), (E) Fluorodifen.

### 3.3.6.2. Peroxidase, POX (EC 1.11.-.-)

POX activity in the enzyme extracts was measured following the method proposed by Drotar and coworkers in 1985. Guaiacol (2-methoxyphenol) (Fluka, Steinheim, Germany) was used as substrate. The reaction buffer was 50 mM Tris-HCl pH 6.0. The formation of tetraguaiacol ( $\epsilon = 26.6 \text{ mM}^{-1}\text{cm}^{-1}$ ) (Fig. 6) was followed measuring absorbance at a wavelength of 420 nm for 5 min. The reaction started by adding 10  $\mu\text{L}$  sample to 190  $\mu\text{L}$  of the reaction mix containing 190  $\mu\text{M}$   $\text{H}_2\text{O}_2$  and 68  $\mu\text{M}$  guaiacol.

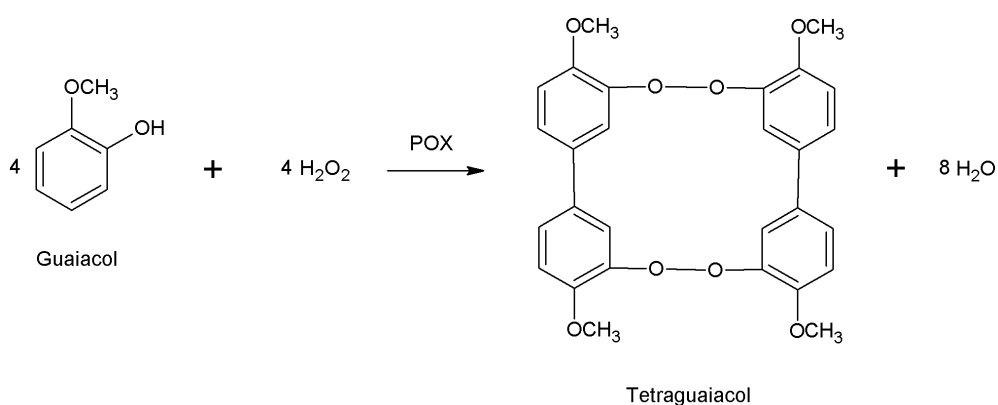


Figure 6: Oxidation of guaiacol to tetraguaiacol by the enzyme peroxidase (POX) in presence of  $\text{H}_2\text{O}_2$ . This reaction is used in the photometric enzyme assay to measure POX activity in plant extracts.

### 3.3.6.3. Ascorbate peroxidase, APOX (EC 1.11.1.11)

APOX activity was determined after Vanacker et al., 1998. The oxidation of ascorbic acid ( $\epsilon = 2.8 \text{ mM}^{-1}\text{cm}^{-1}$ ) was recorded following the decrease in its concentration photometrically at 290 nm. The reaction started after adding 20  $\mu\text{L}$  of the enzyme extract to 180  $\mu\text{L}$  of the reaction mix containing 1 mM  $\text{H}_2\text{O}_2$  and 250  $\mu\text{M}$  ascorbic acid in 55.56 mM  $\text{KH}_2\text{PO}_4$  (pH 7.0). The reaction was started by mixing 180  $\mu\text{L}$  reaction mix with 20  $\mu\text{L}$  enzyme and was followed for 5 min.

### 3.3.6.4. Glutathione reductase, GR (EC 1.6.4.2)

GR activity was determined after Zhang and Kirkham (1996). The reaction was initiated by adding 10  $\mu\text{L}$  of the enzyme extract to 190  $\mu\text{L}$  of a reaction mixture containing 1 mM oxidized glutathione (GSSG) (Fluka, Steinheim, Germany) and 2 mM NADPH in 100 mM Tris-HCl buffer (pH 7.5) with 0.1 mM EDTA. The reduction of glutathione disulphide (GSSG) to the sulfhydryl form glutathione (GSH) (Fig. 7) was measured by monitoring the consumption in NADPH at a wavelength of 340 nm ( $\epsilon = 6.22 \text{ mM}^{-1}\text{cm}^{-1}$ ).



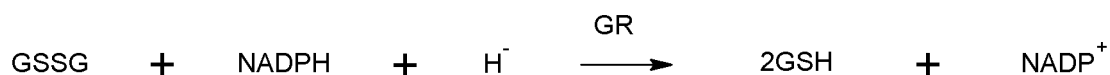


Figure 7: Reduction of glutathione disulphide (GSSG) to the sulfhydryl form glutathione (GSH) by the enzyme glutathione reductase (GR). GR activity can be determined photometrically monitoring the consumption in NADPH.

### 3.3.6.5. Proteomics analyses

Ultra-pure deionized water with a conductivity of 0.055  $\mu\text{S}/\text{cm}$  and total organic carbon of 2 ppb was produced on demand from a GenPure (TKA, Niederelbert, Germany) system equipped with a UV lamp, an internal 0.1 micron ultrafilter and a 0.45  $\mu\text{m}$  end filter. Modified trypsin was purchased from Promega (Mannheim, Germany) and was prepared using the company's own reconstitution solution and protocol, and was heat-activated for 15 min at 37  $^{\circ}\text{C}$  prior to use. Ammonium hydrogen carbonate ( $\geq 98\%$  Ph. Eur.), 1,4-dithiothreitol ( $\geq 99\%$  p. A.), trifluoroacetic acid (for peptide synthesis), acetone ( $\geq 99.9\%$ ) acetonitrile with 0.1% formic acid (LC-MS grade) and water with 0.1% formic acid (LC-MS grade) were purchased from Carl Roth (Karlsruhe, Germany). Iodoacetamide (BioUltra) was purchased from Sigma (Taufkirchen, Germany).

Total protein was measured on a Roche c701 clinical chemical analyser (Mannheim, Germany), using the Biuret method. All chemicals were used without further purification.

Medium samples were centrifuged at 17,000 x g for 10 min at 4  $^{\circ}\text{C}$ . To 15 mL supernatant were added 13.5 mL of acetone. After mixing, the sample was stored at -20  $^{\circ}\text{C}$  for one hour. The sample was then centrifuged at 17,000 x g for 10 min at 4  $^{\circ}\text{C}$  and the supernatant was discarded. The pellet was resuspended in 900  $\mu\text{L}$  acetone and was transferred to a 1.5 mL plastic tube. After centrifuging at 17,000 x g for 10 min at 4  $^{\circ}\text{C}$ , the supernatant was carefully aspirated. The remaining pellet was dried at ambient temperature overnight.

The pellet was taken up with 100  $\mu\text{L}$   $\text{NH}_4\text{HCO}_3$  (100 mM) and then reduced with 5  $\mu\text{L}$  DTT (200 mM in 100 mM  $\text{NH}_4\text{HCO}_3$ ) for 20 min at 90 °C, shaken at 300 rpm, in an Eppendorf Thermomixer C (Eppendorf, Hamburg, Germany). This was followed by cysteine-S-alkylation via the addition of 10  $\mu\text{L}$  iodoacetamide (500 mM in 100 mM  $\text{NH}_4\text{HCO}_3$ ) and was shaken for 1 hour at 300 rpm in the dark. An additional reduction was then performed by adding 20  $\mu\text{L}$  of the above DTT solution followed by shaking for 30 min at 300 rpm at ambient temperature. The sample was digested at 37 °C overnight in the dark with shaking (300 rpm) using 10  $\mu\text{L}$  of freshly prepared trypsin to every 2  $\mu\text{g}$  of total protein.

Proteomic experiments were conducted on a Bruker maXis 4g plus q-TOF equipped with a Captive Spray source (Bremen, Germany). The lock mass (Agilent G1982-85001, 1221.990637 m/z, Heilbronn, Germany) was applied directly onto the air intake filter. The system was calibrated before each analytical sequence using the enhanced quadratic algorithm with Agilent ESI L tuning mix (G1969-85000).

The source was operated in the positive ion mode using active focus and sum of intensities concerning line spectral calculation. The ionisation voltage was set to 1,400 V. Dry gas flow ( $\text{N}_2$ ) and dry temperatures were 3 L/min and 150 °C, respectively. Ion funnel 1 RF was operated at 400 Vpp and multipole RF was set to 400 Vpp. The quadrupole energy was set to 6 eV with low mass of 322 m/z. The transfer time and pre-pulse storage time were 120  $\mu\text{s}$  and 10  $\mu\text{s}$ , respectively. The TOF mass range was set to 50 – 2200 m/z with a sampling time of 0.5 sec. The auto MS/MS parameters were as follows: Inclusion m/z 300 – 1221.9 and 1224.5 – 1400. The collision cell was operated with a RF of 1200 Vpp and at different energies depending on the target mass and width which are listed in Table 12.

The LC system Ultimate 3000 (ThermoFisher Scientific, Dreieich, Germany) consisted of a binary nano high pressure gradient pump and a tertiary low pressure gradient loading pump, a column oven, a degasser for the loading pump and an autosampler. Mobile phase A was 90% acetonitrile/10% water (v/v) with 0.1% formic acid (v/v)

and mobile phase B was 100% water with 0.1% formic acid (v/v). The mobile phases were degassed via ultra sonication for 15 min prior to each sequence.

Table 12: Collision cell operating parameters during proteomics experiments.

Type	Mass	Width	Collision	Charge state
Base	300.0000	3.00	34.00	1
Base	500.0000	4.80	39.00	1
Base	1,000.0000	6.00	52.00	1
Base	2,000.0000	9.00	55.00	1
Base	300.0000	3.00	26.00	2
Base	500.0000	4.80	34.00	2
Base	1,000.0000	6.00	40.00	2
Base	2,000.0000	9.00	45.00	2
Base	300.0000	3.00	21.00	3
Base	500.0000	4.80	28.00	3
Base	1,000.0000	6.00	36.00	3
Base	2,000.0000	9.00	40.00	3

The column temperature was set to 40 °C, the injection volume was 5  $\mu$ L ( $\mu$ L pickup mode). The flow rate was 300 nL/min. The autosampler was equipped with a 20  $\mu$ L PEEK sample loop, a 15  $\mu$ L PEEK needle and the temperature was set at 6 °C. The pick-up fluid was the same as the trap column wash mobile phase. The trap column (C4 PepMap 300, 5  $\mu$ m, 300 Å, 300  $\mu$ m id x 5 mm) was washed for 4 min post injection at 30  $\mu$ L/min with a mobile phase consisting of 245 mL water, 5 mL acetonitrile and 125  $\mu$ L TFA (v/v/v).

Peptides were separated on an Acclaim PepMap® RSLC C18 nano column 75  $\mu$ m x 250 mm, 2  $\mu$ m, 100 Å using the following gradient: 98% B, 0-4 min, linear to 65% B at 50 min; linear to 2% B at 94 min, isocratic to 98% B at 104 min, stop at 120 min.

MS/MS data were imported into Protein Scape version 3.1. Mascot version 2.51 (Matrix Science, Boston, USA) was used to upload data to the SwissProt database using default search parameters from maXis\_allOrg (Bruker, Bremen) except that the peptide tolerance was set to 7 ppm, the MS/MS tolerance to 0.05 Da and FDR to 5%.

### 3.4. Analytical techniques

#### 3.4.1. Chemicals

Acetonitrile (HPLC grade), water with 0.1% formic acid (LC–MS grade), acetonitrile with 0.1% formic acid (LC–MS grade) were obtained from Carl Roth (Karlsruhe, Germany). Ultrapure water (MilliQ, Millipore Corporation) was used for sample preparation. Analytical standards of carbamazepine (CBZ), oxcarbazepine, carbamazepine-10,11-epoxide (CBZE), 10,11-dihydro-10-hydroxycarbamazepine (10-OH-CBZ), 3-hydroxycarbamazepine (3-OH-CBZ), 10,11-dihydro-10,11-dihydroxycarbamazepine (10,11-diOH-CBZ), acridine and acridone, (all  $\geq 97\%$  purity) were purchased from Sigma-Aldrich (Taufkirchen, Germany). L-Glutathione reduced ( $\geq 98.0\%$ ) and L-Cysteine (97%) were purchased from Sigma-Aldrich (Taufkirchen, Germany).

#### 3.4.2. In vitro synthesis of glutathione related metabolites

The conjugates 10,11-dihydro-10-hydroxy-11-glutathionyl-CBZ (CBZE-GSH) and 10,11-dihydro-10-hydroxy-11-cysteinyl-CBZ (CBZE-CYS) were synthesized chemically according to Bu and co-workers, 2005. Briefly, 80  $\mu\text{L}$  of CBZE were incubated with GSH or cysteine (5 mM) in 0.1 M potassium phosphate buffer (pH 7.4) for 2 h at 37 °C. Subsequently, samples were evaporated to dryness under  $\text{N}_2$  after mixing them with 2 volumes of acetonitrile. Residues were reconstituted in ultrapure water (MS grade) with 0.1% formic acid and stored at -20 °C before analysis.

#### 3.4.3. Extraction of carbamazepine and transformation products from plant tissues

For the extraction of CBZ and its metabolites, the plant tissue was homogenized with a glass mortar under liquid nitrogen and 0.5 g of the resulting powder was extracted in 1 mL of methanol 80% by vortexing for 1 min and sonicating for 10 min. Samples were then centrifuged at 13,000  $\times g$  for 10 min. The supernatants were transferred to a new tube and were evaporated to dryness in a centrifugal evaporator. The residues obtained were reconstituted in methanol 10% with the help of the pipette. Samples were frozen and stored at -20 °C until analysis.

#### 3.4.4. Sample preparation for HPLC and LC-QTOF-MS/MS analysis

Samples from culture media were centrifuged at 13,000 x g for 10 min, and the pellet containing cells and debris was discarded. Prior to HPLC or LC-QTOF-MS/MS analysis, samples from nutrient media or plant extracts were subjected to protein precipitation. Samples were mixed with 45 mg/mL 5-Sulfosalicylic acid (99,9%, Sigma-Aldrich, Taufkirchen, Germany) (1:10, v:v), vortexed briefly and centrifuged for 5 min at 13,000 x g. The protein-free supernatant was used for CBZ quantification or metabolite identification after filtration through a 0.22 µm pore size PVDF filter. Supernatants were stored at - 20 °C for further analyses.

#### 3.4.5. Quantification of CBZ by HPLC

CBZ concentration in nutrient solutions or in plant tissue was determined by HPLC (Varian ProStar 410). All samples were prepared in triplicate. CBZ and their metabolites were separated on a C18 ProntoSIL Spheribond ODS 2 (5 µM, 125 \* 4 mm) column under reversed phase conditions, applying a linear gradient of eluents. Mobile phases consisted of 0.1% aqueous trifluoroacetic acid (TFA) (solvent A) and acetonitrile with 0.1% TFA (solvent B) run at a constant flow rate of 0.85 mL/min (Table 13).

Table 13: HPLC solvent gradient used for quantification of carbamazepine.

Time (min)	% Solvent A	% Solvent B
0	95	5
2.5	95	5
17.5	5	95
21	5	95
23	95	5

Detection of CBZ was at 210 nm using a UV/vis detector (Varian ProStar 410). Identification of CBZ was performed by comparison of the spectra and the retention time of an authentic standard supplied by Sigma-Aldrich. Chromatograms were analyzed using MS Workstation version 6.9.3 (Varian). Concentration of CBZ in nutrient media or in plant tissue was determined

using a calibration curve performed with a CBZ analytical standard (99.9%, Sigma-Aldrich, Taufkirchen, Germany) (Fig. 8).

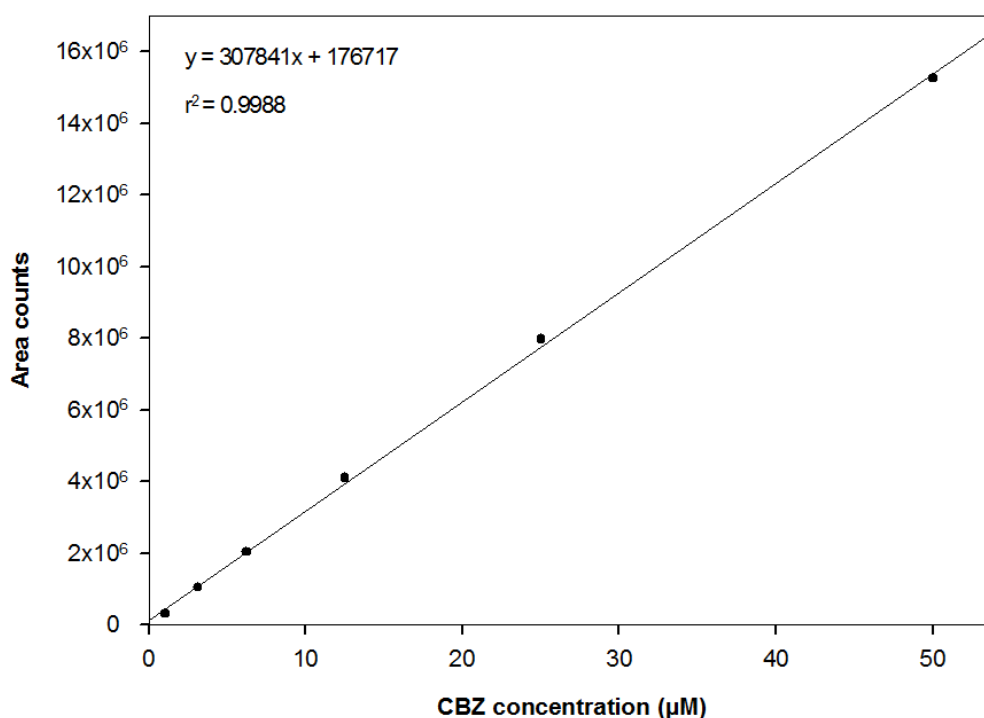


Figure 8: Standard curve for the quantification of carbamazepine (CBZ) in nutrient media and plant extracts.

### 3.4.6. LC-QTOF-MS/MS analysis for TPs identification

LC-QTOF-MS/MS experiments were conducted on an Ultimate 3000 LC system (ThermoFisher) coupled to an ultra-high resolution maXis 4 g plus QTOF mass spectrometer (Bruker) equipped with an electrospray source. The TOF-MS was operated in positive polarity mode with active focus under the following conditions: capillary voltage, 5,000 V; nitrogen dry gas temperature, 225 °C; dry gas flow, 10 L/min; nebulizer pressure, 2 bar. The TOF-MS was calibrated daily with ESI-L tuning mix (Agilent) using the enhanced quadratic algorithm. MS scans were recalibrated using Hexakis (<sup>1</sup>H, <sup>1</sup>H, <sup>4</sup>H-hexafluorobutyloxy) phosphazine (Agilent) as a lock mass. The LC conditions were as follows: the column was a Phenomenex Synergi HYDRO-RP column (C18, polar endcapped; particle size 4 µm; 50×2.00 mm). CBZ and its metabolites were separated using a linear gradient of eluents: buffer A (H<sub>2</sub>O, 0.1% formic acid) and buffer B (acetonitrile, 0.1% formic acid). Elution gradient: 0–2 min 97% buffer A (isocratic); 2–10 min 95% buffer B (linearly increasing); 10–12 min 95% buffer B (isocratic); 12–12.5 min 97% buffer

A (linearly decreasing); 12.5–17 min 97% A (isocratic) (Table 14). The flow rate was 0.3 mL/min. All solvents used for LC–MS were of the highest grade available.

Table 14: LC solvent gradient used for LC-QTOF-MS/MS analysis of carbamazepine and its transformation products.

Time (min)	% Solvent A	% Solvent B
0	97	3
2	97	3
10	5	95
12	5	95
12.5	97	3
17	97	3

#### 3.4.7. Identification of carbamazepine transformation products

TPs were hypothesized using the software Compound Crawler (Bruker, Bremen, Germany). Only compounds with molecular ions at  $m/z$  within  $\pm 10$  ppm of the exact molar mass were considered. TPs were identified after LC-QTOF-MS/MS separation using different collision energies. Fragmentation patterns were compared to those obtained from analytical standards. When analytical standards were not available, fragmentation patterns were predicted using the competitive fragmentation model by Allen et al., 2015. Only TPs with a fragmentation pattern matching standards or predicted patterns were considered.

### 3.5. Statistical treatment of data

Statistical treatment of the data obtained from enzyme activities, CBZ removal and TPs accumulation in liquid media were performed using the software MS Excel (Microsoft, USA). The differences between means and/or the effect of treatment were determined by Student t-tests or one-way analysis of variance.

## 4. Results

To answer the questions addressed in this study, results have been divided in two chapters. The first part emphasizes conditions similar to those found in CWs, investigating the potential of reed plants to remove CBZ from polluted waters and the identity and characteristics of the endophytic community of exposed plants. In a second part, a mechanistic study sheds light on interactions between isolated endophytic bacteria and plant roots exposed to the pharmaceutical using a horseradish HR culture as model system.

### 4.1. Carbamazepine removal by reed plants and its endophytic bacteria from nutrient solutions: a view on close-to-real conditions in CWs

#### 4.1.1. Carbamazepine removal from nutrient media by *Phragmites australis*

The capacity of *P. australis* to remove CBZ was investigated under semi-hydroponic conditions. Adult plants were grown individually in pots containing perlite and Hoaglands solution. At  $t=0$ , plants were transferred to a solution containing 5 mg/L of CBZ (21.16  $\mu\text{M}$ ). Aliquots from the nutrient solution were taken after 0, 1, 4 and 9 days of incubation and CBZ concentration was determined by HPLC.

The initial CBZ concentration measured was  $17.84 \pm 0.30 \mu\text{M}$  in the control pots and  $17.52 \pm 0.41 \mu\text{M}$  in pots containing plants. The difference observed between expected and real concentration can be attributable to the rapid adsorption of the compound to the walls of pots and perlite. Rapid uptake of the substance was observed within 24 hours (Fig. 9). Whereas in controls without plants 5% of the compound was lost, 35% of CBZ disappeared from pots with plants after one day. The initial uptake rate decreased after 4 and 9 days, but still significant amounts were taken up into the plant. After 4 days, 66% were removed, and after 9 days only 10% were left, whereas the concentration in the control pots remained constant.



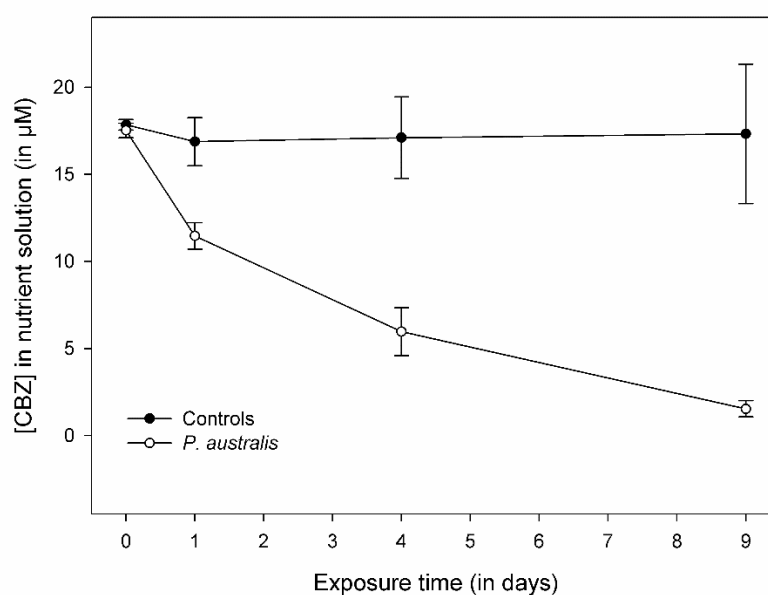


Figure 9: Carbamazepine (CBZ) removal from the nutrient solution by *Phragmites australis*. Adult reed plants were exposed to 21  $\mu\text{M}$  CBZ for 9 days. Pots without plants but containing perlite were used as control. Data are means  $\pm$  SD of three replicates.

#### 4.1.2. Oxidative stress and enzymatic defence responses in *Phragmites australis*

No visual signs of toxicity were detected in *P. australis* plants exposed to CBZ during the incubation time. The activity of the ROS scavenging enzymes GR, POX APOX in plant cytosolic protein extracts was determined by photometric assays. Adult plants were grown in semi-hydroponic conditions in pots containing nutrient solution spiked with 100  $\mu\text{M}$  CBZ in ethanol for 48 h. Pots containing nutrient solution and spiked with the same volume of ethanol were used as controls. Plants were harvested after 24 and 48 h and cytosolic enzymes were extracted from leaves, roots and rhizomes.

The activity of GR in treated plants was slightly higher than in control plants in all tissues after 48 h of incubation with an increase of 47% in leaves, 81% in rhizomes and 10% in roots (Fig. 10). After 24 h of treatment, an induction of GR activity was observed only in leaves, with a two-fold increase. In rhizomes and roots, GR activity was lower in treated plants than in control plants after 24 h, (37% and 59% lower respectively).

Dynamics of POX activity was similar to GR activity in leaves and rhizomes (Fig. 10). An induction of 70% was observed in leaves of treated plants after 24 h of exposure. In these tissues, POX activity decreased after 48 h in treated plants matching values of control plants. In rhizomes, POX activity in treated plants was depleted 23% after 24 h of exposure whereas an induction of 28% in the enzyme activity was observed after 48 h. In roots, the enzyme activity remained almost equal in treated and control plants after 24 h, but decreased a 37% in treated plants after 48 h.

APOX activity was 60% higher in leaves of treated plants than in controls all along the treatment. The opposite trend was observed in root tissues, where activity decreased

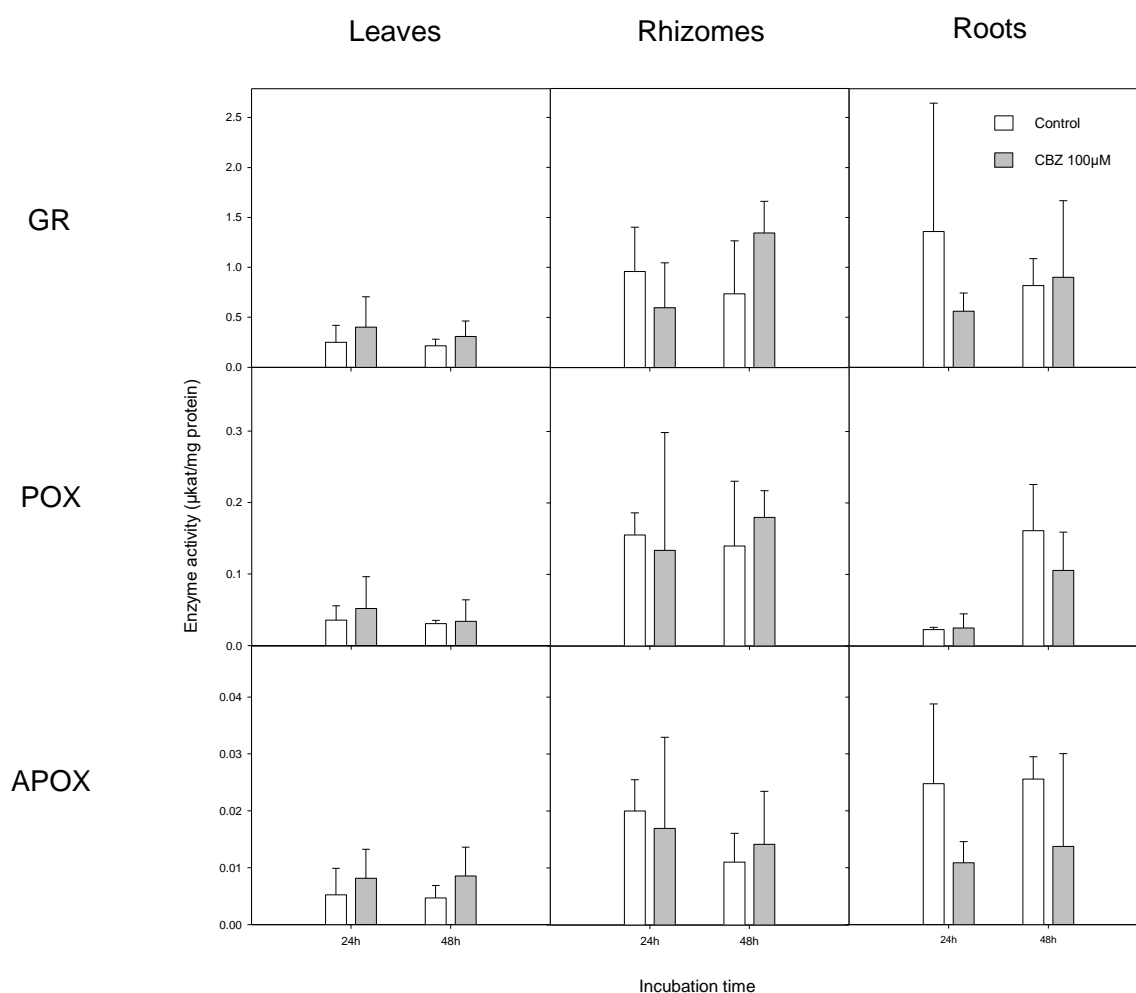


Figure 10: Antioxidant enzyme activities in *Phragmites australis* exposed to carbamazepine (CBZ). Activities of the ROS-scavenging enzymes glutathione reductase (GR), peroxidase (POX) and ascorbate peroxidase (APOX) in cytosolic extracts of *Phragmites australis* exposed to 100 µM CBZ for 48 h. Data are means  $\pm$  SD of three biological replicates.

56% after 24 h and 47% after 48 h of exposure to CBZ. In rhizomes, activity was slightly lower in treated plants after 24 h, but an induction of 27% was observed after 48 h.

GST activity was measured in cytosolic extracts from leaves, rhizomes and roots of *P. australis* plants exposed to 100  $\mu\text{M}$  CBZ after 24 and 48 h using CDNB, pNBC and fluorodifen as substrates in the assays (Fig. 11). In general GST activity was higher in rhizomes than in leaves and roots.

A small induction of GST activity was observed in leaves of treated plants all along the treatment when CDNB was used as substrate, with increases of 16% after 24 h and 28% after 48 h. In rhizomes, GST activity in treated plants decreased after 24 h and increased 84% of the control plants after 48 h. In root tissues, activity in treated plants remained below control values after 24 h and recovered after 48 h.

Dynamics of GST-pNBC was similar to GST-CDNB in rhizomes, where an induction in treated plants was observed only after 48 h. In leaves, activity was 21% lower in treated plants after 24 h but increased 42% after 48 h. In roots of control plants, almost no activity was detected. When CBZ was applied to the medium, GST-pNBC could be detected in treated plants with values of 0.025 and 0.015  $\mu\text{kat}/\text{mg}$  protein after 24 and 48 h respectively.

When fluorodifen was used as substrate, GST activity was found to be induced after CBZ treatment in all tissues and time points except in roots after 48 h. In leaves, activity increased 86% after 24 h and 59% after 48 h. In rhizomes, the highest induction was observed after 48 h with a 190% higher GST activity in treated plants. In roots, activity was 120% higher after 24 h and 14% lower after 48 h.

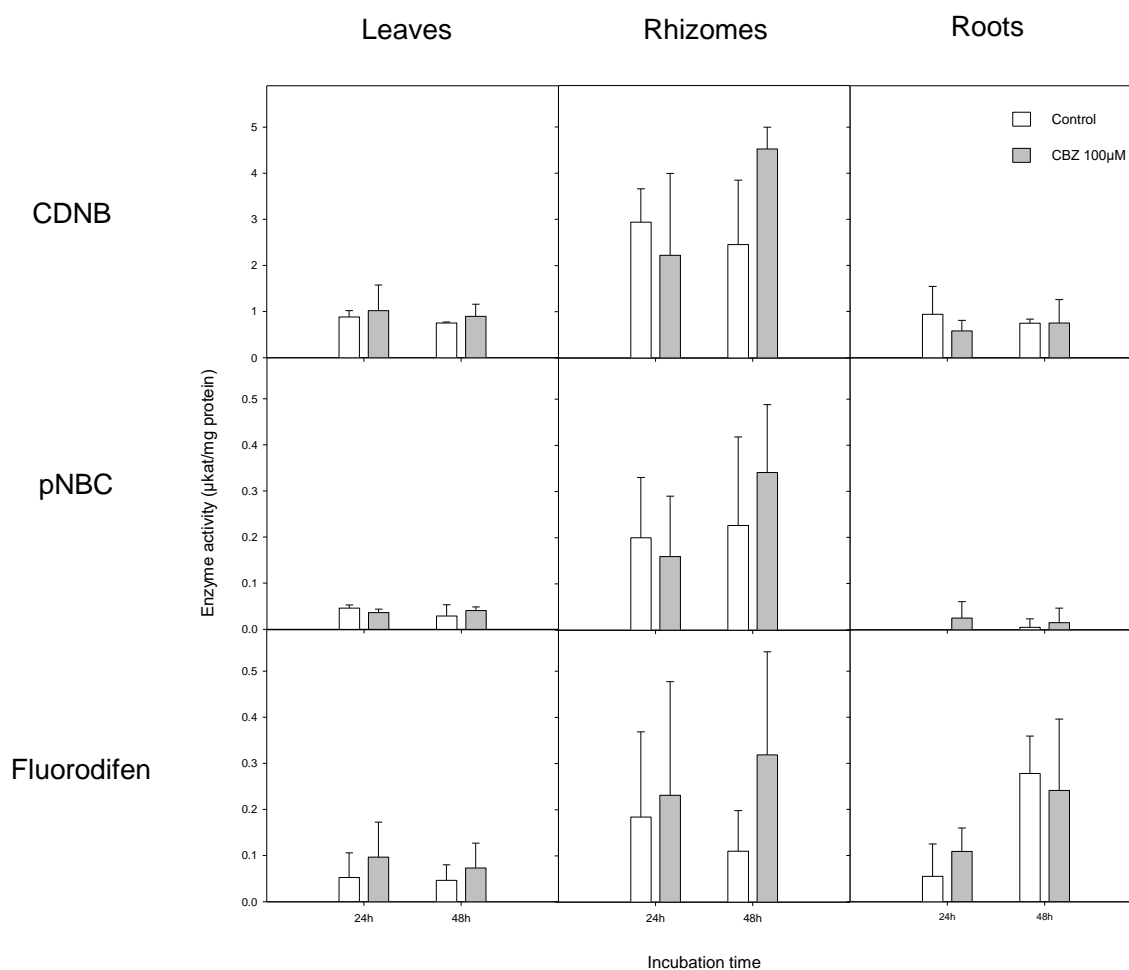


Figure 11: Specific glutathione-S-transferases (GST) activity in *Phragmites australis* exposed to carbamazepine (CBZ). GST activity was measured in leaves, rhizomes and roots of plants exposed to 100 µM CBZ after 24 and 48 h for three different substrates: CDNB, pNBC and fluorodifen. Data are means  $\pm$  SD of three biological replicates.

## 4.2. Microbial communities associated to *Phragmites australis*

Plants and their microbiota form an inseparable and unique entity known as holobiont. Microorganisms inhabiting inside and outside plant tissues (endosphere and ectosphere) contribute to some biological functions such as plant nutrition or resistance to biotic and abiotic stresses (Vandenkoornhuyse et al., 2015). Therefore, the impact of the microbiota associated with *P. australis* on CBZ uptake and plant fitness was investigated using cultivation approaches.

#### 4.2.1. Rhizome-associated microbial communities

Physiological characterization of rhizoplane and root-endosphere-associated bacterial communities was performed using the BIOLOG GEN III microplate. Inocula were prepared from fresh rhizomes harvested in the greenhouse and after incubation in R2A medium. Rhizomes used for the preparation of the endophytic inocula were first surface sterilized in a solution of sodium hypochlorite. Biochemical characteristics concerning assimilation of different carbon sources and sensitivity to several chemicals, antibiotics or acidic conditions were determined. Among the 94 physiological traits, differences between rhizoplane and endophytic communities could be observed in 18 of them (Table 15).

The endophytic community inhabiting reed rhizomes could assimilate a wider range of carbon sources than the community in the rhizoplane. Only in the cases of  $\alpha$ -D-lactose and L-arginine, this was reversed. Both communities could assimilate the rest of the 71

Table 15: Differential biochemical characteristics of rhizoplane and endosphere rhizome-associated microbial communities in *Phragmites australis*.

	Rhizoplane	Endosphere
<b>Assimilation of</b>		
$\alpha$ -D-Lactose	+	-
Methyl pyruvate	-	+
D-Arabitinol	-	+
D-Lactic acid methyl ester	-	+
$\alpha$ -Hydroxybutyric acid	-	+
L-Arginine	+	-
$\alpha$ -Ketobutyric acid	-	+
D-Fucose	-	+
Glucuronamide	-	+
Acetoacetic acid	-	+
D-Malic acid	-	+
Propionic acid	-	+
D-Turanose	-	+
Acetic acid	-	+
Stachyose	-	+
Formic acid	-	+
<b>Growth on</b>		
pH5	+	-
Potassium tellurite	+	-

carbon sources except L-galacturonic acid, 3-methyl glucose, D-aspartic acid and N-acetyl neuremic acid were no growth was observed (Table 16). In contrast to its endophytic homologous, rhizoplane community could grow in presence of potassium tellurite as well as in acidic conditions (pH 5). Both communities grew in 1% NaCl, 1% sodium lactate, guanidine HCl, tetrazolium violet, D-serine, Niaproof 4, tetrazolium blue, and pH 6 (Table 16). They were resistant to the antibiotics troleandomycin, linconmycin, vancomycin and rifamycin Sv, but sensitive to 4% and 8% NaCl, nalidixic

Table 16: Biochemical characteristics conserved in endophytitic and rhizoplane rhizome-associated microbial communities of *Phragmites australis*.

			Rhizoplane	Endosphere			
<b>Assimilation of</b>							
{ D-Raffinose α-D-Glucose D-Sorbitol Gelatin Pectin Sucrose Tween 40 { Dextrin D-Mannose D-Mannitol Glycyl-L-proline D-Galacturonic acid γ -Aminobutyric acid D-Maltose D-Mellibiose D-Fructose L-Alanine } { L-Galacturonic acid 3-Methyl glucose }	D-Threulose	α-Ketoglutaric acid	}	}			
	β-Methyl-D-glucoside	p-Hydroxyphenylacetic acid					
	D-Galactose	N-Acetyl-β-D-mannosamine					
	Myoinositol	L-Fucose					
	D-Gluconic acid	D-Fructose 6PO <sub>4</sub>					
	D-Lactic acid	L-Histidine					
	β-Hydroxy-D,L- butyric acid	Mucic acid					
	D-Cellobiose	N-Acetyl-D-galactoseamine					
	D-Salicin	L-Rhiamnose					
	Glycerol	L-Pyroglutamic acid					
	L-Aspartic acid	Quinic acid					
	D-Glucuronic acid	L-Malic acid					
	Citric acid	Inosine					
	Gentobiose	D-Serine, L-serine					
	N-Acetyl-D-glucoseamine	D-Saccharic acid					
	D-Glucose 6 PO <sub>4</sub>	Bromo-succinic acid					
	L-Glutamic acid						
	D-Aspartic acid	N-Acetyl neuremic acid			-	-	
	<b>Growth on</b>						
	{ 1% NaCl 1% Sodium lactate Guanidine HCl Tetrazolium violet }	D-Serine			Troleandomycin	}	}
Niaproof 4		Linconmycin					
Tetrazolium blue		Vancomycin					
pH 6		Rifamycin Sv					
{ 4% NaCl 8% NaCl Nalidixic acid }	Aztreonam	Sodium butyrate	}	}			
	Fusidic acid	Sodium bromide					
	Lithium chloride	Minocycline					

acid, aztreonam, fusidic acid, lithium chloride, sodium butyrate, sodium bromide and the antibiotic minocycline.

#### 4.2.2. Isolation of endophytic bacteria

Extracts were prepared from roots and rhizomes of healthy plants after surface sterilization. No colonies grew on plates inoculated with the last rinsing water, indicating a good efficiency of the sterilization phase. Serial dilutions of these extracts were plated on PDA and R2A agar media.

Colonies showing different morphotypes grew on the agar plates after some days of incubation at room temperature. Distinct morphotypes were identified based on the form, elevation, margins, surface, opacity and pigmentation of their colonies. To ensure purity and viability, colonies of each morphotype were selected and sub-cultured in their corresponding medium. After three subcultures, 41 isolates corresponding to distinct morphotypes were obtained and further characterized. Total DNA was extracted from pure cultures and used to amplify bacterial 16S rRNA encoding genes. After sequencing of the fragments, all morphotypes could be classified into different taxonomic groups, and finally 22 redefined distinct species could be identified (Table 17).

Phylogenetic analysis of the sequences revealed that most of the isolates belonged to *Proteobacteria* (72.7%, Fig. 12 and 13). Other isolates were affiliated with *Bacteroidetes* (13.6%), *Actinobacteria* (9.1%) and *Firmicutes* (4.5%). The genus *Pseudomonas* ( $\gamma$ -*Proteobacteria*) was represented by the highest number of identified species (22.7% of the total of isolates) followed by the genus *Rhizobium* ( $\alpha$ -*Proteobacteria*) with 13.6% and *Acidovorax* ( $\beta$ -*Proteobacteria*) with 9.1%.

Table 17: Taxonomic identification of endophytic bacteria isolated from *Phragmites australis* plants exposed to carbamazepine based on the 16S rDNA region sequence compared to validated type strain sequences deposited in the EzTaxon database.

Isolate	Plant tissue	Closest match	Similarity	Group
Cb35	Roots	<i>Achromobacter mucicolens</i> LMG 26685(HE613446)	100,0	$\beta$ -Proteobacteria
Cb52	Roots, rhizomes	<i>Acidovorax radialis</i> N35 (AFBG01000030)	98,87	$\beta$ -Proteobacteria
Cb22	Roots	<i>Acidovorax temperans</i> CCUG 11779 (AF078766)	99,49	$\beta$ -Proteobacteria
Cb2	Stems	<i>Aquabacterium citratiphilum</i> B4 (AF035050)	98,64	$\beta$ -Proteobacteria
Cb59	Roots	<i>Candidatus Rhizobium massilae</i> 90A (AF531767)	99,14	$\alpha$ -Proteobacteria
Cb69	Roots, rhizomes	<i>Cedecea davisae</i> DSM 4568 (ATDT01000040)	100,0	$\gamma$ -Proteobacteria
Cb66	Rhizomes	<i>Chitinophaga sancti</i> NBRC 15057 (AB078066)	98,87	Bacteroidetes
Cb47	Roots, rhizomes	<i>Chryseobacterium taeansense</i> PHA3-4 (AY883416)	98,69	Bacteroidetes
Cb55	Rhizomes	<i>Diaphorobacter nitroreducens</i> NA10B (AB064317)	99,86	$\beta$ -Proteobacteria
Cb56	Rhizomes	<i>Eiseniicola composti</i> YC06271 (FJ791048)	98,17	$\beta$ -Proteobacteria
Cb17	Roots	<i>Flexibacter aurantiacus</i> ATCC 23107 (M62792)	99,78	Bacteroidetes
Cb4	Roots	<i>Kocuria palustris</i> DSM 11925 (Y16263)	99,93	Actinobacteria
Cb62	Rhizomes	<i>Leifsonia lichenia</i> strain 2Sb (AB278552)	100,00	Actinobacteria
Cb46	Roots, rhizomes	<i>Microvirgula aerodenitrificans</i> DSM 15089 (JHVK01000054)	99,86	$\beta$ -Proteobacteria
Cb36	Roots	<i>Pseudomonas arsenicoxydans</i> VC-1 (FN645213)	99,7	$\gamma$ -Proteobacteria
Cb65	Roots, rhizomes	<i>Pseudomonas corrugata</i> ATCC 29736 (D84012)	99,86	$\gamma$ -Proteobacteria
Cb31	Roots	<i>Pseudomonas lini</i> CFBP 5737 (AY035996)	100,0	$\gamma$ -Proteobacteria
Cb49	Rhizomes	<i>Pseudomonas moorei</i> RW10 (AM293566)	100,00	$\gamma$ -Proteobacteria
Cb61	Roots, rhizomes	<i>Pseudomonas veronii</i> CIP 104663 (AF064460)	100,00	$\gamma$ -Proteobacteria
Cb54	Rhizomes	<i>Rhizobium daejeonense</i> KCTC 12121 (AY341343)	97,69	$\alpha$ -Proteobacteria
Cb58	Rhizomes	<i>Rhizobium radiobacter</i> ATCC 19358 (AJ389904)	100,00	$\alpha$ -Proteobacteria
Cb1	Stems	<i>Staphylococcus epidermidis</i> ATCC 14990 (L37605)	99,89	Firmicutes

Other members belonging to the phylum of *Proteobacteria* were identified as *Achromobacter*, *Aquabacterium*, *Diaphorobacter*, *Eiseniicola* and *Microvirgula* ( $\beta$ -*Proteobacteria*) and *Cedecea* ( $\gamma$ -*Proteobacteria*) representing 4.5% of the total of isolates. The rest of the isolates (54.6%) were identified as members of different genera distributed within *Actinobacteria* (*Leifsonia*, *Kocuria*), *Bacteroidetes* (*Chryseobacterium*, *Flavobacterium* and *Chitinophaga*) and *Firmicutes* (*Staphylococcus*), each of them representing 4.5% of the culturable community.

Differences in the genotypic composition of the isolated bacterial community were observed when using PDA and R2A as isolation media. The diversity of cultivable bacteria was higher when using R2A medium (Fig. 14). Bacteria affiliated to 6 distinct classes were identified in R2A agar plates. In PDA agar plates, only 4 different classes



were isolated. Bacteria belonging to *Actinobacteria*, *Bacteroidetes*,  $\beta$ -*Proteobacteria* and  $\gamma$ -*Proteobacteria* were identified in both media, but *Firmicutes* and  $\alpha$ -*Proteobacteria* classes were associated only to R2A medium.

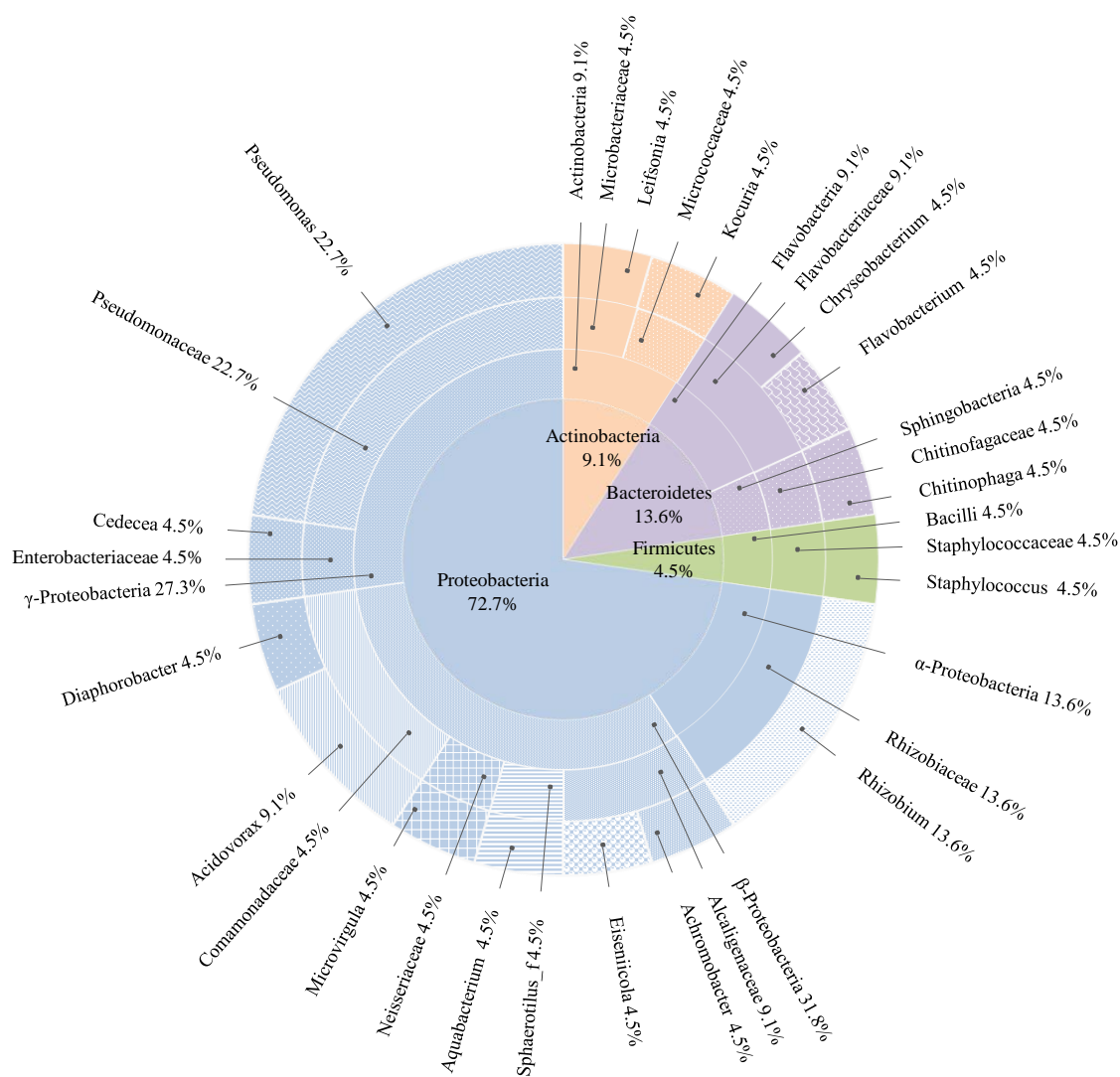


Figure 12: Taxonomic breakdown of 16S rDNA gene sequences of total cultivable endophytic bacterial community composition isolated from *Phragmites australis* plants exposed to 21  $\mu$ M of carbamazepine for 9 days. The central pie shows phylum distribution in percentages and each outer ring breaks progressively down to lowest taxonomic levels (class, family, genera) (Adapted from Sauvêtre and Schröder, 2015).

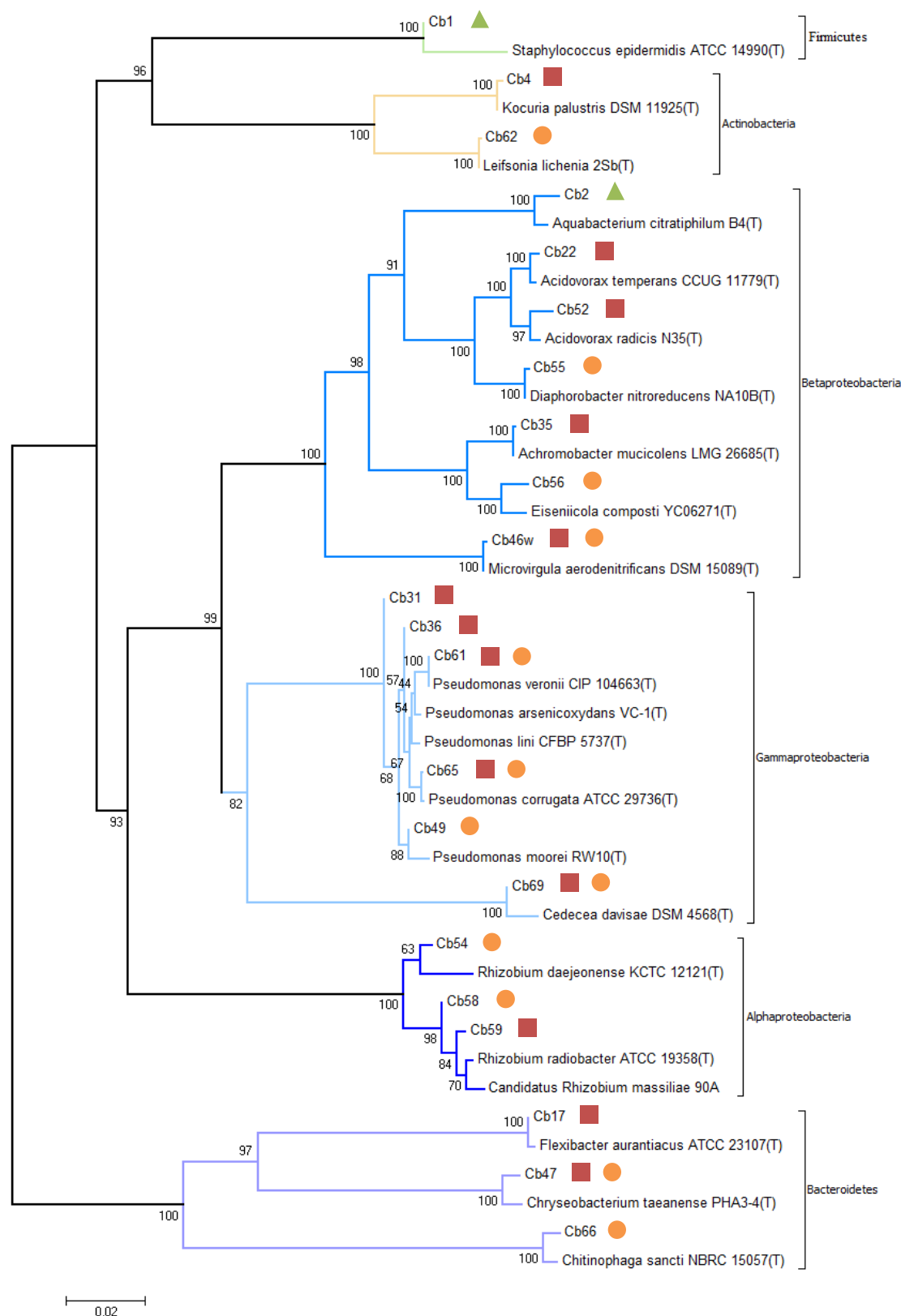


Figure 13: Evolutionary relationships of isolates from Reed plants exposed to carbamazepine based on 16S rDNA sequences obtained from all isolates and closely related sequences from EzTaxon database. The tree is drawn to scale, with branch lengths in the same units as those of the evolutionary distances used to infer the phylogenetic tree. The percentage of replicate trees in which the associated taxa clustered together in the bootstrap test (2,000 replicates) is shown next to the branches. The evolutionary distances were computed using the Maximum Composite Likelihood method. Endophytic bacteria isolated from stems (▲), rhizomes (●) and roots (■) (Sauvêtre and Schröder, 2015).

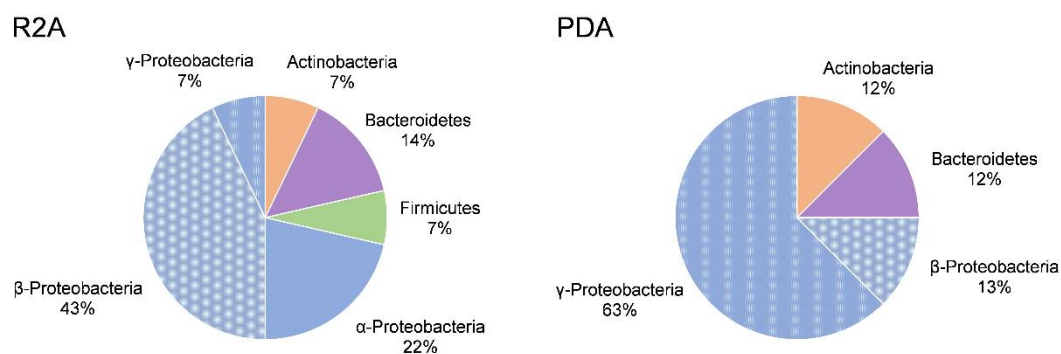


Figure 14: Genotypic characterization of the cultivable bacterial population of *Phragmites australis* exposed to 21 µM CBZ, grown in two different agar media: PDA and R2A.

A second classification was done taking in account the plant tissue. The taxonomic compositions of endophytic bacteria isolated from roots and from rhizomes are represented in Fig. 15. A similar distribution was found in both tissues, presenting small differences at species level.

Endophytic cultivable community associated to roots were predominantly represented by *Proteobacteria* with 72.7% of the isolates (Fig 15 A). The rest of the isolates belonged to *Bacteroidetes* (18.2%) and *Actinobacteria* (9.1%). No isolates from *Firmicutes* phylum were found in root compartments. The genera *Pseudomonas* and *Acidovorax* represented the higher number of species with 36.4% and 18.2% respectively. The rest of the root cultivable endophytic community were identified as *Kocuria*, *Chryseobacterium*, *Flavobacterium*, *Rhizobium* and *Achromobacter* with 9.1% of the total isolates each of them.

Concerning the endophytic bacteria associated to rhizomes, a similar distribution of phyla was found, with 76.9% of the isolates belonging to *Proteobacteria*, 15.4% to *Bacteroidetes* and 7.7% to *Actinobacteria* (Fig 15 B). The genera *Pseudomonas* and *Rhizobium* represented the highest number of identified species with 23.1% and 15.4% respectively. The rest of the rhizome endobacteria were identified as *Leifsonia* (*Actinobacteria*), *Chitinophaga* and *Chryseobacterium* (*Bacteroidetes*), *Acidovorax*, *Diaphorobacter*, *Eiseniicola* and *Microvirgula* (*β-Proteobacteria*) and *Cedecea* (*γ-Proteobacteria*) with a representation of 7.7%. The genera *Achromobacter*, *Aquabacterium*, *Flavobacterium* and *Kocuria* were lacking among these isolates.

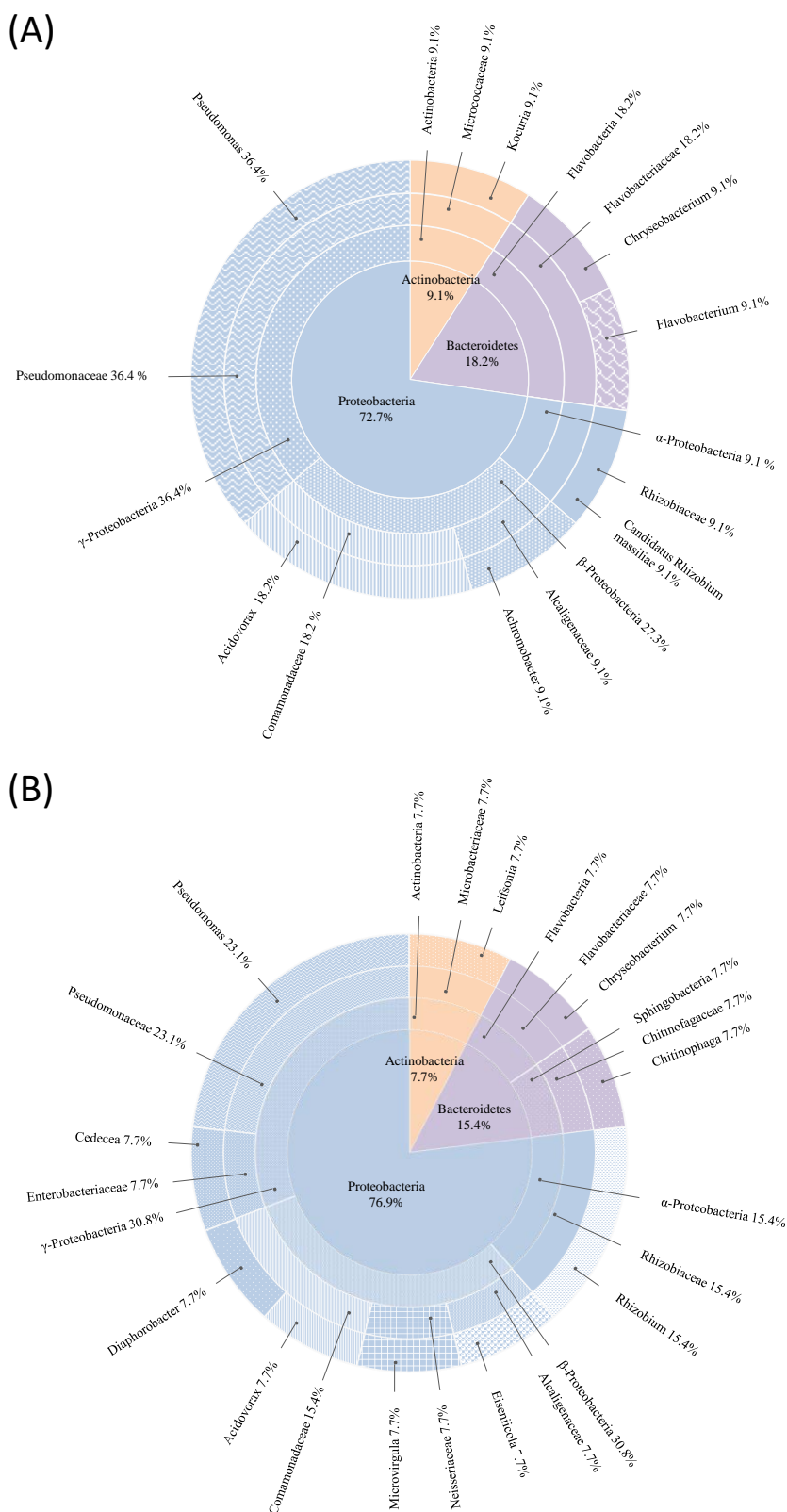


Figure 15: Taxonomic breakdown of 16S rDNA gene sequences of total (A) and rhizomes (B) culturable endophytic bacterial community composition isolated from *Phragmites australis* plants exposed to 21  $\mu$ M of carbamazepine for 9 days. The central pie shows phylum distribution in percentages and each outer ring breaks progressively down to lowest taxonomic levels (class, family, genera) (Adapted from Sauv tre and Schr der, 2015)

### 4.2.3. Carbamazepine removal from liquid medium by endophytic bacteria

Bacterial isolates were tested for CBZ removal from liquid media. Strains were grown for 5 days in small liquid LB-Lennox/10 cultures supplemented with 50  $\mu$ M CBZ. Slight differences in CBZ removal were observed between the tested strains (Fig. 16). Few strains could remove the compound from the growth medium, with rates ranging from 0.1% to 2.4%. *Rhizobium daejeonense* ( $\alpha$ -Proteobacteria) was the strain showing the highest removal rate with 2.45%, followed by *Chryseobacterium taeaneense* (Bacteroidetes) with 2.18% and *Achromobacter mucicolens* and *Diaphorobacter nitroreducens* ( $\beta$ -Proteobacteria) with 1.93% and 1.78% respectively. Additionally, *Pseudomonas moorei*, one isolate affiliated to *Pseudomonaceae* family ( $\gamma$ -Proteobacteria) showed a weak removal of the pharmaceutical (0.12%).

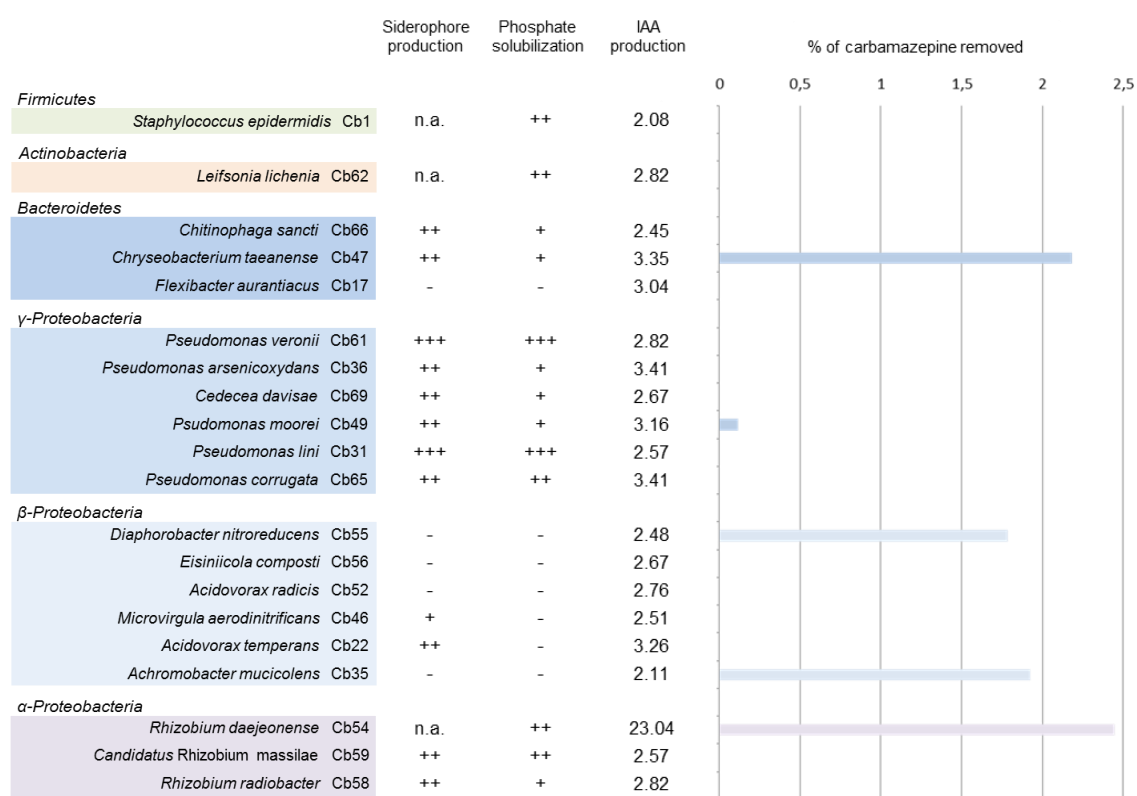


Figure 16: Carbamazepine (CBZ) removal from liquid cultures by endophytic bacteria associated to *P. australis* and plant growth promoting traits. Bacterial clones are grouped by taxonomic groups (class). Siderophore production and phosphate solubilization are represented by +, ++ or +++. Production of IAA is indicated in  $\mu$ g/mL. The percentage indicates the removal capacity after 5 days in LB-Lennox/10 medium supplemented with 50  $\mu$ M CBZ (Adapted from Sauv tre and Schr der, 2015).

#### 4.2.4. Plant growth promoting characteristics

The capacity of the isolates for phosphate solubilization, siderophore production, and auxin production were determined following qualitative or quantitative methods. 90% of the isolates could produce indoleacetic acid, whereas 59% of them could solubilize mineral phosphate and 54% secreted siderophores into the growth medium (Fig. 16). All isolates had at least one of the PGP traits tested and 45% of the isolates presented the three PGP traits tested. Most of these isolates belong to *γ-Proteobacteria*, *α-Proteobacteria* and *Bacteroidetes*. Several isolates had two of the three PGP traits tested. From them, 59% could solubilize phosphate and produce IAA and 45% could produce siderophores and solubilize phosphate.

Strains producing IAA were present in all plant tissues, with values ranged between 2.08 and 3.41 μg/mL in the most of the cases. All strains isolated from rhizomes could produce IAA and among them, *Rhizobium daejeonense* showed an exceptional high production (23.04 μg/mL). Siderophore producers were equally distributed in root as well as in rhizomes (69% of root and 67% of rhizomes isolates could produce siderophores) whereas phosphate solubilizers were more predominant in rhizomes (75% of rhizomes isolates against 54% of root isolates). None of the *β-Proteobacteria* isolates could solubilize phosphate.

The group of bacterial strains having the three PGP traits tested was comprised by all members of *γ-Proteobacteria* (*Pseudomonas veronii*, *Pseudomonas lini*, *Pseudomonas moorei*, *Pseudomonas arsenicoxydans*, *Pseudomonas corrugata* and *Cedecea davisae*), two members from *α-Proteobacteria* (*Rhizobium radiobacter* and *Candidatus Rhizobium massilae*) and two members from *Bacteroidetes* (*Chitinophaga sancti* and *Chryseobacterium taeanense*). In total, 10 from the 22 isolates presented simultaneously, the three PGP traits tested.

#### 4.2.5. Enrichment cultures

Enrichment cultures were performed to isolate bacterial strains that could potentially use CBZ as carbon source. Fresh rhizomes and roots were harvested in the greenhouse and transferred to sterile minimal medium AB supplemented with 0.4 mM CBZ as sole carbon source. These cultures were sub-cultured three times, once every two weeks and then serial dilutions were prepared and spread onto agar plates. Enrichment cultures were prepared from sterilized and non-sterilized segments of roots and rhizomes to distinguish rhizoplane from endophytic bacteria.

Eighteen isolates were obtained and after sequencing the 16S-rRNA encoding gene, seven distinct species were identified among the isolates (Table 18). At phylum level, six strains were affiliated to *Proteobacteria* and one to *Actinobacteria*. *Pseudomonas* ( $\gamma$ -*Proteobacteria*) was the most represented genus with three distinct species (*P. monteilii*, *P. hunanensis*, and *P. japonica*). *Achromobacter* ( $\beta$ -*Proteobacteria*) was represented by two species: *A. dolens* and *A. denitrificans*. The other two isolates were *Sphingopyxis ummariensis* ( $\alpha$ -*Proteobacteria*) and *Cellumonas gelida* (*Actinobacteria*).

Table 18: Taxonomic identification of root and rhizome associated bacteria from *Phragmites australis* plants isolated using enrichment cultures with carbamazepine as sole carbon source. Taxonomy classification was based on the 16S rDNA region sequence compared to validated type strain sequences deposited in the EzTaxon database.

Isolate	Closest related type strain	Sequence similarity	Sequence coverage	Group
E1	<i>Cellumonas gelida</i> DSM 20111	93,36	1083	<i>Actinobacteria</i>
E2	<i>Achromobacter dolens</i> LMG 26840	99,93	1431	$\beta$ - <i>Proteobacteria</i>
E3	<i>Pseudomonas monteilii</i> CIP 104883	96,63	1076	$\gamma$ - <i>Proteobacteria</i>
E4	<i>Sphingopyxis ummariensis</i> UI2	99,78	1377	$\alpha$ - <i>Proteobacteria</i>
E5	<i>Pseudomonas monteilii</i> CIP 104833	97,68	1438	$\gamma$ - <i>Proteobacteria</i>
E6	<i>Pseudomonas monteilii</i> CIP 104833	99,86	1424	$\gamma$ - <i>Proteobacteria</i>
E7	<i>Pseudomonas monteilii</i> CIP 104833	99,86	1409	$\gamma$ - <i>Proteobacteria</i>
E8	<i>Pseudomonas monteilii</i> CIP 104833	97,76	1366	$\gamma$ - <i>Proteobacteria</i>
E9	<i>Achromobacter dolens</i> LMG 26840	100	1376	$\beta$ - <i>Proteobacteria</i>
E10	<i>Pseudomonas hunanensis</i> LV	99,73	753	$\gamma$ - <i>Proteobacteria</i>
E11	<i>Pseudomonas monteilii</i> CIP 104883	99,86	1411	$\gamma$ - <i>Proteobacteria</i>
E12	<i>Achromobacter denitrificans</i> DSM 30026	99,86	1389	$\beta$ - <i>Proteobacteria</i>
E13	<i>Pseudomonas monteilii</i> CIP 104833	97,93	1419	$\gamma$ - <i>Proteobacteria</i>
E14	<i>Pseudomonas monteilii</i> CIP 104833	99,86	1389	$\gamma$ - <i>Proteobacteria</i>
E15	<i>Pseudomonas japonica</i> IAM 15071	98,33	1095	$\gamma$ - <i>Proteobacteria</i>
E16	<i>Pseudomonas monteilii</i> CIP 104833	95,80	1395	$\gamma$ - <i>Proteobacteria</i>
E18	<i>Pseudomonas monteilii</i> CIP 104833	97,18	1039	$\gamma$ - <i>Proteobacteria</i>

Isolates were maintained in agar plates, growing in the isolation media. All isolates were able to grow in liquid complex media but failed to grow in minimal media containing CBZ as sole carbon source (data not shown).

### **4.3. Metabolism of carbamazepine in *Armoracia rusticana* hairy roots and interactions with endophytic bacteria**

A HR culture derived from horseradish (*Armoracia rusticana*) was used to unravel interactions between the endophytic bacteria isolated from *P. australis* and plant roots exposed to CBZ. Such a model allowed the study of plant-bacteria interactions in a rapid and easy manner, in a controlled and axenic environment, limiting all the external factors that would add more uncertainty to the research question. The focus of interest here were to describe CBZ metabolism in plant roots, and to determine the role of endophytic bacteria in the detoxification of the compound and in the antioxidant responses in the host.

#### **4.3.1. Carbamazepine removal from nutrient media by hairy roots and endophytic bacteria**

CBZ removal in HR cultures void of or inoculated with endophytic bacteria previously isolated from *P. australis* was studied in short time experiments. Growth medium was spiked with CBZ to obtain final concentrations of 10 and 25  $\mu\text{M}$ . HRs and inoculated HRs with the endophytic strains *Rhizobium radiobacter* and *Diaphorobacter nitroreducens* were incubated in the spiked growth medium for six days. Samples from the nutrient solution were taken at  $t=0$  and after one, three and six days of incubation and analysed for CBZ concentration.

HR cultures alone removed 5% of the compound when they were incubated with 10  $\mu\text{M}$  CBZ and 4% when they were incubated with 25  $\mu\text{M}$  (Fig. 17). When cultures were inoculated with *R. radiobacter*, the amount of CBZ removed increased significantly to 21% and 13% in treatments with 10  $\mu\text{M}$  and 25  $\mu\text{M}$  respectively. These rates represented a 4-fold and 3-fold increase in the removal capacity of HRs alone at initial



concentrations of 10  $\mu\text{M}$  and 25  $\mu\text{M}$ , respectively. HRs inoculated with *D. nitroreducens* also showed an increase in CBZ removal with rates of 10% in 10  $\mu\text{M}$  treatment and 9% in treatments with 25  $\mu\text{M}$ . The increase in removal rates was lower, but still represented twice the amount of CBZ removed by HRs not assisted by endophytic bacteria.

The total amount of CBZ removed increased with the initial concentration of the compound. In treatments with 10  $\mu\text{M}$  CBZ, the removal of CBZ in HR cultures after 6 days was 3.5  $\mu\text{g/g}$  FW (Fig. 17). In inoculated HRs, this amount increased to 8  $\mu\text{g/g}$  FW (*D. nitroreducens*) and to 17.5 (*R. radiobacter*). In treatments with 25  $\mu\text{M}$ , total removal was higher: 9  $\mu\text{g/g}$  FW in HRs, 28  $\mu\text{g/g}$  FW in HRs inoculated with *D. nitroreducens* and 34  $\mu\text{g/g}$  FW in HRs inoculated with *R. radiobacter*. Hence, in all conditions applied, CBZ removal was strongly correlated with initial concentrations in the media ( $r=0.99$ ) (Fig. 18).

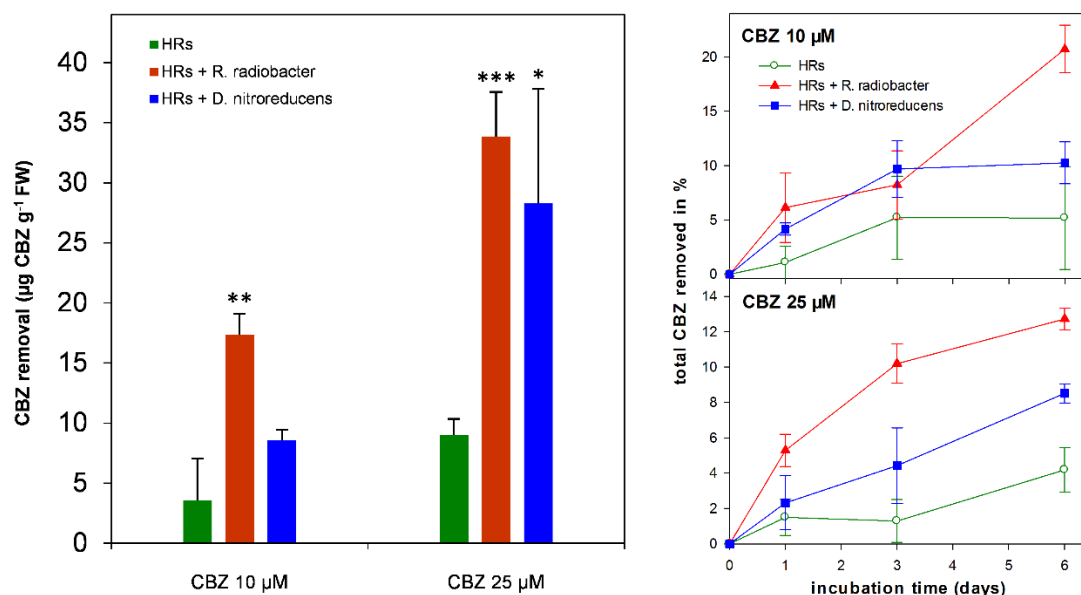


Figure 17: Carbamazepine (CBZ) removal in *A. rusticana* hairy root cultures and effect of inoculation with the endophytic bacteria *R. radiobacter* and *D. nitroreducens* isolated from *P. australis*. The left panel shows the removal of CBZ after 6 days of incubation, expressed in  $\mu\text{g}$  of CBZ removed per g of root tissue (FW). The right panel shows the total removal of CBZ in % during the incubation time. Data are means  $\pm$  SD of three replicates. The values labelled by asterisk are statistically significant (Analysis of variance: \*  $P < 0.05$ , \*\*  $P < 0.01$ , \*\*\*  $P < 0.001$ , compared with HR groups).

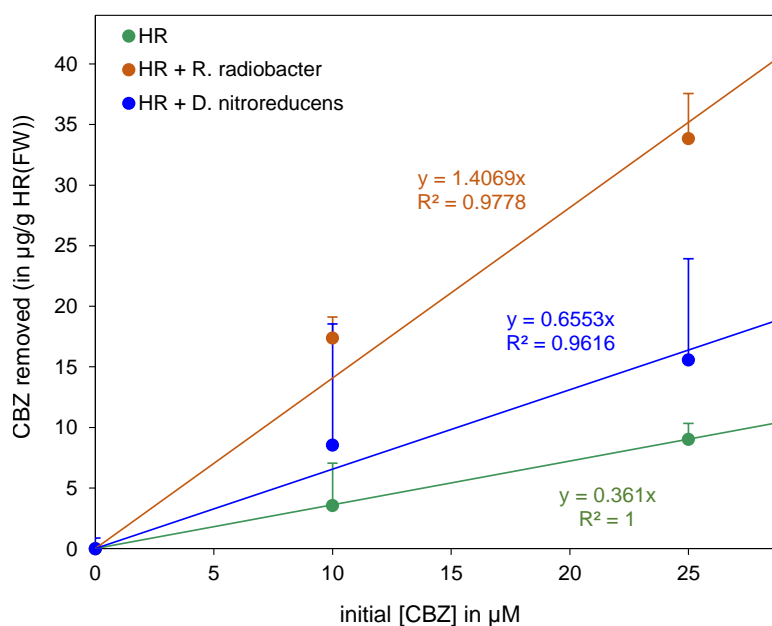


Figure 18: Relationship between the initial concentration of carbamazepine (CBZ) in the growth medium and the removal by HR cultures after 6 days of incubation. Values are means  $\pm$  SD of three replicates

#### 4.3.2. Oxidative stress and antioxidant responses in HRs

The activity of the ROS scavenging enzymes GR, POX and APOX and the detoxification enzymes GSTs, was determined in cytosolic extracts of *A. rusticana* HR cultures. HRs void of or inoculated with the endophytic bacteria *R. radiobacter* and *D. nitroreducens* were grown in Erlenmeyer flasks containing nutrient solution spiked with 250  $\mu\text{M}$  CBZ in ethanol for 48 h. HRs and inoculated HRs growing in flasks containing nutrient solution and spiked with the same volume of ethanol were used as controls. Roots were harvested after 48 h and cytosolic enzymes were extracted.

The activity of GR in HR cultures treated with CBZ was three-fold higher than in control cultures (3.97 against 1.32  $\mu\text{kat/g FW}$ ) (Fig. 19). In the same way, treatment with CBZ resulted in an increase of GR activity when HRs were inoculated with endophytic bacteria. However, this increase was lower than in non-inoculated samples (2-fold in roots inoculated with *R. radiobacter* and 1.4-fold in roots inoculated with *D. nitroreducens*).

POX activity also increased in all samples after CBZ treatment. The increase was higher in roots inoculated with *D. nitroreducens*. In this case POX activity rose from 0.031 to 0.278  $\mu\text{kat/g FW}$  after treatment, denoting a 9-fold increase. Increase in POX activity was lower in cultures inoculated with *R. radiobacter*: 0.297 to 0.427  $\mu\text{kat/g FW}$  (1.4-fold) and almost non-observable in non-inoculated roots, with a constant enzyme activity around 0.020  $\mu\text{kat/g FW}$ .

APOX remained almost constant in HRs after exposure to CBZ with values around 0.010  $\mu\text{kat/g FW}$ . In cultures inoculated with endophytic bacteria, the enzyme activity was higher when roots were grown without CBZ (around 0.050  $\mu\text{kat/g FW}$ ). Treatment with CBZ resulted in the inhibition of this enzyme, with a 2-fold decrease in roots

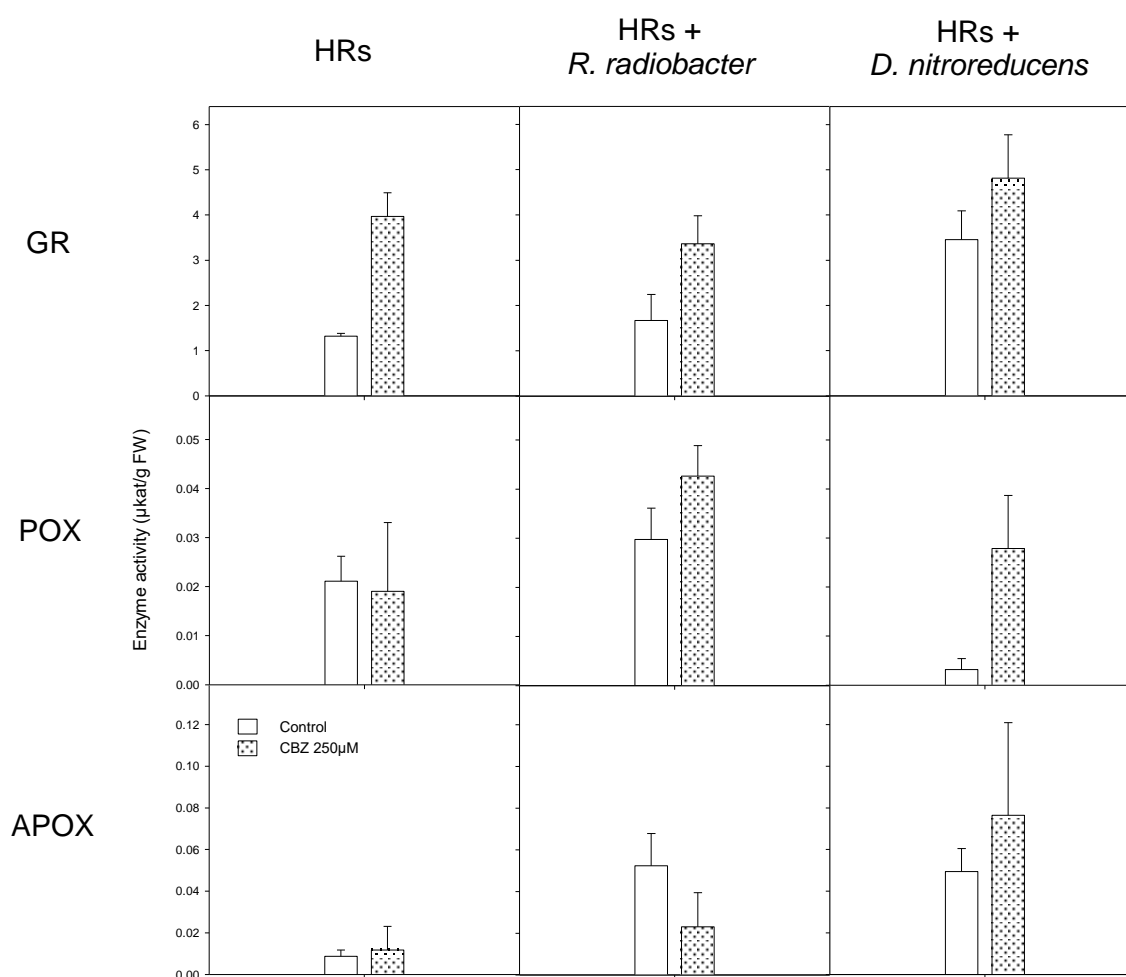


Figure 19: Antioxidant enzyme activities in *Armoracia rusticana* hairy root cultures and endophytic bacteria exposed to carbamazepine (CBZ). Activities of the ROS-scavenging enzymes glutathione reductase (GR), peroxidase (POX) and ascorbate peroxidase (APOX) were measured in cytosolic extracts of *A. rusticana* hairy roots void of or inoculated with the endophytic bacteria *R. radiobacter* and *D. nitroreducens* exposed to 250  $\mu\text{M}$  CBZ for 48 h.

inoculated with *R. radiobacter*. In contrast, CBZ treatment resulted in an induction of APOX activity in roots inoculated with *D. nitroreducens* with an increase of 50%.

GST activity was analysed in cytosolic extracts using different substrates. When CDNB was used as substrate, no induction could be observed in HRs after exposure to CBZ (Fig. 20). The same effect was observed in HRs inoculated with *R. radiobacter* where even a decrease was observed. In contrast, inoculated roots with *D. nitroreducens* responded to CBZ treatment with an increase of 70% in GST activity. When pNBoC was used as substrate, treatment with CBZ induced GST activity in all samples. Elevated activity was observed in roots inoculated with *D. nitroreducens* where GST activity rose from 0.067 to 0.259  $\mu\text{kat/g}$  FW. In roots inoculated with *R. radiobacter*, GST activity increased from 0.084 to 0.225  $\mu\text{kat/g}$  FW. In this case, the activity was lower in non-inoculated HRs (0.001 and 0.059  $\mu\text{M/g}$  FW before and after CBZ treatment

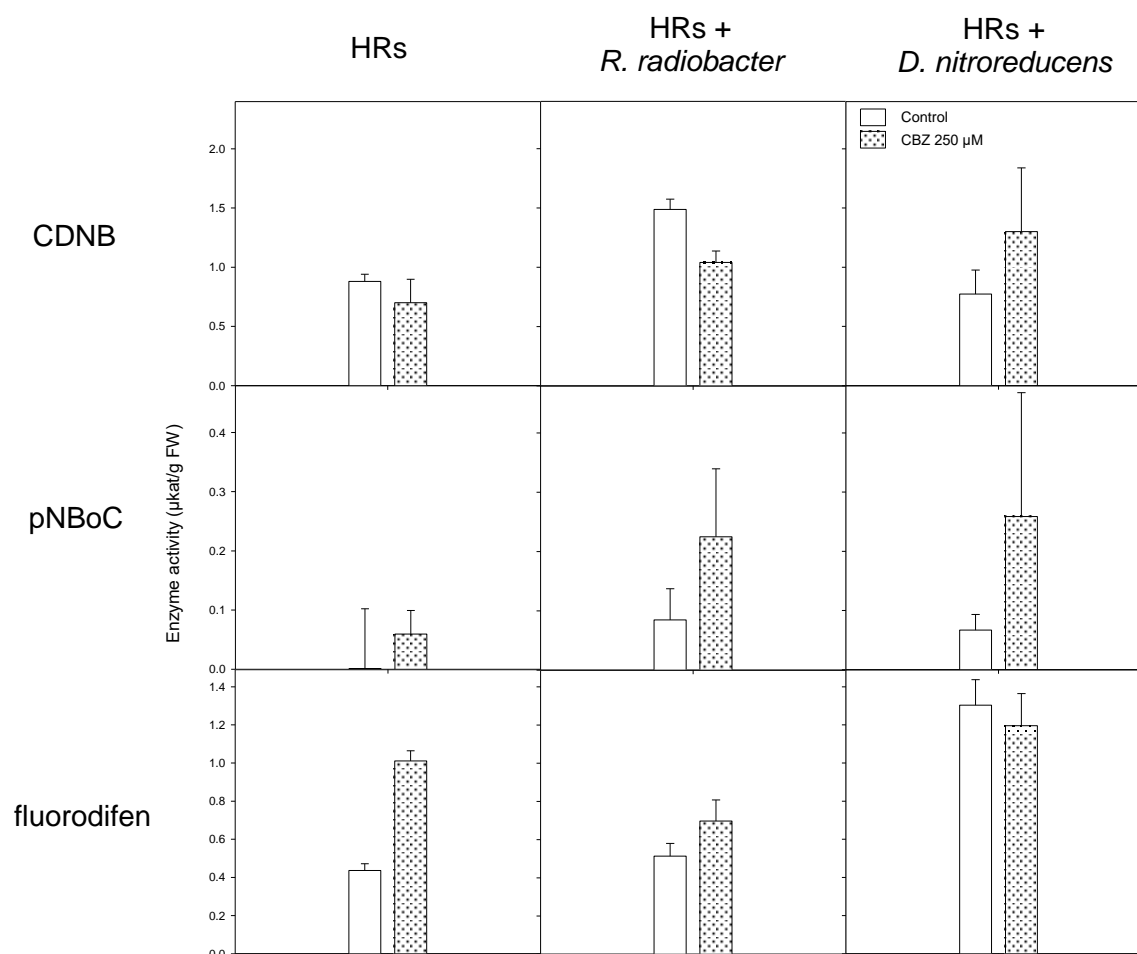


Figure 20: Specific glutathione-S-transferases (GST) activity in *Armoracia rusticana* hairy roots exposed to CBZ. GST activity was measured in cytosolic extracts of hairy root cultures void of or inoculated with *R. radiobacter* or *D. nitroreducens* and exposed to 250  $\mu\text{M}$  CBZ after 48 h for three different substrates: CDNB, pNBC and fluorodifen.

respectively. Using fluorodifen as substrate, changes in GST activity were not observed in roots inoculated with *D. nitroreducens*. Still, GST activities were the highest measured in all samples (1.30  $\mu\text{kat/g FW}$  in non-treated samples and 1.19  $\mu\text{kat/g FW}$  in samples exposed to CBZ). In non-inoculated roots, a 2.3-fold increase was recorded and a small increment was observed in roots inoculated with *R. radiobacter* (0.51  $\mu\text{kat/g FW}$  before and 0.70  $\mu\text{kat/g FW}$  after treatment).

### 4.3.3. Metabolism of carbamazepine in hairy roots and endophytic bacteria

Metabolism of CBZ in HRs was studied at initial concentration of 250  $\mu\text{M}$ . HRs and inoculated HRs with the endophytic strains *R. radiobacter* and *D. nitroreducens* were incubated in the spiked growth medium for 21 days. Samples from the nutrient solution were taken at  $t_0$  and after 1, 4, 8, 14 and 21 days of incubation and analysed for CBZ TPs by LC-QTOF-MS/MS. In total, 13 TPs were identified in the growth media (Table 19). These TPs were clustered in four hypothetical pathways, the development of which during the incubation time was followed in the growth media. The composition of TPs in root extracts was determined at the end of the incubation. For reasons of clarity of the presentation, references on the composition of the pathways are presented in the discussion section of this thesis (see below).

#### 4.3.3.1. The 10,11-diol pathway

The 10,11-diol pathway has previously been described in plants and involves three TPs. CBZ is first oxidized to CBZ-10,11-epoxide (reaction A, Fig. 21). This is a common metabolite that serves as starting point for other sub-pathways.

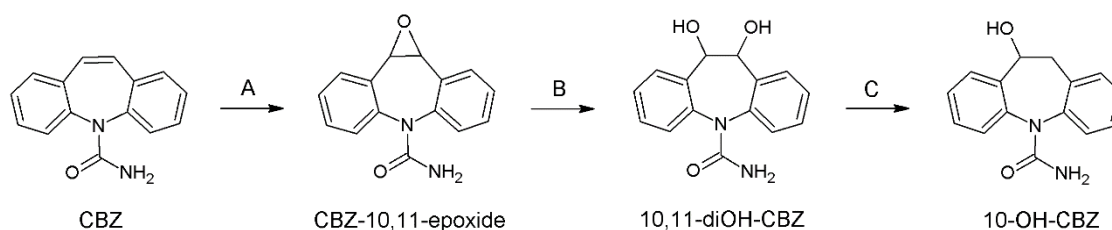


Figure 21: Carbamazepine metabolism in *A. rusticana* hairy roots assisted by endophytic bacteria: the 10,11-diol pathway

Table 19: CBZ structure and transformation products identified in the liquid media during degradation by *A. rusticana* hairy root cultures and the endophytic bacteria *R. radiobacter* and *D. nitroreducens*.

Name	Exact Mass (Da)	Chemical formula	Structure	Identification	Rt (min)	log Kow
<b>CBZ-10,11-epoxide</b>	253.0971	C <sub>15</sub> H <sub>12</sub> N <sub>2</sub> O <sub>2</sub>		Standard	6.02	2.54
<b>10,11-dihydro-10,11-dihydroxy-CBZ</b>	271.1077	C <sub>15</sub> H <sub>14</sub> N <sub>2</sub> O <sub>3</sub>		Standard	5.37	1.16
<b>10,11-dihydro-10-hydroxy-CBZ</b>	255.1128	C <sub>15</sub> H <sub>14</sub> N <sub>2</sub> O <sub>2</sub>		Standard	5.67	2.15
<b>2,3-dihydro-2,3-dihydroxy-CBZ</b>	271.1077	C <sub>15</sub> H <sub>14</sub> N <sub>2</sub> O <sub>3</sub>		Proposed	5.7	0.49
<b>2,3-dihydroxy-CBZ</b>	269.0921	C <sub>15</sub> H <sub>12</sub> N <sub>2</sub> O <sub>3</sub>		Proposed	5.82	1.85
<b>CBZ-2,3-quinone</b>	267.0764	C <sub>15</sub> H <sub>10</sub> N <sub>2</sub> O <sub>3</sub>		Proposed	5.67	1.36
<b>CBZE-GSH</b>	560.1809	C <sub>25</sub> H <sub>29</sub> N <sub>5</sub> SO <sub>8</sub>		Proposed	5	-3.83
<b>CBZE-cys-gly</b>	431.1384	C <sub>20</sub> H <sub>22</sub> N <sub>4</sub> SO <sub>5</sub>		Proposed	4.93	-1.25
<b>CBZE-cys</b>	374.1169	C <sub>18</sub> H <sub>19</sub> N <sub>3</sub> SO <sub>4</sub>		Synthesized	4.87	-0.90
<b>acridine</b>	180.0808	C <sub>13</sub> H <sub>9</sub> N		Standard	4.95	3.17
<b>9-acridine carboxaldehyde</b>	208.0757	C <sub>14</sub> H <sub>9</sub> NO		Proposed	7.8	3.49
<b>9-OH-acridine</b>	196.0757	C <sub>13</sub> H <sub>9</sub> NO		Proposed	4.8	3.48
<b>acridone</b>	196.0757	C <sub>13</sub> H <sub>9</sub> NO		Standard	6.5	2.57

All chromatograms obtained from treated cultures showed multiple peaks corresponding to a theoretical  $m/z$  253.1071. This  $m/z$  corresponds to an epoxidation or a hydroxylation of the parent compound and is shared by several plausible epoxidized or hydroxylated CBZ TPs. This result revealed the co-elution of other epoxidized or hydroxylated TPs formed during the incubation impeding a quantification for this metabolite.

The first epoxidation is followed by cleavage and hydroxylation of the epoxy bond to form 10,11-dihydro-10,11-dihydroxy-CBZ (10,11-diOH-CBZ) (reaction B, Fig. 21). This metabolite was found in the media from the first day and accumulated constantly until the last day of incubation in HR cultures (Fig 22). When HRs were inoculated with endophytic bacteria, an acceleration in the formation of this TP was observed during the first day. A decrease in the concentration measured in the growth medium followed between the first and the fourth day of incubation, and after the fourth day, the peak area increased with lower rates than in control HR cultures.

The compound 10,11-dihydro-10-hydroxy-CBZ (10-OH-CBZ) can be formed from the intermediate 10,11-diOH-CBZ (reaction C, Fig.21). This compound was identified in the media from HR cultures and HR cultures inoculated with *D. nitroreducens*. In both cases, the peak area increased slowly from the first day on, although reaching a higher concentration in non-inoculated HRs.

The metabolites 10,11-dihydro-10,11-dihydroxy-CBZ and 10-OH-CBZ were found in negative controls consisting of autoclaved HRs incubated with CBZ (Fig 23). The formation of these compounds in absence of biological matrices reveals a chemical oxidative degradation independent from plants or bacteria. However, the total amount of products accumulated was always lower than in biological samples. When autoclaved HRs were inoculated with endophytic bacteria, 10,11-dihydro-10,11-dihydroxy-CBZ was formed with a trend similar to rates observed in healthy HRs but in lower amounts. Thus, we can conclude that bacteria and plants can degrade CBZ through the 10,11-diol pathway although plants are more efficient.

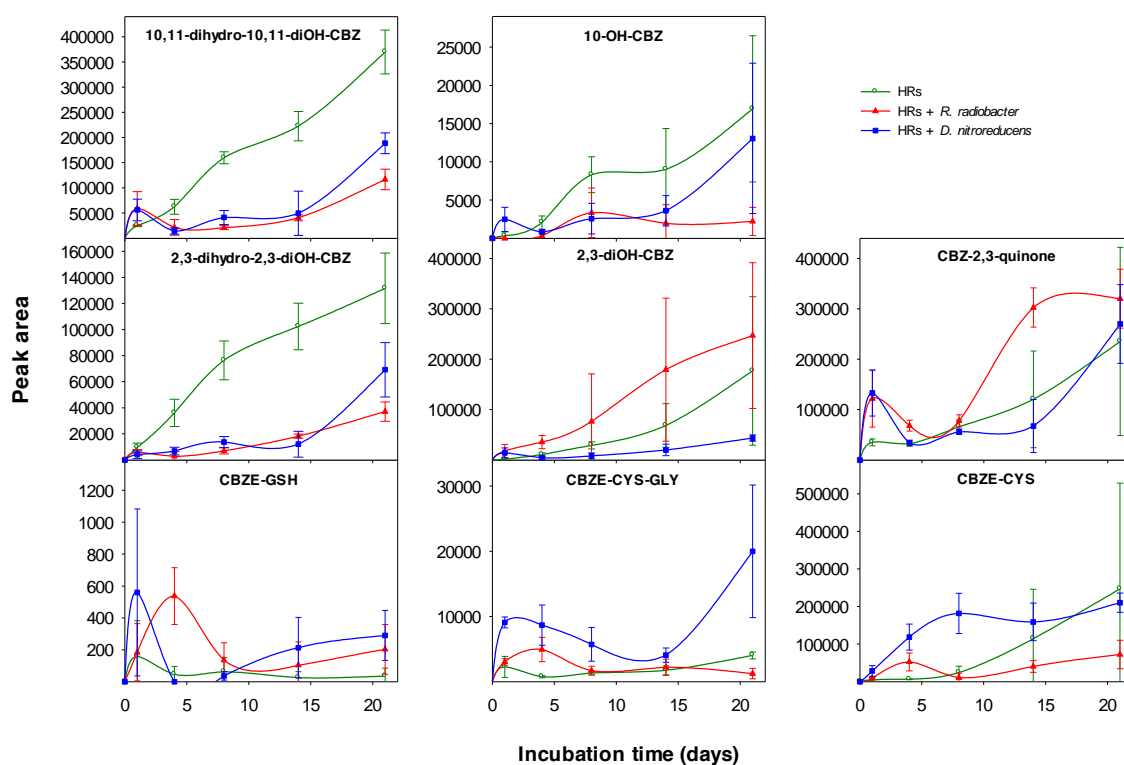


Figure 22: Carbamazepine (CBZ) transformation products in *A. rusticana* hairy root cultures I. Evolution of CBZ transformation products during degradation by *A. rusticana* hairy root cultures and effect of the inoculation with the endophytic bacteria *R. radiobacter* and *D. nitroreducens* isolated from *P. australis*: 10,11-diol, 2,3-diol and GSH subpathways. CBZ initial concentration was 250  $\mu\text{M}$ . Peak area is in unit of mAU/g FW. Data are means  $\pm$  SD of three replicates.

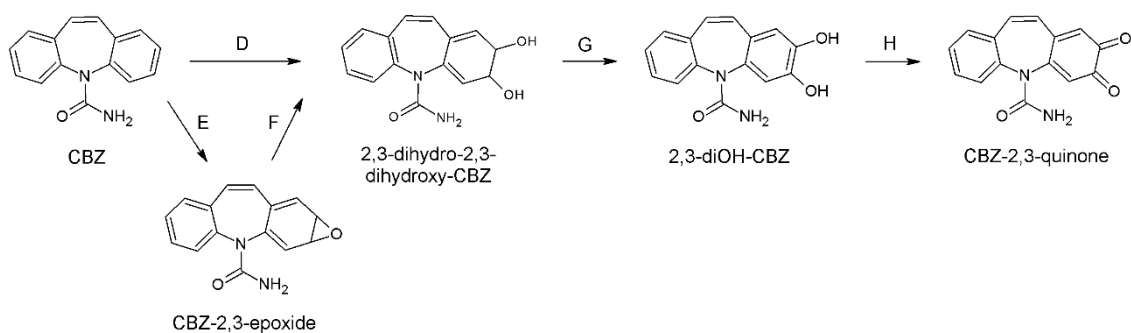


Figure 23: Carbamazepine metabolism in *A. rusticana* hairy roots assisted by endophytic bacteria: the 2,3-diol pathway.

9-acridine carboxaldehyde  $10^8$

acridine

9-OH-acridine

$10^7$

$10^6$

$10^5$

$10^4$



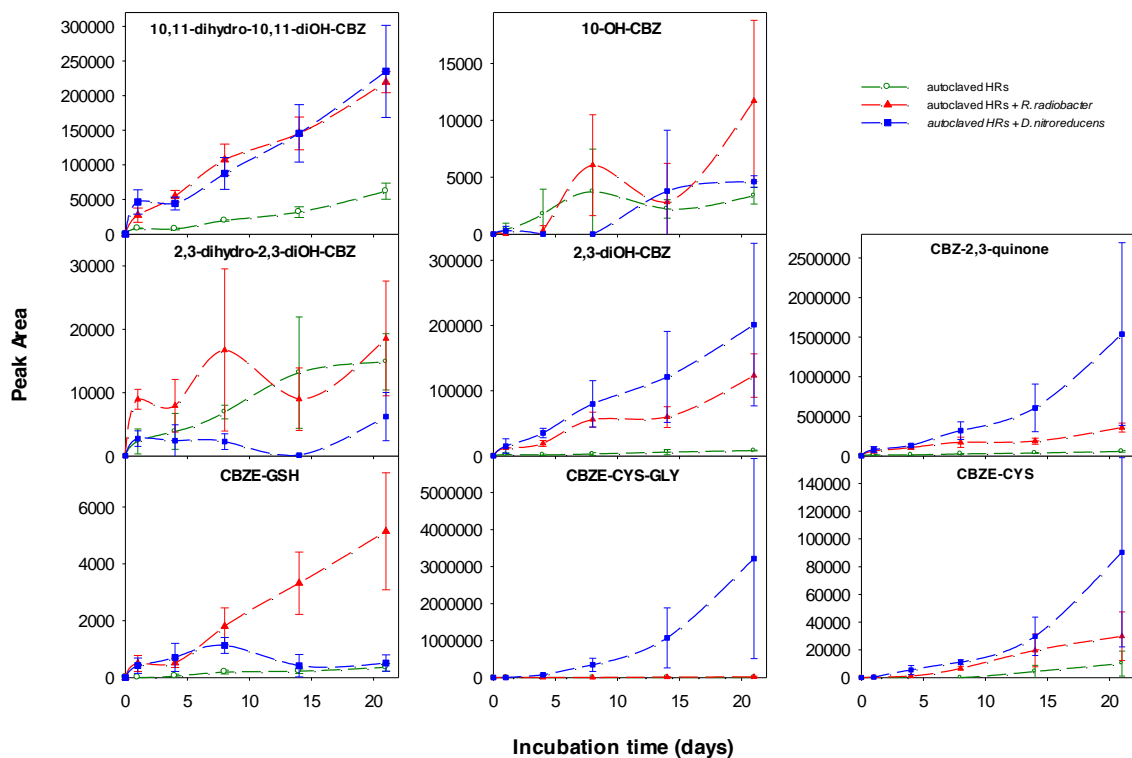


Figure 24: Carbamazepine (CBZ) transformation products in control *A. rusticana* hairy root cultures I. Evolution of CBZ transformation products in controls corresponding to autoclaved *A. rusticana* hairy root cultures and autoclaved hairy roots inoculated with the endophytic bacteria *R. radiobacter* and *D. nitroreducens* isolated from *P. australis*: 10,11-diol, 2,3-diol and GSH subpathways. CBZ initial concentration was 250  $\mu$ M. Peak area is given in unit of mAU/g FW. Data are means  $\pm$  SD of three replicates.

(  
 ]  
 (  
 (  
 ]  
 ]  
 (  
 (  
 4  
 (  
 7  
 (  
 ]  
 ]

The next step in this pathway is the oxidation of 2,3-dihydro-2,3-dihydroxy-CBZ to 2,3-dihydroxy-CBZ (2,3-diOH-CBZ) (reaction G, Fig. 24). The formation of dihydrodiols and subsequent diol compounds is a conserved mechanism in bacterial degradation of PAHs such phenanthrene, naphthalene, fluoranthene, pyrene and benzopyrene and is generally achieved by dehydrogenases.

Finally, 2,3-diOH-CBZ was oxidized to CBZ-2,3-quinone (reaction H, Fig. 24). This reaction can be catalyzed by a catechol oxidase, an enzyme of the polyphenol oxidase family, present in plants. The same reaction has been postulated to occur non-enzymatically during the oxidation of 1,2-dihydroxynaphthalene to 1,2-naphthaquinone in bacterial metabolism of naphthalene.

The 2,3-diol pathway exhibited a behaviour comparable to the 10,11-diol pathway in its first steps (Fig. 22). Evolution of the TPs 2,3-dihydro-2,3-dihydroxy-CBZ and 10,11-dihydro-10,11-dihydroxy-CBZ in the growth media of HRs was similar, with amounts approximately 30% lower in the case of 2,3-dihydro-2,3-dihydroxy-CBZ. In contrast, 2,3-diOH-CBZ and CBZ-2,3-quinone were more significant in HRs inoculated with endophytic bacteria and specially with *R. radiobacter*. Additionally, 2,3-diOH-CBZ and CBZ-2,3-quinone were identified in negative controls inoculated with bacteria while there were negligible in autoclaved HRs (Fig. 23).

#### 4.3.3.3. GSH pathway

To investigate phase II metabolism, TPs resulting from GSH conjugation were searched for. Glutathione-S-transferases (GSTs) are detoxifying enzymes responsible for the conjugation of xenobiotics with glutathione. GSTs initiated the GSH pathway in CBZ metabolism (reaction I, Fig. 25).

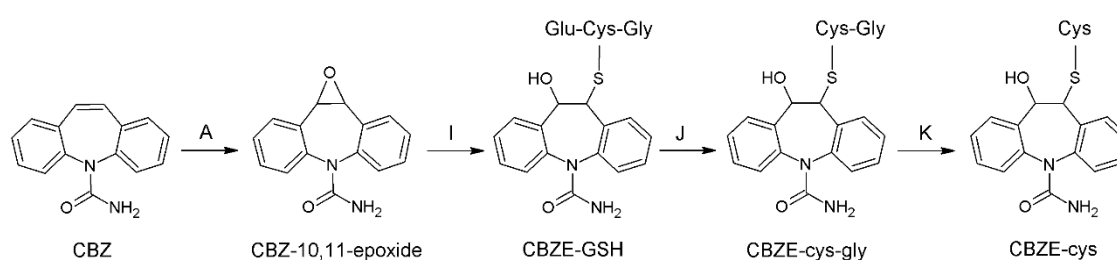


Figure 25: CBZ metabolism in horseradish HRs assisted by endophytic bacteria: the GSH pathway

Several TPs derived from GSH conjugates were identified and designated following their  $m/z$  ratios: TP374, TP431 and TP560. To confirm the nature of these TPs, chemical conjugation with GSH and cysteine was performed *in vitro*, and the products were analysed under the same analytical conditions as the samples. A molecular ion peak at  $m/z$  560.1809 was observed when CBZ-10,11-epoxide was incubated with GSH. The respective ion chromatogram showed a double peak eluting at 4.99-5.04 min, corresponding to the GSH adduct (Fig. 26 A). Identical retention and fragmentation patterns were obtained during collision experiments on the precursor ion in biological samples and in chemically synthesized GSH adducts (Fig. 26 B). Therefore, TP560 was identified as 10,11-dihydro-10-hydroxy-11-glutathionyl-CBZ (CBZE-GSH). TP560 was found only in trace levels in HR cultures and HRs inoculated with endophytes (Fig. 22), but in greater amounts when autoclaved roots were grown with *R. radiobacter* (Fig. 23).

Following GSH conjugation, CBZE conjugate can be further degraded to the respective  $\gamma$ -glutamylcysteinyl- and subsequent cysteinyl-moieties by carboxypeptidases or to cysteinylglycyl- and subsequent cysteinyl- moieties by  $\gamma$ -glutamyl-transpeptidase ( $\gamma$ -GT) (reaction J, Fig. 25). Cysteinylglycine adducts (TP431) were detected in the media of HR cultures. Fragment ions with identical  $m/z$  ratios were observed when TP560

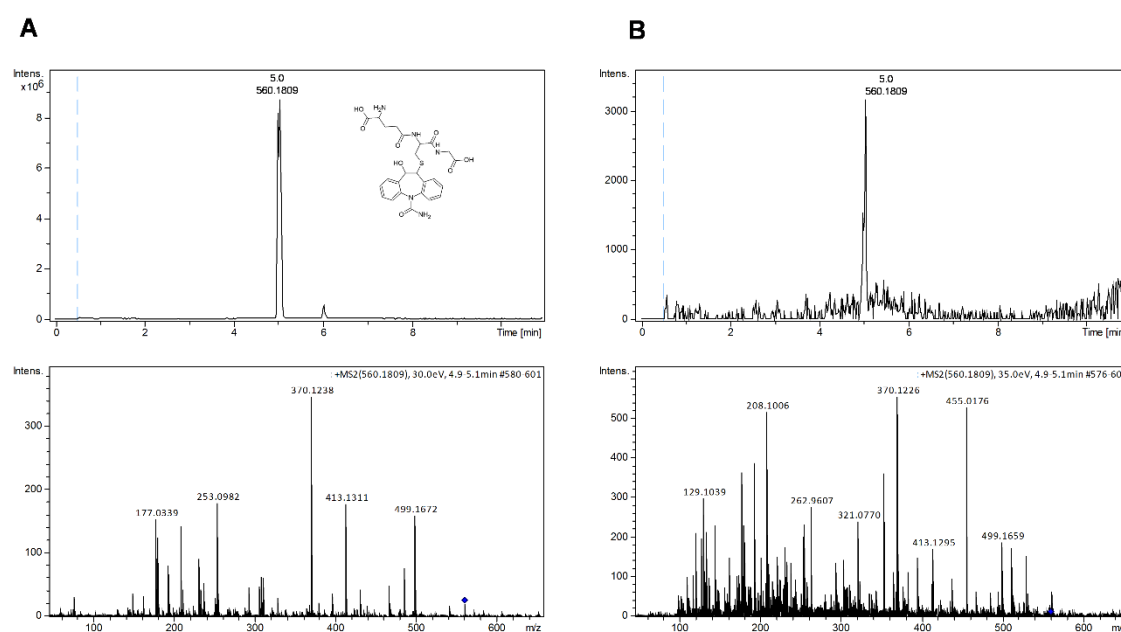


Figure 26: Identification of TP560 as 10,11-dihydro-10-hydroxy-11-glutathionyl-CBZ (CBZE-GSH). Chromatograms showing the elution and fragmentation pattern of the GSH conjugate formed with carbamazepine-10,11-epoxide after chemical synthesis (A) and in biological samples (B).

and TP431 were subjected to collision. Additionally, retention times revealed a very similar hydrophobicity of CBZE-GSH and TP461. For this reasons, TP431 was identified as 10,11-dihydro-10-hydroxy-11-cysteinylglycinyl-CBZ (CBZE-CYS-GLY). TP431 was likewise detected in the growth media of autoclaved HRs inoculated with endophytic bacteria, suggesting a bacterial engagement in GSH conjugation and successive degradation of CBZ (Fig. 23). The  $\gamma$ -glutamylcysteinyl adduct (CBZE-GLU-CYS) was not found in the media of any of the experimental conditions.

TP374, with a theoretical  $m/z$  matching to the cysteine CBZE adduct was identified in all culture media. When CBZE was incubated with cysteine, a double peak at 4.88-4.92 min and  $m/z$  374.1169 corresponding to a cysteine adduct was observed. Collision experiments on the precursor ion  $m/z$  374.1169 showed conserved fragments in biological and chemical samples ( $m/z$  = 180.0821, 210.0928, 253.0985, 313.1025, 339.0819), proving that TP374 is in fact 10,11-dihydro-10-hydroxy-11-cysteinyl-CBZ (CBZE-CYS) (Fig. 27). TP374 was detected in autoclaved HR culture media at low levels only after 14 days of incubation (Fig. 23). These results indicate that besides biological formation of CBZE-CYS, chemical conjugation with free cysteine may occur in the media.

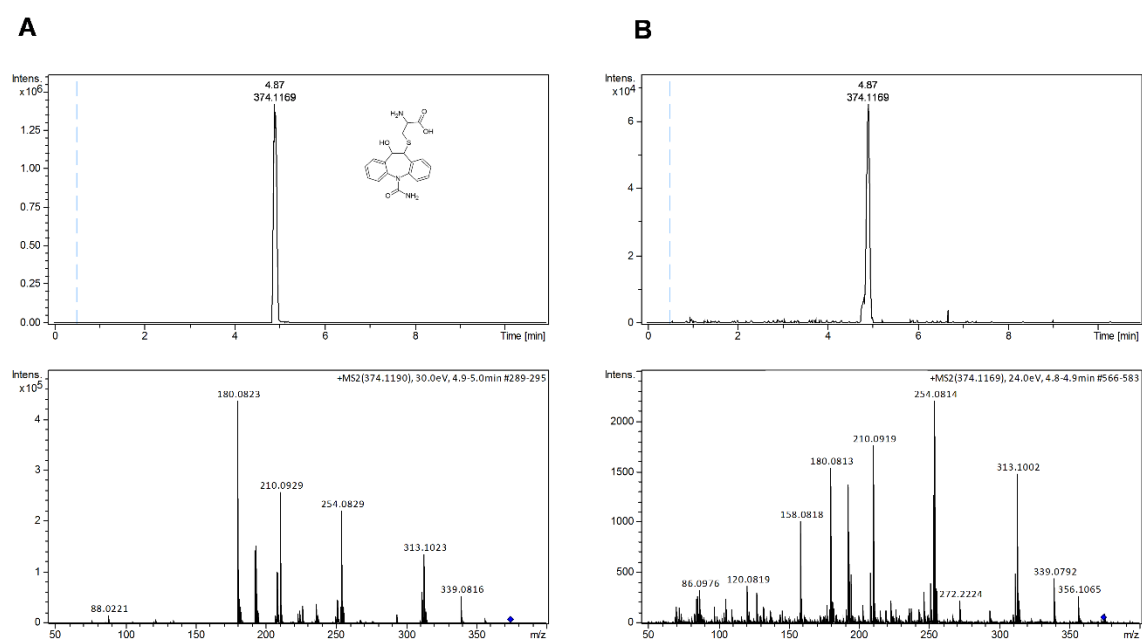


Figure 27: Identification of TP374 as 10,11-dihydro-10-hydroxy-11-cysteinyl-CBZ (CBZE-cys). Chromatograms showing the elution and fragmentation pattern of the cysteine conjugate formed with carbamazepine-10,11-epoxide after chemical synthesis (A) and in biological samples (B).

The trends of the intermediate (CBZE-CYS-GLY) and the final (CBZE-CYS) metabolites in the GSH degradation pathway displayed phases at different time points during the incubation where concentration decreased significantly (Fig. 22). In media of roots inoculated with *D. nitroreducens*, CBZE-CYS-GLY decreased from the first to the eighth day of incubation, to accumulate again up to the last day, whereas CBZE-CYS decreased between days 8 and 14. In media of roots inoculated with *R. radiobacter*, CBZE-CYS reached a maximum in the fourth day, and decreased between days 4 and 8, suggesting further degradation of the cysteine conjugate when plants were inoculated with endophytic bacteria. Hypothetical TPs derived from further catabolism were not identified.

#### 4.3.3.4. Acridine pathway

The acridine pathway involves a contraction of the seven-membered of the central ring of CBZE into a six-membered ring. This pathway is initiated by cleavage of the carbamoyl group of CBZE (reaction L, Fig. 28).

Several TPs with an acridine-like structure were detected in the growth media of HR cultures (Fig. 29). The order of the reactions involved in this pathway was deduced

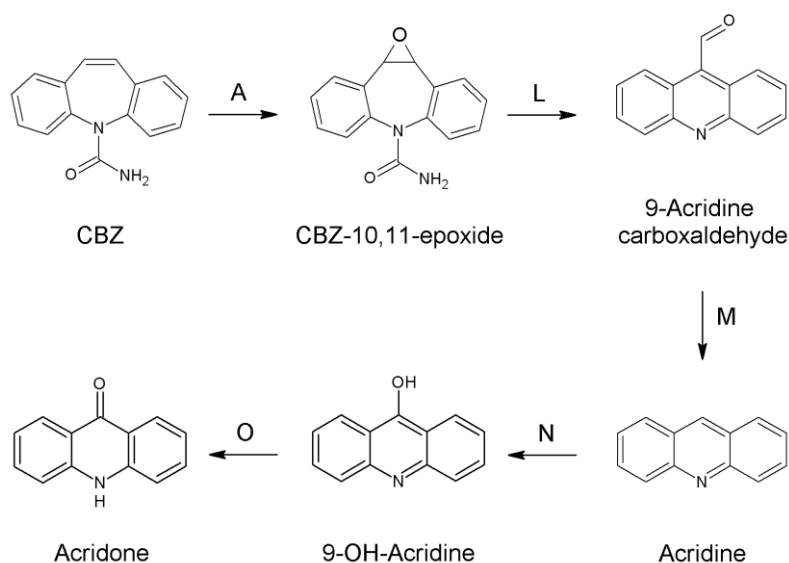


Figure 28: Carbamazepine metabolism in *A. rusticana* hairy roots assisted by endophytic bacteria: the acridine pathway

from the observation of trends and absolute amounts exhibited by each of the compounds.

The first TP of this pathway is 9-acridine carboxaldehyde which is formed from CBZ-10,11-epoxide after cleavage of the carbamoyl group and contraction of the seven-membered central ring to a six-membered ring (reaction L, Fig. 28). The aldehyde moiety is then cleaved to form acridine. Both TPs are known to be toxic and reactive.

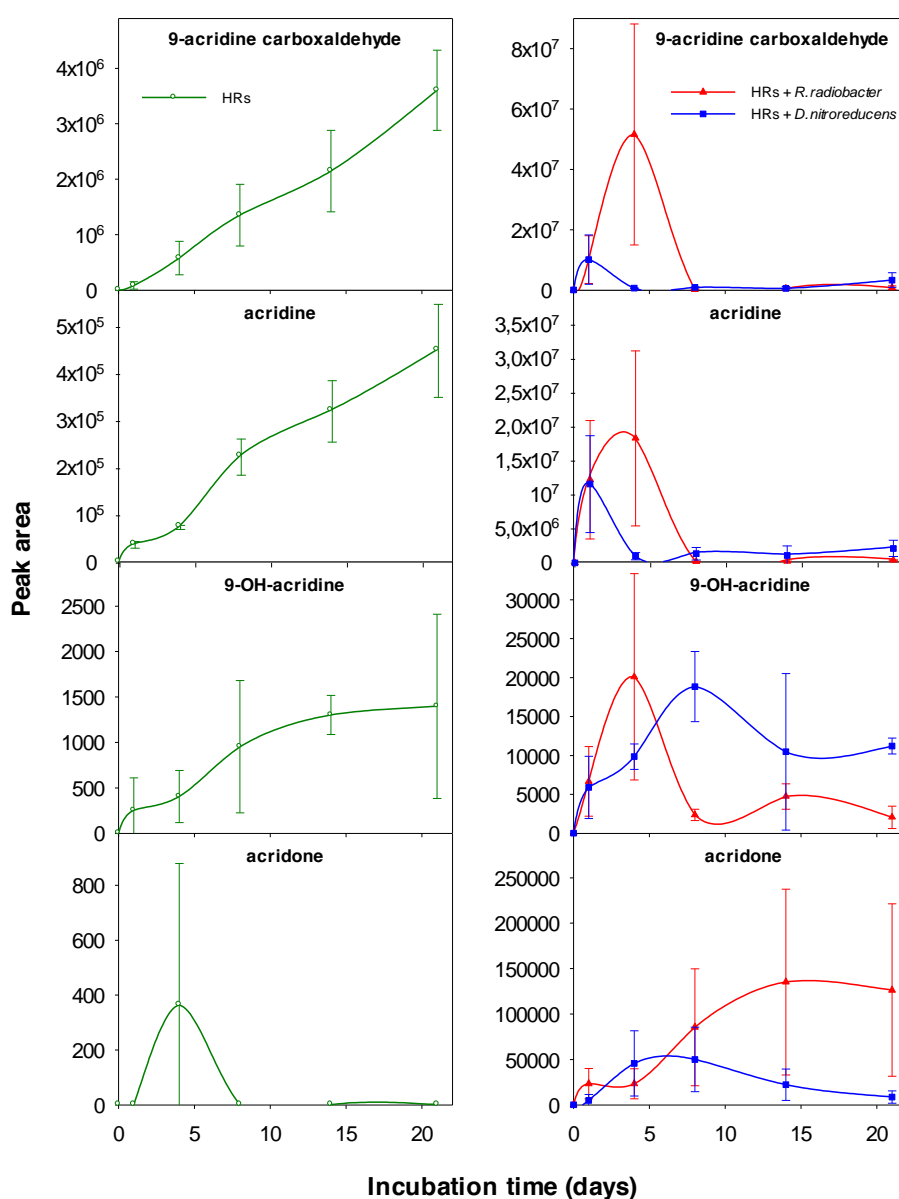


Figure 29: Carbamazepine (CBZ) transformation products in *A. rusticana* hairy root cultures II. Evolution of CBZ transformation products belonging to the acridine pathway during degradation by *A. rusticana* hairy root cultures and effect of the inoculation with the endophytic bacteria *R. radiobacter* and *D. nitroreducens* isolated from *P. australis*. CBZ initial concentration was 250  $\mu$ M. Peak area is in unit of mAU/g FW. Data are means  $\pm$  SD of three replicates.

Acridine is finally oxidized to acridone, a non-toxic compound, in two steps, with the formation of the intermediate 9-OH-acridine (reaction O, Fig. 28).

The first three compounds (9-acridine carboxaldehyde, acridine and 9-OH-acridine) showed an increase in the culture medium of HRs and an accumulation at the end of the incubation time. The total amount of each of these three TPs after 21 days of incubation was 10-fold lower than this of its predecessor. These TPs were identified in

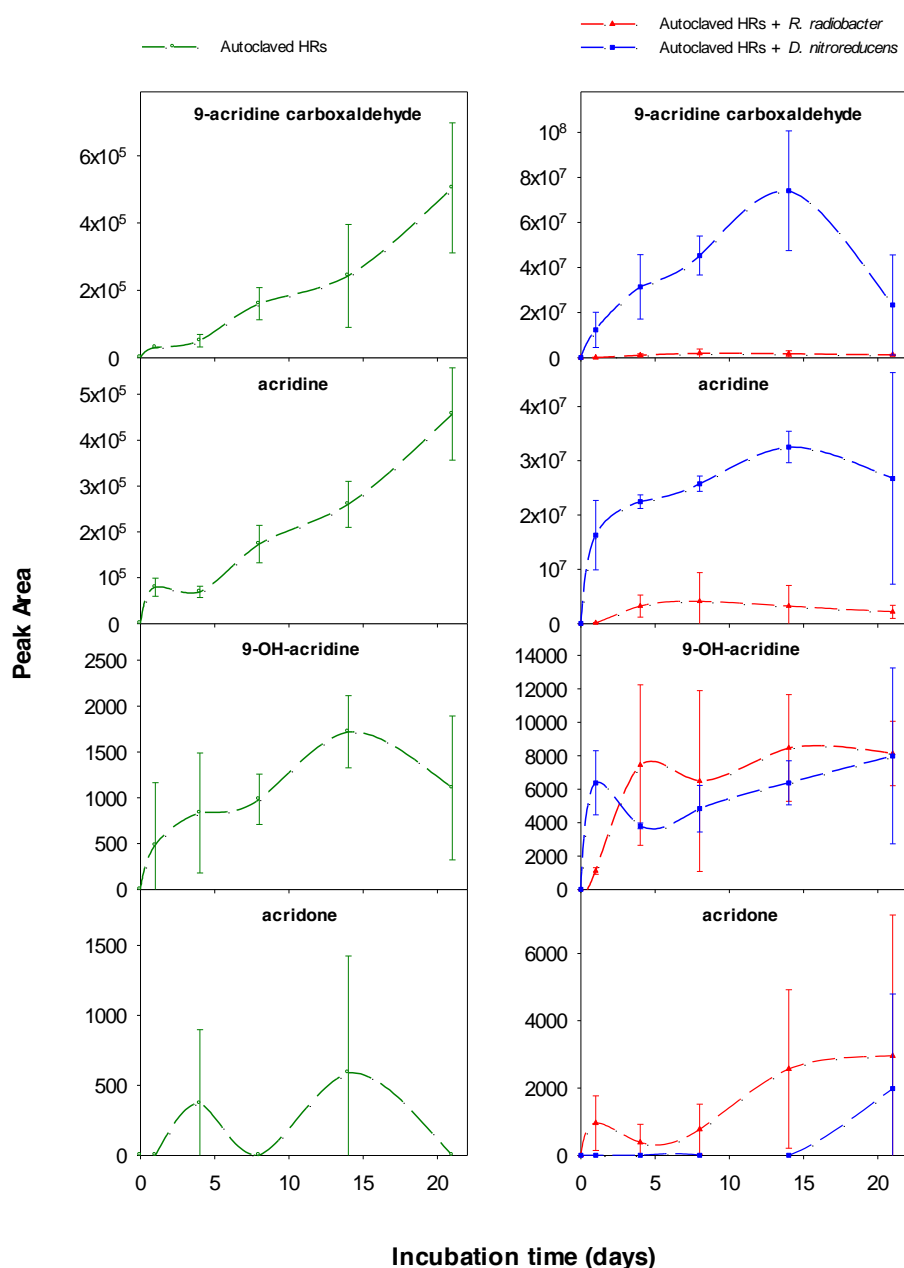


Figure 30: Carbamazepine (CBZ) transformation products in control *A. rusticana* hairy root cultures II. Evolution of CBZ transformation products belonging to the acridine pathway in controls corresponding to autoclaved *A. rusticana* hairy root cultures and autoclaved hairy roots inoculated with the endophytic bacteria *R. radiobacter* and *D. nitroreducens* isolated from *P. australis*. CBZ initial concentration was 250  $\mu\text{M}$ . Peak area is in unit of mAU/g FW. Data are means  $\pm$  SD of three replicates.

the media of autoclaved HRs showing trends and amounts like those exhibited in living roots (Fig. 30), suggesting that these compounds are formed by chemical oxidation.

Inoculation of HRs with *R. radiobacter* induced acridine pathway strongly, causing a burst in the synthesis of 9-acridine carboxaldehyde, acridine and 9-OH-acridine during the first days of incubation. A maximum in their concentration was reached after 4 days of incubation and was followed by a strong decrease. Acridone accumulated in these samples from the fourth day on, but this increase was not comparable to the decreasing trend of the upstream TPs. Similar trends were observed when HRs were inoculated with *D. nitroreducens*. At the end of the incubation, even the acridone signal decreased, suggesting the existence of further steps in the metabolic pathway of acridine-like TPs in inoculated roots. However, no TP related to further metabolism could be identified under the conditions used.

#### **4.3.3.5. Transformation products in root extracts**

After 21 days of incubation, metabolites were extracted from the root cultures. The composition of TPs identified previously in the media was determined in root extracts (Fig. 31). The amount of CBZ found in root extracts inoculated with endophytic bacteria was twice as high as in HR extracts, confirming the observations made in removal experiments with concentrations 10 and 25  $\mu\text{M}$  (Fig. 17). TPs of the diol pathways were equally distributed in HRs and inoculated HRs with a slight higher prevalence for the 2,3-diol pathway in roots inoculated with *R. radiobacter*. Acridine-related TPs were ten-fold higher in HRs inoculated with *D. nitroreducens*. This strain caused a high accumulation particularly of 9-acridine carboxaldehyde and acridine in root tissues with 10-fold and 20-fold increases respectively. Considering absolute amounts, this was the most relevant metabolic sub-pathway found in root extracts. Metabolites derived from GSH conjugation and subsequent degradation products were present in higher amounts in non-inoculated HRs. Particularly, CBZE-CYS was accumulated in great amounts in root tissues after 21 days of incubation.



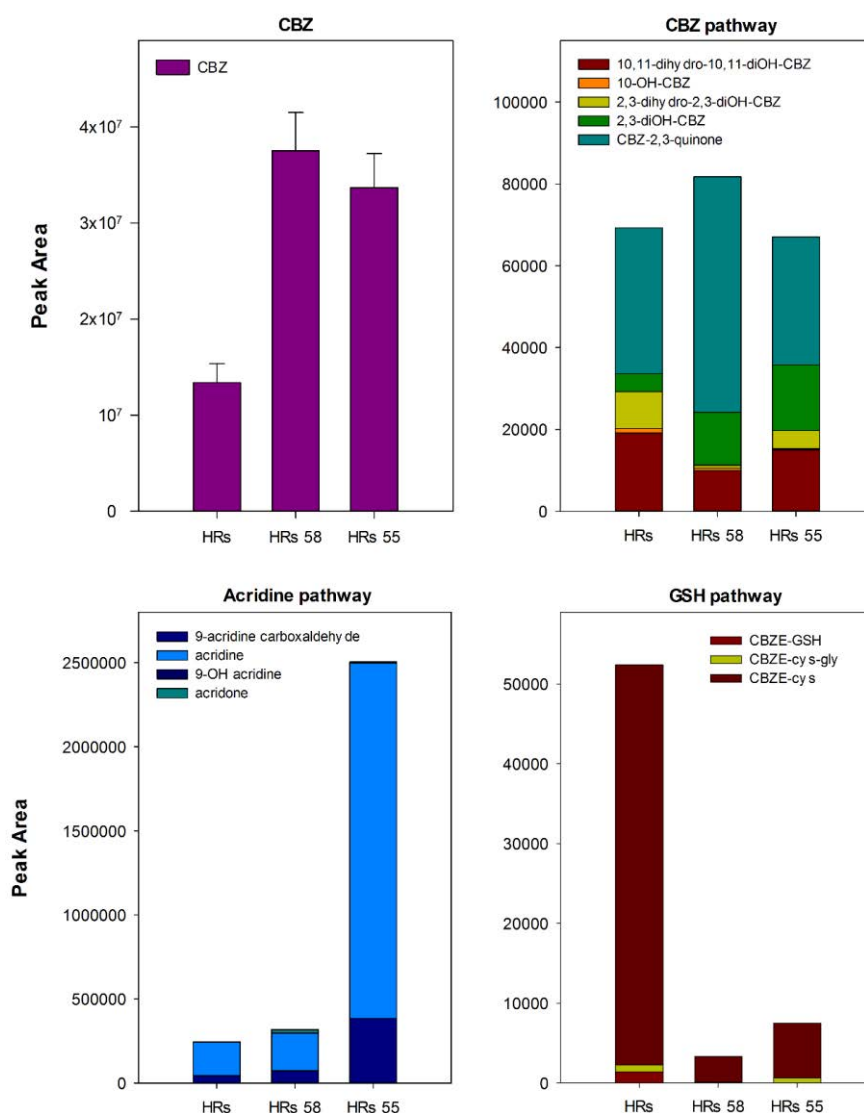


Figure 31: Summarizing carbamazepine (CBZ) transformation products in root extracts. Composition of the different transformation products identified in root extracts during carbamazepine metabolism in *A. rusticana* hairy roots (HRs) and hairy roots inoculated with the endophytic bacteria *R. radiobacter* (HRs 58) and *D. nitroreducens* (HRs 55). Extracts were performed after 21 days of incubation in 250  $\mu$ M CBZ.  $\mu$ M Peak area is in unit of mAU/g FW. Data are means  $\pm$  SD of three replicates.

#### 4.3.4. Proteomics analyses in hairy root cultures

To study in more detail the nature of interactions established between endophytic bacteria and plant roots, extracellular proteins in the media of HR cultures exposed to CBZ were characterized by tandem mass spectrometry. Samples from three independent biological replicates were harvested and analysed in a LC-QTOF mass spectrometer. Sampling was done after 4 days of incubation, once bacterial population were presumably well established and metabolically active inside the root tissues.

MS/MS spectra obtained were assigned to distinct tryptic peptides, allowing the identification of non-redundant proteins using the SwissProt database. Differences in the composition of the exoproteomes between treated and non-treated HRs as well as between treated HRs and treated HRs inoculated with endophytic bacteria were observed and analysed.

When HRs were cultivated in MS medium, 32 different plant proteins were identified in the growth medium (Table 20). Proteins were classified per biological processes in which they were involved. The main functions found were redox homeostasis and oxidative stress with 34% of the total proteins, biosynthesis of primary metabolites (amino acids, carbohydrates and lipids) with 19%, and defence response with 13%. Other minor functional categories were identified such as growth, cell wall structure and organization, protein signalling, transport and degradation, signalling, and lipid transport and metabolism, with 3% of the proteins in each of them.

When CBZ was added to the nutrient medium, the total amount of plant proteins detected increased to 90 (Table 21). The functional composition of the secreted proteome displayed some significant variations depending on treatment (Fig. 32). Two functional groups showed a decrease in the number of proteins affiliated to them: proteins involved in biosynthesis of primary metabolites dropped from 19 to 14% of the total proteins and proteins involved in redox homeostasis and oxidative stress decreased from 34 to 28%. On the other hand, identified proteins involved in cell wall structure and organization, signalling and defence increased when HRs were exposed to CBZ.

Table 20: Proteins identified in the nutrient medium of *A. rusticana* hairy roots after 4 days of incubation.

Entry	Protein name	Functional classification
P38562	Glutamine synthetase root isozyme 4 (EC 6.3.1.2)	Aminoacids biosynthesis
Q94JQ4	Reactive Intermediate Deaminase A, chloroplastic (EC 3.5.99.10)	
Q42656	$\alpha$ -galactosidase (EC 3.2.1.22)	Carbohydrate metabolism
Q9C525	$\beta$ -glucosidase 21 (EC 3.2.1.21)	
Q9SSG3	HIPL1 protein	
P86074	Malate dehydrogenase, mitochondrial (EC 1.1.1.37)	
Q38913	Extensin-1	Cell wall structure and organisation
O04310	Jacalin-related lectin 34	Defence
Q42952	Non-specific lipid-transfer protein 1	
Q9LLR6	Non-specific lipid-transfer protein 4 (LTP 4)	
Q9LSB4	TSA1-like protein	
Q42783	Biotin carboxyl carrier protein of acetyl-CoA carboxylase, chloroplastic	Fatty acid biosynthesis
Q9FM65	Fasciclin-like arabinogalactan protein 1	Growth
Q1H583	GDSL esterase/lipase 22 (EC 3.1.1.-)	Lipids transport and catabolism
P32746	Dihydroorotate dehydrogenase (quinone), mitochondrial (EC 1.3.5.2)	Nucleotide biosynthesis
P69310	Ubiquitin	Protein signaling and degradation
Q05431	L-ascorbate peroxidase 1, cytosolic (EC 1.11.1.11)	Redox homeostasis/ oxidative stress
Q96518	Peroxidase 16 (EC 1.11.1.7)	
Q9LSY7	Peroxidase 30 (EC 1.11.1.7)	
Q9LHB9	Peroxidase 32 (EC 1.11.1.7)	
Q96522	Peroxidase 45 (EC 1.11.1.7)	
Q43731	Peroxidase 50 (EC 1.11.1.7)	
P80679	Peroxidase A2 (EC 1.11.1.7)	
P00433	Peroxidase C1A (EC 1.11.1.7)	
P15233	Peroxidase C1C (EC 1.11.1.7)	
P00434	Peroxidase P7 (EC 1.11.1.7)	
O22263	Protein disulfide-isomerase like 2-1 (EC 5.3.4.1)	
Q9M8T0	Probable inactive receptor kinase At3g02880	Signalling
Q9SJ81	Fasciclin-like arabinogalactan protein 7	Unclassified
Q9ZWA8	Fasciclin-like arabinogalactan protein 9	
Q8W4H8	Inactive GDSL esterase/lipase-like protein 23	
Q39366	Putative lactoylglutathione lyase (EC 4.4.1.5)	

Table 21 Proteins identified in the nutrient medium of *A. rusticana* hairy roots exposed to 250  $\mu$ M carbamazepine after 4 days of incubation.

Entry	Protein name	Functional classification
Q67XZ3	$\beta$ -fructofuranosidase, insoluble isoenzyme CWINV3 (EC 3.2.1.80)	Carbohydrate metabolism
P45582	$\beta$ -galactosidase (Lactase) (EC 3.2.1.23)	
Q9SCV4	$\beta$ -galactosidase 8 (Lactase 8) (EC 3.2.1.23)	
Q9C525	$\beta$ -glucosidase 21 (EC 3.2.1.21)	
Q9SJQ9	Fructose-bisphosphate aldolase 6, cytosolic (EC 4.1.2.13)	
Q9LF98	Fructose-bisphosphate aldolase 8, cytosolic (EC 4.1.2.13)	
P46257	Fructose-bisphosphate aldolase, cytoplasmic isozyme 2 (EC 4.1.2.13)	
Q9ZU91	Glucan endo-1,3-beta-glucosidase 3 (EC 3.2.1.39)	
Q93Z08	Glucan endo-1,3-beta-glucosidase 6 (EC 3.2.1.39)	
Q9SSG3	HIPL1 protein	
Q43744	Malate dehydrogenase, mitochondrial (EC 1.1.1.37)	
Q38913	Extensin-1	Cell wall structure and organization
Q9LXD9	Probable pectinesterase/pectinesterase inhibitor 51	
Q38910	Probable xyloglucan endotransglucosylase/hydrolase protein 23 (EC 2.4.1.207)	
Q9FKL8	Putative xyloglucan endotransglucosylase/hydrolase protein 13 (EC 2.4.1.207)	
Q38857	Xyloglucan endotransglucosylase/hydrolase protein 22 (EC 2.4.1.207)	
P24806	Xyloglucan endotransglucosylase/hydrolase protein 24 (EC 2.4.1.207)	
Q9FZ37	Putative UDP-glucuronate:xylan alpha-glucuronosyltransferase 4 (EC 2.4.1.-)	
P80828	54 kDa cell wall protein	
P34893	10 kDa chaperonin, mitochondrial (Chaperonin 10)	Defence
P19172	Acidic endochitinase (EC 3.2.1.14)	
P28814	Barwin	
P19171	Basic endochitinase B (EC 3.2.1.14)	
Q06209	Basic endochitinase CHB4 (EC 3.2.1.14)	
F4HWQ8	Cell wall / vacuolar inhibitor of fructosidase 1 (AtC/VIF1)	
Q9LNU1	CO(2)-response secreted protease (EC 3.4.14.10)	
O24331	Defensin-like protein 4	
O04310	Jacalin-related lectin 34	
P05087	Leucoagglutinating phytohemagglutinin (PHA-L)	
Q941R6	MLP-like protein 31	
Q9ZVF3	MLP-like protein 328	
Q9C7F7	Non-specific lipid transfer protein GPI-anchored 1	
A0A161	Non-specific lipid-transfer protein 1	
Q9LLR6	Non-specific lipid-transfer protein 4 (LTP 4)	
Q9FMH8	Probable cysteine protease RD21B (EC 3.4.22.-)	
Q9LSB4	TSA1-like protein	

Entry	Protein name	Functional classification
Q42533	Biotin carboxyl carrier protein of acetyl-CoA carboxylase 1, chloroplastic	Fatty acid biosynthesis
Q9LLC1	Biotin carboxyl carrier protein of acetyl-CoA carboxylase 2, chloroplastic	
Q9FM65	Fasciclin-like arabinogalactan protein 1	Growth
Q9SZ11	Glycerophosphodiester phosphodiesterase GDPDL3 (EC 3.1.4.46)	
Q9SHY6	Putative expansin-B2	
Q9ZPW9	Non-specific lipid-transfer protein 8	Lipid transport and catabolism
Q1H583	GDSL esterase/lipase 22 (EC 3.1.1.-)	
Q42342	Cytochrome b5 isoform E	Oxidation-reduction
P00052	Cytochrome c	
O80517	Uclacyanin-2	
O04496	Aspartyl protease AED3 (EC 3.4.23.-)	Protein signalling, transport and degradation
Q56WF8	Serine carboxypeptidase-like 48 (EC 3.4.16.-)	
Q7XA74	Inactive GDSL esterase/lipase-like protein 25	
Q6NMS0	Glutathione S-transferase U12 (EC 2.5.1.18)	Redox homeostasis and oxidative stress
Q9SVG4	Berberine bridge enzyme-like 19 (EC 1.1.1.-)	
P22196	Cationic peroxidase 2 (EC 1.11.1.7)	
Q9SI17	Peroxidase 14 (EC 1.11.1.7)	
Q9SI16	Peroxidase 15 (EC 1.11.1.7)	
O23044	Peroxidase 3 (EC 1.11.1.7)	
P24101	Peroxidase 33 (EC 1.11.1.7)	
Q9SUT2	Peroxidase 39 (EC 1.11.1.7)	
Q9SZB9	Peroxidase 47 (EC 1.11.1.7)	
Q43731	Peroxidase 50 (EC 1.11.1.7)	
Q9SZE7	Peroxidase 51 (EC 1.11.1.7)	
Q9FG34	Peroxidase 54 (EC 1.11.1.7)	
Q9LXG3	Peroxidase 56 (EC 1.11.1.7)	
Q9FKA4	Peroxidase 62 (EC 1.11.1.7)	
Q9FMI7	Peroxidase 70 (EC 1.11.1.7)	
P80679	Peroxidase A2 (EC 1.11.1.7)	
P00433	Peroxidase C1A (EC 1.11.1.7)	
P15233	Peroxidase C1C (EC 1.11.1.7)	
P59121	Peroxidase E5 (EC 1.11.1.7)	
Q42517	Peroxidase N (EC 1.11.1.7)	
P00434	Peroxidase P7 (EC 1.11.1.7)	
Q9XI01	Protein disulfide isomerase-like 1-1 (EC 5.3.4.1)	
Q9SRG3	Protein disulfide isomerase-like 1-2 (EC 5.3.4.1)	
O22263	Protein disulfide-isomerase like 2-1 (EC 5.3.4.1)	
Q39241	Thioredoxin H5	
Q9LV60	Cysteine-rich repeat secretory protein 55	Signalling
O82328	Gibberellin-regulated protein 7	
Q9M8T0	Probable inactive receptor kinase At3g02880	
Q9LUL4	Protein STRUBBELIG-RECEPTOR FAMILY 7	

Entry	Protein name	Functional classification
Q9SIT1	Receptor-like kinase TMK3 (EC 2.7.11.1)	Signalling
Q9SA89	Berberine bridge enzyme-like 12 (EC 1.1.1.-)	Unclassified
Q9FKU9	Berberine bridge enzyme-like 25 (EC 1.1.1.-)	
Q9SK27	Early nodulin-like protein 1	
Q9SU13	Fasciclin-like arabinogalactan protein 2	
Q9SJ81	Fasciclin-like arabinogalactan protein 7	
Q9ZWA8	Fasciclin-like arabinogalactan protein 9	
Q8W4H8	Inactive GDSL esterase/lipase-like protein 23	
Q9LE22	Probable calcium-binding protein CML27	
Q39366	Putative lactoylglutathione lyase (EC 4.4.1.5)	
P55748	Serine carboxypeptidase II-2 (EC 3.4.16.6)	
P48522	Trans-cinnamate 4-monooxygenase (EC 1.14.13.11)	

When HRs were inoculated with *D. nitroreducens*, 84 distinct proteins were identified in the nutrient media after 4 days. When roots were inoculated with *R. radiobacter*, this number even increased to 120 proteins. From the total number of distinct proteins identified in all conditions, 16 proteins were found in the nutrient medium when HRs were incubated with or without previous inoculation (Fig. 33). Five proteins were found in the nutrient medium of HRs and inoculated HRs with *R. radiobacter*. This number increased to 38 proteins shared by HRs and HRs inoculated with *D.*

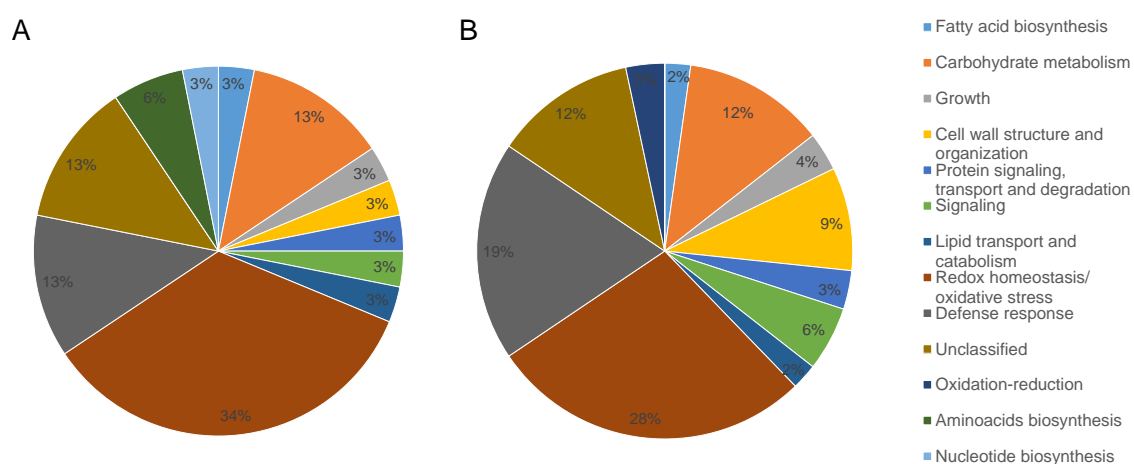


Figure 32: Functional classification of proteins identified after 4 days in the nutrient media of *A. rusticana* hairy root cultures (A) and hairy root cultures exposed to 250 µM carbamazepine (B). Samples were taken in triplicates from the nutrient media after 4 days of incubation and analysed by tandem mass spectrometry. Proteins were identified and assigned to biological processes using the SwissProt database.

*nitroreducens*. 5 proteins were identified in both media of inoculated HRs. Still, big differences were found between the different conditions, and some proteins seemed to be very exclusive for each condition. Roots inoculated with the endophytic strain *R. radiobacter* presented the highest number of exclusive proteins. Indeed, from a total of 294 proteins, 93 proteins were identified only in the nutrient medium of HRs inoculated with *R. radiobacter* (Table 22). Finally, 30 proteins were exclusive to non-inoculated HRs whereas 24 were specific to inoculated HRs with *D. nitroreducens*. (Table 23).

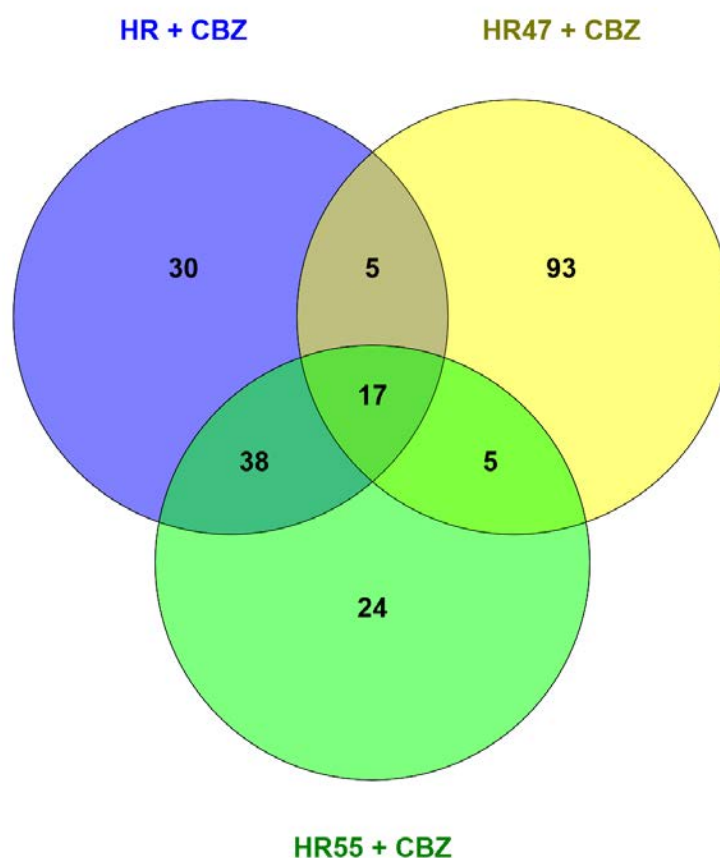


Figure 33: Venn diagram showing the number of plant proteins identified in nutrient media from *A. rusticana* hairy root cultures void of or inoculated with endophytic bacteria and exposed to 250  $\mu$ M carbamazepine. The numbers of proteins detected through identification is indicated in each category (HRs, HRs inoculated with *R. radiobacter* (HR47) and HRs inoculated with *D. nitroreducens* (HR55)). Samples were taken after 4 days of incubation.

Table 22: Proteins identified in the nutrient medium of inoculated *A. rusticana* hairy root cultures with *R. radiobacter* and exposed to 250  $\mu$ M carbamazepine, after 4 days of incubation.

Entry	Protein names	Functional classification
O50039	Ornithine carbamoyltransferase, chloroplastic (EC 2.1.3.3)	Amino acid biosynthesis
O65396	Aminomethyltransferase, mitochondrial (EC 2.1.2.10)	
O50008	5-methyltetrahydropteroyltriglutamate--homocysteine methyltransferase 1 (EC 2.1.1.14)	
P46248	Aspartate aminotransferase, chloroplastic (EC 2.6.1.1)	
O04937	Glutamate dehydrogenase A (GDH A) (EC 1.4.1.3)	
Q9SRV5	5-methyltetrahydropteroyltriglutamate--homocysteine methyltransferase 2 (EC 2.1.1.14)	
P31265	Translationally-controlled tumor protein 1 (TCTP1)	Auxin homeostasis
P48491	Triosephosphate isomerase, cytosolic (TIM) (EC 5.3.1.1)	Carbohydrate metabolism
P93819	Malate dehydrogenase 1, cytoplasmic (EC 1.1.1.37)	
Q9SML8	Malate dehydrogenase, cytoplasmic (EC 1.1.1.37)	
O04955	Glutathione reductase, cytosolic (GR) (EC 1.8.1.7)	Cell redox homeostasis
Q93WJ8	Monodehydroascorbate reductase 2 (EC 1.6.5.4)	
Q9M5K3	Dihydrolipoyl dehydrogenase 1, mitochondrial (EC 1.8.1.4)	
Q9XEX2	Peroxiredoxin-2B (EC 1.11.1.15)	
Q9M9P3	UTP--glucose-1-phosphate uridylyltransferase 2 (EC 2.7.7.9)	Cell wall organization, stress response
Q96266	Glutathione S-transferase F8, chloroplastic (EC 2.5.1.18)	Defence response
O81235	Superoxide dismutase [Mn] 1, mitochondrial (EC 1.15.1.1)	
P22953	Probable mediator of RNA polymerase II transcription subunit 37e (Heat shock 70 kDa protein 1)	
Q1JPL7	Pectinesterase/pectinesterase inhibitor 18 (EC 3.1.1.11)	
Q9SRZ6	Cytosolic isocitrate dehydrogenase [NADP] (EC 1.1.1.42)	
Q9SSK7	MLP-like protein 34	
QQJJ01	BTB/POZ domain and ankyrin repeat-containing protein NPR2	Defence response, protein degradation
P85121	Ferredoxin	Electron transport chain
Q42783	Biotin carboxyl carrier protein of acetyl-CoA carboxylase, chloroplastic (BCCP)	Fatty acid biosynthesis
P21820	Triosephosphate isomerase, cytosolic (TIM) (EC 5.3.1.1)	Glycolysis



Entry	Protein names	Functional classification
O04499	2,3-bisphosphoglycerate-independent phosphoglycerate mutase 1 (EC 5.4.2.12)	
Q42962	Phosphoglycerate kinase, cytosolic (EC 2.7.2.3)	
Q9FXM5	Glucose-6-phosphate isomerase, cytosolic (GPI) (EC 5.3.1.9)	
Q9LD57	Phosphoglycerate kinase 1, chloroplastic (EC 2.7.2.3)	
Q9M9K1	Probable 2,3-bisphosphoglycerate-independent phosphoglycerate mutase 2 (EC 5.4.2.12)	
Q9SAJ4	Phosphoglycerate kinase 3, cytosolic (EC 2.7.2.3)	
Q96262	Plasma membrane-associated cation-binding protein 1	Ion response
Q9SYT0	Annexin D1	Ion transport
Q93ZR6	O-acyltransferase WSD1 (Diacylglycerol O-acyltransferase) (EC 2.3.1.20)	Lipid biosynthesis
P42643	14-3-3-like protein GF14 chi	Metabolism
P57751	UTP--glucose-1-phosphate uridylyltransferase 1 (EC 2.7.7.9)	
Q56XG6	DEAD-box ATP-dependent RNA helicase 15 (EC 3.6.4.13)	mRNA transport
Q9LMK7	Ran-binding protein 1 homolog a (Ran-binding protein siRanBP)	
Q9M7P6	Nucleoside diphosphate kinase (EC 2.7.4.6)	Nucleotide biosynthesis
P00063	Cytochrome c	Oxidation-reduction
P26852	Cytochrome b (Complex III subunit 3)	
P15232	Peroxidase C1B (EC 1.11.1.7)	Oxidative stress
P17180	Peroxidase C3 (EC 1.11.1.7)	
P21276	Superoxide dismutase [Fe] 1, chloroplastic (EC 1.15.1.1)	
Q9FPF0	Protein DJ-1 homolog A	
Q9MOV6	Ferredoxin--NADP reductase, root isozyme 1, chloroplastic (EC 1.18.1.2)	Photosynthesis
O23715	Proteasome subunit alpha type-3 (EC 3.4.25.1)	Protein degradation
P35135	Ubiquitin-conjugating enzyme E2-17 kDa (EC 2.3.2.23)	
P69310	Ubiquitin	
Q8LC69	RING-H2 finger protein ATL8 (EC 2.3.2.27)	
Q9SVD7	Ubiquitin-conjugating enzyme E2 variant 1D	

Entry	Protein names	Functional classification
P24525	Peptidyl-prolyl cis-trans isomerase (PPlase) (EC 5.2.1.8)	Protein folding
Q38867	Peptidyl-prolyl cis-trans isomerase CYP19-3 (PPlase CYP19-3) (EC 5.2.1.8)	Protein folding
Q38900	Peptidyl-prolyl cis-trans isomerase CYP19-1 (PPlase CYP19-1) (EC 5.2.1.8)	Protein folding
Q8GUM2	Heat shock 70 kDa protein 9, mitochondrial	Protein folding
Q9LDZ0	Heat shock 70 kDa protein 10, mitochondrial	Protein folding, defence
Q9ASS6	Photosynthetic NDH subunit of lumenal location 5, chloroplastic (EC 5.2.1.8)	Protein folding, transport
P31542	ATP-dependent Clp protease ATP-binding subunit ClpA homolog CD4B, chloroplastic	Protein metabolism
P42730	Chaperone protein ClpB1	Protein metabolism
P84557	GTP-binding nuclear protein Ran	Protein transport
Q53PC7	Coatomer subunit beta-1	Protein transport
Q9CA23	Ubiquitin-fold modifier 1	Protein Ufmylation
Q9ZSK4	Actin-depolymerizing factor 3 (ADF-3)	Response to oxidative stress
Q42418	Profilin-2	Root development
Q9M0A7	$\gamma$ -glutamyl peptidase 1 (EC 3.4.19.-)	Secondary metabolism
Q944P7	Leucine aminopeptidase 2, chloroplastic (EC 3.4.11.1)	Senescence
P34790	Peptidyl-prolyl cis-trans isomerase CYP18-3 (EC 5.2.1.8)	Signaling
Q01525	14-3-3-like protein GF14 omega	
Q43348	Acid beta-fructofuranosidase 3, vacuolar (EC 3.2.1.26)	
Q38882	Phospholipase D alpha 1 (EC 3.1.4.4)	Signaling, lipid catabolism
P30184	Leucine aminopeptidase 1 (EC 3.4.11.1)	Stress response
P39207	Nucleoside diphosphate kinase 1 (EC 2.7.4.6)	
P55852	Small ubiquitin-related modifier 1	
Q9LZ66	Assimilatory sulfite reductase (ferredoxin), chloroplastic (EC 1.8.7.1)	Transcription regulation
P42731	Polyadenylate-binding protein 2 (PABP-2)	
P93736	Valine-tRNA ligase, mitochondrial 1 (EC 6.1.1.9)	
Q39779	Acyl-CoA-binding protein (ACBP)	Transport
O04487	Probable elongation factor 1-gamma 1 (EF-1-gamma 1)	Unclassified

---

<b>Entry</b>	<b>Protein names</b>	<b>Functional classification</b>
O80699	Putative Tubby-like protein 4 (AtTLP4)	
P07803	Non-symbiotic hemoglobin	
P0DH95	Calmodulin-1 (CaM-1)	
P41372	Profilin-1	
P48006	Elongation factor 1-delta 1 (EF-1-delta 1)	
P85919	Unknown protein 14 (Fragment)	
Q2PS27	Translationally-controlled tumor protein homolog (TCTP)	
Q41649	FK506-binding protein 2 (EC 5.2.1.8)	
Q7G7C7	Signal peptide peptidase-like 1 (EC 3.4.23.-)	
Q8L831	Nudix hydrolase 3 (EC 3.6.1.-)	
Q93ZA3	Berberine bridge enzyme-like 13 (EC 1.1.1.194)	
Q944W6	Translationally-controlled tumor protein homolog (TCTP)	
Q94AZ4	Probable calcium-binding protein CML13	
Q9FM19	Hypersensitive-induced response protein 1	
Q9LPC3	Berberine bridge enzyme-like 1 (EC 1.1.1.-)	

---

Table 23: Proteins identified in the nutrient medium of inoculated hairy root cultures with *D. nitroreducens* and exposed to 250  $\mu$ M carbamazepine, after 4 days of incubation.

Entry	Protein names	Functional classification
Q94JQ4	Reactive Intermediate Deaminase A, chloroplastic (EC 3.5.99.10)	Aminoacid biosynthesis
Q9FXT4	$\alpha$ -galactosidase (EC 3.2.1.22)	Carbohydrate metabolism
Q9SLA0	$\beta$ -glucosidase 14 (EC 3.2.1.21)	
Q8VZJ2	Probable glucan endo-1,3-beta-glucosidase (EC 3.2.1.39)	
Q56UD1	$\beta$ -fructofuranosidase, insoluble isoenzyme 5 (EC 3.2.1.26)	
A7PZL3	Probable polygalacturonase (PG) (EC 3.2.1.15)	
Q6NKW9	Glucan endo-1,3-beta-glucosidase 8 (EC 3.2.1.39)	Carbohydrate metabolism, cell wall, defence
Q9FS16	Extensin-3	Cell wall organization
Q9ZSU4	Xyloglucan endotransglucosylase/hydrolase protein 14 (EC 2.4.1.207)	
O80803	Probable xyloglucan endotransglucosylase/hydrolase protein 17 (EC 2.4.1.207)	
Q84LF2	5-epi-aristolochene synthase 3 (EC 4.2.3.61)	Defence response
Q9FLG1	$\beta$ -D-xylosidase 4 (EC 3.2.1.37)	
O65719	Heat shock 70 kDa protein 3	
Q8W593	Probable lactoylglutathione lyase, chloroplastic (EC 4.4.1.5)	
Q93ZH0	LysM domain-containing GPI-anchored protein 1	
Q9SD84	PLASMODESMATA CALLOSE-BINDING PROTEIN 2	
P00059	Cytochrome c	Oxidation-reduction
Q05431	L-ascorbate peroxidase 1, cytosolic (AP) (EC 1.11.1.11)	Oxidative stress
Q9SN20	Putative F-box protein	Protein degradation
Q9LRJ9	Cysteine-rich repeat secretory protein 38	Signaling
Q9AWS0	AP2/ERF and B3 domain-containing protein	Transcription
P21529	Serine carboxypeptidase 3 (EC 3.4.16.5)	Unclassified
Q9FZP1	Heparinase-like protein 3 (EC 3.2.-.-)	
Q9M5J9	Polygalacturonase inhibitor 1	

## 5. Discussion

Fresh water is one of the most important natural resources for human activities. On the planetary scale, only the 3% of total water in earth is fresh water, the rest is sea water. Over two thirds of the fresh water is immobilized in glaciers and polar caps. A very small fraction is present on the surface and atmosphere, and the biggest part of exploitable fresh water is stored as groundwater. Unfortunately, groundwater recharge is dramatically decreasing in the last years due to climate change (Gleeson et al., 2012). Moreover, the continuous growth of the world population and the intensive urbanization is leading to an increase of water usage for human activities. To face this increasing demand in fresh water and to decrease the stress on the water cycle, the reuse of treated wastewater is an option gaining importance.

To ensure “good ecological and chemical status” for all Community waters, the European Union has established a Community framework for water protection and management. In this context, the EU Water Framework Directive was published in 2000, aiming at intensifying the monitoring of pollutants in ecosystems and enhancing the control of contaminants release, to keep waterbodies clean and safe (EU Water Framework Directive 2000). In 2008, 33 priority substances were identified as dangerous to water and 13 other were proposed to be identified as priority substances (Directive 2008/105/EC, 2008). This list was updated in 2013 to 45 priority substances (Directive 2013/39/EU, 2013). Besides the traditional pollutants, emerging contaminants are of increasing concern. In recent years, pharmaceutical compounds and metabolites have been found not only in surface and ground water, but even in the drinking water supplies of many countries. In 2015, for the first time, the European commission included three pharmaceuticals in a watch list of 17 compounds that must be monitored in surface waters within the EU (Decision 2015/495/EU, 2015). Some of these compounds have shown to be very recalcitrant, and are not completely removed using traditional methods. To meet appropriate water quality requirements, the use of plants is a complementary tool to other physicochemical treatments that may not be sufficient. In fact, plants can act as living filters for such compounds, and can be used to phytoremediate polluted waters (Schröder et al., 2002).

CWs are currently used to treat wastewater effluents. These artificial systems are based on the ability of natural wetlands to remove pollutants from water and improve water quality. Physical, chemical and biological processes favouring the removal of pollutants occur simultaneously in these complex systems (Zhang et al., 2014). Thus, the control of factors like volatilization, sorption, sedimentation, photodegradation, plant uptake or microbial degradation, will determine the final removal efficiency of the system for a given compound. Plant uptake depends on the physicochemical properties of the compound, the plant species and the environmental conditions. Considering that the first and the last are predetermined by the location and the compound to remove, the choice of the plant species will determine the degree of achievement and applicability of CWS for the removal of contaminants. For an efficient removal of compounds consistently found in wastewater worldwide, the plant should have a high biomass, an extended root system, high transpiration rate and an ample distribution and adaptation to different habitats. *P. australis* meets all these constraints and therefore is the second most used species in CWS (Vymazal, 2011).

In this chapter, the previously presented experimental results are critically discussed in context with the current scientific knowledge in the field and recommendations for applications in wastewater treatment are given.

## **5.1. Phytoremediation of carbamazepine: plant uptake and oxidative stress**

### **5.1.1. Carbamazepine uptake in *Armoracia rusticana* hairy roots**

CBZ removal by HRs was studied in short time experiments with initial CBZ concentrations of 10 and 25  $\mu\text{M}$  spiked to the media. These concentrations were chosen because of their ecological relevance, representing concentrations frequently found in WWTP effluents (Zhang et al., 2008). HRs removed about 5% and 4% of the initial concentration (10 and 25  $\mu\text{M}$  respectively) after 6 days of incubation. The total amount of CBZ removed increased with the initial concentration of the treatment. Given that the removal of CBZ strongly correlated with the initial concentration in the media ( $r = 0.99$ ), we suggest that CBZ moves into root tissues driven by simple diffusion. Generally, it is expected that organic xenobiotics with optimum hydrophobicity ( $\log K_{ow}$  between 0.5 and 3.5) are readily taken up by plants (Barac et al., 2004).

### 5.1.2. Carbamazepine uptake in *Phragmites australis*

Several studies have reported CBZ uptake into crop plants such as lettuce (Hurtado et al., 2016), maize (Ryšlavá et al., 2015) or cucumber (Shenker et al., 2011) among others. Recently the uptake of CBZ into the wetland species *Typha latifolia* has been demonstrated (Dordio et al., 2011). The authors performed a treatment with 2 mg/L CBZ and showed a removal of 28% after 7 days. In our study with *P. australis*, removal of 90% was observed after 9 days of incubation using a higher initial concentration (5 mg/L). CBZ removal after 7 days could be estimated to 80% of the initial amount, still much higher than the results obtained with *Typha*. Measurements of CBZ remaining in the control pots after 9 days revealed no adsorption to the perlite or vessel walls over the time. Some studies have shown a correlation between uptake rates of organic xenobiotics in *Phragmites* and log  $K_{OW}$  and  $pK_a$  values of the xenobiotic. Compounds exhibiting log  $K_{OW}$ s between 1 and 3 present are taken up in higher amounts by this plant species (Schröder et al., 2008). CBZ, with a log  $K_{OW}$  of 2.45 shows better uptake in *Phragmites* than in *Typha* suggesting a greater transport from roots to shoots, a process highly influenced by the transpiration rate of the plant. However, Chazarenc and coworkers (2010) were not able to attribute any differences in evapotranspiration rates to the morphology of both species. Hence, other effects like plant biomass, ionic interactions, sorption etc. might be responsible for the higher retention of CBZ in *Phragmites* tissues.

The effect of macrophyte species selection on pollutant removal in subsurface-flow CWs has been summarized in a review of 35 experimental studies published in peer-reviewed journals and proceedings (Brisson and Chazarenc, 2009). The authors found differences between plant species, even though these were not generalized, giving in some cases opposite results in different studies. Hijosa-Valsero and coworkers studied in 2010 the removal efficiency of CBZ among other PPCPs in seven mesocosm-scale CWs differing in some design parameters, including plant species (Hijosa-Valsero et al., 2010). In their study, they could not see any difference in the removal of CBZ in summer (48%), but they found small differences in winter, when *P. australis* removed higher amounts of CBZ than *Typha angustifolia* (36% against 34%). These observations led to the assumption that plant species does matter, although there are other factors like the composition of microbial communities that may play an important role in the removal efficiency in real conditions.

### 5.1.3. Antioxidants responses in *Phragmites australis* and role of GSTs

When plants are exposed to stressful biotic or abiotic conditions, the production of reactive oxygen species (ROS) increases and can result in cell damage. To protect themselves against these oxidants, they need to maintain cellular redox homeostasis. Therefore, plants have evolved ROS-scavenging enzymes (superoxide dismutase (SOD), catalase (CAT), monodehydroascorbate reductase (MDAR), dihydroascorbate reductase (DHAR), glutathione reductase (GR), glutathione peroxidase (GP), ascorbate peroxidase (APOX) and peroxidase (POX)) and antioxidant molecules like ascorbic acid,  $\alpha$ -tocopherols, glutathione, prolin, flavonoids and carotenoids (Trchounian et al., 2016). The underlying enzymatic network is referred to as the Halliwell-Asada-cycle, buffering ROS and their possible detrimental effects. The ability of the plant to surmount the overproduction of ROS and maintain the redox balance in the cells will determine its potential for CBZ uptake and accumulation. Thus, it seemed important to study ROS-scavenging enzymes in *P. australis* exposed to CBZ.

Bartha (2012) showed a strong induction of the ROS scavenging enzymes GR, APOX and cytosolic POX in *Typha latifolia* shoots after 1 day of exposure to 1 mg/L of the pharmaceutical diclofenac (Bartha, 2012). From the third day onwards, the induction decreased and even was reverted in the case of GR and POX. In root tissues, POX was strongly induced from the first day on, reaching a maximum after 7 days and equalling values of control plants after 30 days. No differences between control and treated plants were observed in GR and APOX activities in roots. From these observations, it is obvious that plants react rapidly to xenobiotic exposure, and that it is generally possible to observe changes in ROS-scavenging enzymatic activities already after one day.

Consequently, the antioxidant enzymatic responses of *P. australis* plants exposed to CBZ after 24 and 48 h were investigated in this study. The activity of GR, APOX and cytosolic POX was assayed in protein extracts from roots, rhizomes and leaves of plants exposed to 100  $\mu$ M CBZ. No statistically significant differences in any enzyme activity were observed between control and treated plants. GR, POX and APOX activities in leaves increased sensibly after treatment with CBZ. In roots, POX and APOX activities decreased after CBZ treatment and were lower for the next 48 h, while GR decreased immediately after treatment but recovered after 48 h. In rhizomes, there was a small induction only after 48 h. The Halliwell-Asada cycle is obviously set



to buffer the initial ROS dependent stress reaction. In general rhizomes showed a higher activity of these enzymes revealing a high metabolic activity in these tissues. However, the low reactive antioxidant enzymatic activity was concentrated in leaves and not in rhizomes revealing that metabolism of the compound takes place in the leaves and/or that the reactive metabolites are rapidly transported to the aerial part of the plant. Especially important is the role of peroxidases as they may be directly involved in the metabolism of CBZ, during the first oxidation steps of the parent compound.

These findings suggest that *Phragmites* can deal well with this concentration of CBZ in the medium. Moreover, plants did not show any visible phytotoxic symptoms, maintaining a healthy appearance throughout the experiment. Together with the removal rates observed in our previous experiment, these results confirm that *P. australis* is a well-suited macrophyte species to remove CBZ from polluted water. Similar results were obtained in a study realized on ibuprofen uptake and transformation (He et al., 2017).

Glutathione-S-transferases are a large enzyme family present in all plants. They are involved in a large array of functions including detoxification of xenobiotics and endobiotics, primary and secondary metabolism, stress tolerance, and cell signalling. They can be regarded as loosely connected to the Halliwell-Asada-cycle via the availability of GSH, It has been shown that GSTs tag xenobiotic molecules by conjugating them with glutathione for their vacuolar import by ABC transporters (Edwards and Dixon, 2005). Their elevated expression is gaining acceptance as marker for plant response to stress (Labrou et al., 2015).

We determined the activity of GST enzymes in leaves, rhizomes and roots of treated plants, using different substrates to roughly identify the distribution of different isoforms of the enzyme in plant tissues. Again, higher activity was found in rhizomes. GST activity was slightly higher after treatment in leaves, without big differences between substrates used. In rhizomes, GST activity increased significantly after exposure to CBZ, especially after 48 h of incubation. The highest increase was observed after 48 h in rhizomes and using CDNB as substrate. In root tissues, an increase was observed only with fluorodifen after 24 h, recovering control values after 48 h.

An induction of GST activity in leaves and roots from *P. australis* exposed to paracetamol and diclofenac has been reported in previous studies (Neustifter, 2007). Similar observations were made in *Typha* plants (Bartha, 2012). Our results differ in root tissues, showing a faster transport of the compound to metabolically active parts of the plant like rhizomes or leaves. This difference can be attributable to the physicochemical characteristics of the compounds. In fact, compounds too hydrophobic or too hydrophilic cannot cross biological membranes, the first because they cannot dissolve into the phospholipid bilayer, the second because they are repelled by the plasma membrane. Polar compounds with log  $K_{ow}$  between 1 and 3 like CBZ are most appropriate for uptake and translocation into aerial parts.

## **5.2. Isolation of endophytic bacteria from reed to improve phytoremediation**

Plants and their microbiota form an inseparable and unique entity known as holobiont. A wide diversity of microorganisms inhabits inside and outside plant tissues (endosphere and ectosphere) contributing to some biological functions such as plant nutrition or resistance to biotic and abiotic stresses (Vandenkoornhuyse et al., 2015). The development of new omics approaches has shown that the plant microbiome may indeed play an important role in the removal of organic contaminants bringing a vast array of applications to the field of phytoremediation (Thijs et al., 2017).

To study the role of plant microbiome in the plant holobiont metabolic functions such as xenobiotic removal there are two approaches. The first is the use of -omic tools to determine the community structure of exposed plants and to perform functional analyses on metagenomes at community level. The second is the cultivation approach which does not complete the full characterization of the community but allows working with isolated strains in sub-sequent re-inoculation studies. In our work, we investigated the role of *P. australis* associated bacteria in the removal and metabolism of CBZ in plant roots as well as in other beneficial traits like plant fitness and growth using cultivation approaches.

### **5.2.1. Rhizome associated microbial communities**

Our experiments on carbon source utilization and sensitive assays using Biolog GenIII plates showed a difference between rhizoplane and endophytic bacterial communities. Endophytic

bacteria could use more carbon sources than their homologs inhabiting the rhizoplane interface. This observation reveals a higher adaption of endophytic bacteria for utilization of different organic compounds that may be more abundant in the endosphere. Both communities could grow on different harmful substances such as antibiotics or NaCl 1% but were sensitive to higher salt concentrations. Rhizoplane bacteria could growth in more acidic conditions (pH 5) whereas endophytic bacteria were only able to grow at pH 6. These results show that functional traits in communities of plant associated bacteria evolve adapting to the environmental conditions of their niche. In CWs, continuous exposition to xenobiotics could be a driver for adaption to new carbon sources from which certain bacterial species could benefit, avoiding competition with other species. Isolation of these adapted species constitutes a valuable tool for improving pollutant removal and degradation in CWs.

### 5.2.2. Endophytic bacteria from plants exposed to carbamazepine

Considering that *Phragmites* is a wetland plant, its root system is most of the time submerged and therefore the rhizosphere environment remains mainly anoxic. However, in helophyte species like *Phragmites*, oxygen is transported to the roots and rhizomes through the aerenchyma (Schröder et al., 1986). If CBZ can easily cross biological membranes, and be transported into roots and rhizomes as numerous examples in the literature show (Herklotz et al., 2010; Dordio et al., 2011; Shenker et al., 2011; Goldstein et al., 2014; Malchi et al., 2014; Hurtado et al., 2016), endophytic bacteria inhabiting roots and rhizomes are good candidates to perform a fast and complete degradation of the compound because they inhabit a more aerobic environment inside plant cells or in the intracellular space.

Endophytic bacteria were isolated from reed plants exposed to concentrations of CBZ mimicking those found usually in WWTPs. CBZ was always maintained on the culture media during isolation procedure to rapidly isolate and identify the potential beneficial microbiota. The potential of the endophytic community of reed plants for phytoremediation was investigated directly by removal experiments in liquid media and indirectly by determining plant growth promoting (PGP) traits. Besides contribution to CBZ removal, endophytic bacteria can help plants to cope with stress, contributing to plant fitness. Both characteristics are of high importance during treatment of wastewater in CWs. Three PGP traits were selected: the ability to (1) produce auxins and (2) iron chelating siderophores, and (3) to solubilize phosphate was

determined among the isolated strains. Auxins are involved directly in plant growth. The production of siderophores by rhizospheric bacteria could benefit the plant by chelating iron from the surrounding soil and making it available for the plant cell. Still, this property can be useful in an endophytic context. It has been suggested that siderophores can indirectly contribute to disease control by competing with phytopathogens for trace metals (Duffy and Défago, 1999). Endophytes can also contribute to phosphorus uptake by the plant by releasing low molecular weight acids in the root and the rhizosphere environment.

Li and coworkers described the endophytic bacterial community in roots of *P. australis* growing in a wetland in Beijing using a culture-independent technique (Li et al., 2010). They could identify 57 different endophytes, affiliated to *Proteobacteria* (78.9%), *Firmicutes* (9%), *Bacteroidetes* (6.6%), *Fusobacteria* (2.4%) and a few unidentified genera (3%). Interestingly, our results using cultivation methods and a different geographical location show similar results. In our isolates, *Proteobacteria* was also the dominant phylum (72.7%), followed by *Bacteroidetes* (13.6%) and *Firmicutes* (4.5%). In addition, we found members affiliated to Actinobacteria. Fusobacteria were not present among our isolates, surely because they are obligatory anaerobic and our isolation was performed in aerobic conditions.

The choice of the growth media is of great importance when isolating endophytic bacteria. To isolate a representative fraction of the entire community, cultivation techniques should mimic the environmental conditions in which strains grow usually “in planta”. Normally, the use of complex media is not advised because its high amount of nutrients may favor the growth of fast growing bacteria, impeding slow growing bacteria to develop posteriorly. Minimal media, with a limited amount of nutrients, are generally more appropriate because even though bacteria grow slowly, species of slow growing bacteria have more chances to develop. Although conditions like oxygen concentration, osmolarity, pressure or chemical signals derived from cell to cell communication that are characteristic of microhabitats occurring only in intracellular cavities are hard to reproduce on agar plates, most of the studies result in a diverse cultivable community. In fact, some studies have recently shown that the general assumption that only around 0.001–1% of the total endophytic community would be cultivable, may not correspond to the reality (Eevers et al., 2015a). The use of grow media containing plant extracts is an option that some scientists have applied to increase the possibilities for cultivation of recalcitrant

species. Some studies have shown an improvement of growth of endophytic strains that were frozen for a long period but have failed in isolating a higher number of species (Eevers et al., 2015b). For our isolation, we used one classical minimal medium (R2A) and one complex medium (PDA). The diversity of cultivable endophytic bacteria was higher in R2A agar plates from which bacteria affiliated to six different classes could be identified. In PDA agar plates, bacteria belonging to *α-Proteobacteria* and *Firmicutes* groups could not be isolated.

Surprisingly, of 57 strains identified by sequencing, only one was represented among our isolates. This result reveals a high speciation of the root microbiome driven by the plant in response to specific external conditions (e.g., a high concentration of CBZ, substrate and water used in the greenhouse). In fact, we know now that besides the plant (species, cultivar, age, health, and developmental stage), a multitude of abiotic factors modulate structural and functional diversity of the rhizosphere microbiome (Berg et al., 2014). It has also been discussed that external factors imposed via the host plant such as soil, geographic factors, and anthropogenic management shape the overall structure and function of root microbiomes (Gaiero et al., 2013).

*Pseudomonas* (*γ-Proteobacteria*) was the most abundant genus among our isolates. This is often the case when isolating or describing environmental samples and may be due to their adaptability to different external conditions, and in last instance by the flexibility and diversity of their genome (Silby et al., 2011). Their high metabolic diversity is reflected by the fact that several members of this genus have been used for the remediation of soils contaminated with many different organic pollutants such as hydrocarbons (Andria et al., 2009; Afzal et al., 2011). Relevant examples are TCE (Weyens et al., 2009; Weyens et al., 2010), naphthalene (Germaine et al., 2009) toluene (Weyens et al., 2009), and the herbicide 2,4-dichlorophenoxyacetic acid (Germaine et al., 2006). Indeed, the degradation pathways of polycyclic aromatic hydrocarbons (PAHs) have been described to be frequently present in this genus (Seo et al., 2009). Furthermore, *Pseudomonas* has been studied as model for beneficial plant-microbe interaction (Sitaraman, 2015). Among our isolates, *Pseudomonas moorei* showed a slight CBZ removal from the liquid medium. All members affiliated to Pseudomonads showed all PGP traits tested. Two of them showed particularly high values. *Pseudomonas linii* is oxidase-positive, and denitrifies (Delorme et al., 2002) and *Pseudomonas veronii* possesses high oxidase and catalase activity, and

denitrifies (Elomari et al., 1996). Hence, these isolates could be beneficial partners for the phytoremediation of organic pollutants, especially in constructed wetlands, where the removal of excess nitrogen is needed.

*Rhizobium* ( $\alpha$ -*Proteobacteria*) was the second most abundant genus with a representation of 13.6% of all isolates. *Rhizobium meliloti* has been previously applied in PAH removal observing an ability of this strain to stimulate the rhizosphere degrading microflora (Teng et al., 2011). Among our isolates, *Rhizobium daejeonense* showed the highest uptake of CBZ (2.45%) and additionally, the highest production of IAA (23.04  $\mu\text{g/mL}$ ) and phosphate solubilization. The type strain was isolated from a cyanide-degrading bioreactor originally inoculated by an activated sludge from a municipal sewage treatment plant in Daejeon (Korea). This strain shows catalase and oxidase activity, forms nodules in *M. sativa* and contains a *nifH* gene encoding a component of the nitrogenase complex (Quan et al., 2005). Therefore, this strain was thought to be a good candidate for further inoculation studies.

Also  $\beta$ -*Proteobacteria* were widely represented among the isolates. Members of this class (together with  $\gamma$ -*Proteobacteria*) are important for plant development as they can oxidize ammonium to nitrite. Belonging to this group, *Achromobacter xylosoxydans* and *Burkholderia* sp. have been used for phytoremediation of catechol and phenol (Ho et al., 2012) and toluene (Weyens et al., 2012) respectively. Among our isolates, *Achromobacter mucicolens* and *Diaphorobacter nitroreducens* showed CBZ uptake but neither siderophore production nor phosphate solubilization. Nonetheless, *A. mucicolens* can grow in the presence of 3% NaCl, reduces nitrate and nitrite, denitrifies, exhibits oxidase activity and can grow anaerobically (Vandamme et al., 2013). *D. nitroreducens* was initially isolated from activated sludge. This strain has interesting characteristics for phytoremediation, such as denitrification, catalase activity, and degradation of poly(3-hydroxybutyrate) and poly(3-hydroxybutyrate-co-hydroxyvalerate) under aerobic and anaerobic denitrifying conditions (Khan and Hiraishi, 2002).

With 13.6% of all isolates, *Bacteroidetes* was the third group found most abundant. *Chryseobacterium taeanense* showed positive results for the three PGP traits tested and for CBZ removal. *Chryseobacterium* species have been previously isolated from environmental samples,

showing degradation of carbazoles, a group of compounds structurally similar to CBZ (Guo et al., 2008) and organochlorine pesticides like DDT and HCH (Qu et al., 2015).

Another approach is the use of an enrichment culture for the isolation of bacteria involved in the degradation of xenobiotics. This technique consists in enriching a determined strain or group of strains with a selective medium. We used a minimal medium containing CBZ as sole carbon source to enrich CBZ degraders among bacteria from rhizomes. With this approach 7 distinct species could be isolated and identified. Surprisingly, when these strains were grown separately again in liquid media with CBZ, they failed to grow. One hypothesis that could explain this result is that while these strains complete the degradation of CBZ when they grow together each of them participating in one or several steps, when they grow alone, they cannot complete the degradation pathway. The establishment of bacterial consortia for xenobiotic removal has been already observed in studies with triclosan (Hay et al., 2001) or carbazole (Guo et al., 2008). The most significant study was the isolation of a marine microbial consortium from a beach polluted during the Prestige oil spill which is efficient in removing different hydrocarbon present in heavy fuel oil including three to five-ring PAHs (e.g. anthracene, fluoranthene, pyrene, benzo(a)anthracene, chrysene, and BaP) (Vila et al., 2010 reviewed in Ghosal et al., 2016). Further studies with these strains are needed to unravel the mechanisms behind this observation.

In summary, 22 strains were isolated and identified. Distribution of the different endophytic strains was balanced between root and rhizome tissues. PGP traits were found in strains inhabiting both tissues. A higher presence of phosphate solubilizers was observed in rhizomes. In total, five strains could remove CBZ from liquid cultures. Seven isolates were chosen as best candidates for further inoculation studies. Out of these seven, three were able to remove CBZ and have PGP traits (*Rhizobium daejeonense*, *Chryseobacterium taeanense* and *Pseudomonas moorei*), two exhibit strong PGP traits (*Pseudomonas veronii* and *Pseudomonas lini*) and 2 showed CBZ removal but no PGP traits (*Diaphorobacter nitroreducens* and *Achromobacter mucicolens*). The relatively low rates of CBZ removal are in accordance with research published until now. CBZ still remains a notorious compound for its poor elimination in microbial degradation studies. Removal levels were not higher than 30% across 20 studies examining lab and full scale subsurface flow, lab scale sequencing batch reactor, lab scale anaerobic digester,

pilot and lab scale membrane bioreactor, and full, pilot, and lab scale WWTP systems (Onesios et al., 2009). Therefore, cooperation between plants and associated bacteria is necessary for complete elimination of problematic compounds such as CBZ. Alone or in combination, the application of these endophytic strains to its host *P. australis* or other plant species could improve the plant fitness in xenobiotic stress conditions and contribute to CBZ removal in CWs.

### **5.3. Interactions between plant roots and endophytic bacteria: carbamazepine metabolism**

As has been already emphasized, the plant and its microbiome form a unique identity known as holobiont. After exposure and uptake of a xenobiotic, transformation products (TPs) identified in plant tissues are a consequence of this holobiontic metabolism. In addition to the general mechanisms of detoxification present in plants, other microbial mechanisms may play a role during the transformation of a given parent compound in planta. To distinguish between both processes can be a difficult task, if not impossible. The use of a horseradish HR culture as a model to study interactions between plants and endophytic bacteria allowed us to dissect CBZ removal and transformation pathways in the plant holobiont.

#### **5.3.1. Carbamazepine removal from nutrient media**

The role of endophytic bacteria in CBZ removal by HRs was studied in short time experiments with initial CBZ concentrations of 10 and 25. When HRs were inoculated with *R. radiobacter*, removal significantly increased to 21% and 13% in treatments with 10 and 25  $\mu\text{M}$  respectively. Cultures inoculated with *D. nitroreducens* were also able to remove more efficiently the CBZ present in the growth media than HRs alone, but to a lower extent (10% and 9%). Still, this represented twice the amount of CBZ removed by HRs not assisted by endophytic bacteria. As has been assumed previously, CBZ probably moves across membranes by simple diffusion, limiting the overall metabolism to enzymatic processes occurring inside the cell compartment. In absence of a driving force such as transpiration, transformation products with similar physicochemical properties to the parent compound can leave the cell by the same mechanism and will therefore be identifiable in the growth media.



### 5.3.2. Metabolism of carbamazepine in hairy roots and endophytic bacteria

Metabolism of CBZ in HRs was studied at initial concentration of 250  $\mu$ M. A first screening was performed with a group of selected strains. Based on CBZ removal and metabolic profile of the supernatants, two strains were selected to follow metabolism of CBZ in inoculated HRs for 21 days. In total, 13 TPs were identified in the growth media by LC-QTOF-MS/MS. These TPs clustered in four hypothesized pathways, and their evolution during the incubation time was followed.

#### 5.3.2.1. The 10,11-diol pathway

The 10,11-diol pathway has been extensively described in plants. CBZ is first oxidized to CBZ-10,11-epoxide. This is the main TP identified in root and leaves tissues from sweet potato and carrot as well as in leaves of cucumber and tomato (Goldstein et al., 2014; Malchi et al., 2014). This first oxidation seems to be well conserved among different kingdoms, being reported as well in mammals (Lertratanangkoon and Horning, 1982), lignolytic fungi (Seiwert et al., 2015), and soil bacteria (Li et al., 2013b). This first oxidation step is achieved by cytochrome P450 and/or peroxidases and represents the initial activation of the parent compound, leading to other sub-pathways. All chromatograms showed multiple peaks corresponding to a theoretical  $m/z$  253.1071 revealing the co-elution of other epoxidized or hydroxylated TPs formed during the incubation. Thus, a reliable quantification for this metabolite was not feasible; a fact that had previously been observed in WWTP effluents (Bahlmann et al., 2014).

The first epoxidation is followed by cleavage and hydroxylation of the epoxy bond to render 10,11-dihydro-10,11-dihydroxy-CBZ, a reaction known to be catalysed by epoxide hydrolases in rat and human liver (Tybring et al., 1981), enzymes also present in all kingdoms of life. This TP was formed in the media from the first day and accumulated constantly until the last day of incubation in non-inoculated cultures. In HRs inoculated with endophytic bacteria, accelerated formation of the 10,11-dihydro-10,11-dihydroxy-CBZ could be observed during the first day, followed by a decrease during the next three days. From the fourth day of incubation, the peak area increased

with lower rates than in control HR cultures. This trend suggests that the compound was further metabolized by endophytic bacteria, thus accumulating in media in lower amounts.

The TP 10,11-dihydro-10-hydroxy-CBZ (10-OH-CBZ) could be identified in media sampled from control HR cultures and HR cultures inoculated with *D. nitroreducens*. In both cases, the peak area increased slowly from the first day on, albeit in higher concentration in non-inoculated HRs. This metabolite has previously been detected in wastewater (Leclercq et al., 2009) and fungi (Golan-Rozen et al., 2011) but no enzyme has been postulated for this reaction. In mammals, this metabolite has been identified as a product of oxcarbazepine and not of CBZ (Maggs et al., 1997).

10,11-dihydro-10,11-dihydroxy-CBZ and 10-OH-CBZ were found in negative controls consisting of autoclaved HRs incubated with CBZ. The formation of these compounds in absence of biological matrices reveals a chemical oxidative pathway independent from plants or bacteria. However, the total amount accumulated was lower than in biological samples. When autoclaved HRs were inoculated with endophytic bacteria, 10,11-dihydro-10,11-dihydroxy-CBZ was synthesized with a similar trend to this observed in healthy HRs but in lower amounts. Thus, we can conclude that bacteria and plants can degrade CBZ through the 10,11-diol pathway although plants are more efficient.

### **5.3.2.2. The 2,3-diol pathway**

A sub-pathway involving successive oxidation reactions at the carbons 2 and 3 of the aromatic benzene group was identified in all samples with biological activity. CBZ was metabolized to 2,3-dihydro-2,3-dihydroxy-CBZ in HR cultures void of or inoculated with endophytic bacteria. This reaction can be achieved by 2,3 dioxygenation, or proceed via the epoxidation at carbons 2 and 3, followed by hydrolysis. The first is typical for bacterial degradation of polycyclic aromatic hydrocarbons (Seo et al., 2009). The second would include two steps with the participation of a CYP450 or a peroxidase and an epoxide hydrolase, more representative of plant metabolism. Both could occur in our model, one in HR cultures and the other in inoculated roots. Unfortunately,

epoxidation at the 2,3 position of the dibenzazepine ring could not be confirmed, since several peaks corresponding to its theoretical  $m/z$  were identified. As mentioned above, this array of metabolites with  $m/z$  253.0971 could correspond to TPs formed by hydroxylation or epoxidation at different carbons on the aromatic ring (1-OH-CBZ, 2-OH-CBZ, 3-OH-CBZ, 4-OH-CBZ, CBZ-1,2-epoxide, CBZ-2,3-epoxide, CBZ-3,4-epoxide, CBZ-1,4-epoxide) or on the central ring (CBZ-10,11-epoxide, oxcarbazepine) of the parent compound. Some of these metabolites have been found in wastewater and have shown similar, if not the same fragments under different collision energies (Bahlmann et al., 2014).

The 2,3-dihydro-2,3-dihydroxy-CBZ was oxidized to 2,3-dihydroxy-CBZ (2,3-diOH-CBZ). The formation of dihydrodiols and subsequent diol compounds is a conserved mechanism in bacterial degradation of PAHs such phenanthrene, naphthalene, fluoranthene, pyrene, and benzopyrene and is generally achieved by dehydrogenases (Seo et al., 2009).

The 2,3-diOH-CBZ was oxidized to CBZ-2,3-quinone. This reaction can be catalyzed by a catechol oxidase, an enzyme of the polyphenol oxidase family. In plants, these enzymes are involved during oxidation of polyphenols to quinones. Their biological function remains enigmatic, but since they are induced under conditions of stress and pathogen attack, one of their functions seems to be involved in biotic and abiotic stress resistance (Mayer, 2006). The same reaction has been postulated to occur non-enzymatically during the oxidation of 1,2-dihydroxynaphthalene to 1,2-naphthaquinone in bacterial metabolism of naphthalene (Auger, 1995). Since there was a burst in the production of this TP during the first days only in inoculated samples, it is suggested that both strains trigger antioxidant responses in plant roots and therefore activate a set of responses against stress.

The 2,3-diol pathway exhibited a similar trend to the 10,11-diol pathway in its first steps. The evolution of 2,3-dihydro-2,3-dihydroxy-CBZ was comparable to those of 10,11-dihydro-10,11-dihydroxy-CBZ but approximately 30% less. In contrast to 2,3-dihydro-2,3-dihydroxy-CBZ, 2,3-diOH-CBZ and CBZ-2,3-quinone were more significant

in HRs inoculated with endophytic bacteria and specially with *R. radiobacter*. Moreover, 2,3-diOH-CBZ and CBZ-2,3-quinone were identified in negative controls inoculated with bacteria while there were negligible in autoclaved HRs. From these observations, it may be concluded that plants favour the first reaction involving CYP450s/peroxidases and epoxy hydrolases while bacteria prefer the 2,3-diol pathway where dehydrogenases and catechol oxidases would play an important role.

### 5.3.2.3. The GSH pathway

One of the mechanisms adopted by plants to detoxify xenobiotics is glutathione conjugation by GSTs and subsequent vacuolar compartmentation of the conjugates (Dixon et al., 1998). Several TPs derived from GSH conjugates were identified (TP374, TP431 and TP560). To confirm the nature of these TPs, chemical conjugations with GSH and cysteine were performed *in vitro*. When CBZE was incubated with GSH, a molecular ion peak at  $m/z$  560.1809 was observed. The respective ion chromatogram showed a double peak with retention time 4.99-5.04 min, corresponding to the GSH adduct. Previous work had demonstrated that this double peak contains indeed two different diastereomers formed in the absence of biological matrices (Bu et al., 2005). Still, TP560 was found only in trace levels in HR cultures and HRs inoculated with endophytes, but in greater amounts when autoclaved roots were grown with *R. radiobacter*. Identical retention and fragmentation patterns were obtained during collision experiments on the precursor ion in biological samples and in chemically synthesized GSH adducts. These findings allowed us to finally identify TP560 as 10,11-dihydro-10-hydroxy-11-glutathionyl-CBZ (CBZE-GSH).

Following GSH conjugation, xenobiotic conjugates can further be degraded to the respective  $\gamma$ -glutamylcysteinyl- and subsequent cysteinyl-moieties by carboxypeptidases (Wolf et al., 1996) or to cysteinylglycyl- and subsequent cysteinyl-moieties by  $\gamma$ -glutamyl-transpeptidase ( $\gamma$ -GT), both in the vacuole (Edwards et al., 2011). Other studies have suggested a cytosolic pathway for the degradation of GSH conjugates to cysteinyl moieties, involving carboxypeptidase activity of the enzyme phytochelatin synthase (PCS) (Beck et al., 2003). In the present study, cysteinylglycine adducts (TP431) were detected in the media of HR cultures void of or inoculated with

endophytic bacteria. When autoclaved HRs were inoculated with endophytic bacteria, this metabolite was also detected suggesting that enzymes for GSH conjugation and successive degradation of CBZ are also present in bacteria. Fragment ions with identical  $m/z$  ratios were identified when TP560 and TP431 were subjected to collision. Additionally, the retention time revealed a very similar hydrophobicity to CBZE-GSH leading us to the identification of TP431 as 10,11-dihydro-10-hydroxy-11-cysteinylglycyl-CBZ (CBZE-CYS-GLY).

TP374, corresponding to the cysteine adduct was identified in all culture media. When CBZE was incubated with cysteine, a double peak at 4.88-4.92 min corresponding to a cysteine adduct was observed. Collision experiments on the precursor ion ( $m/z$  374.1169) showed conserved fragments in biological and chemical samples ( $m/z$  = 180.0821, 210.0928, 253.0985, 313.1025, 339.0819), showing that in fact TP374 corresponds to 10,11-dihydro-10-hydroxy-11-cysteinyl-CBZ (CBZE-CYS). TP374 was detected in autoclaved HR cultures at low levels only after 14 days of incubation suggesting chemical conjugation with free cysteine in the media.

The  $\gamma$ -glutamylcysteinyl adduct was not found in the media of any of the experimental conditions. In HRs, this could be explained by a dominance of GGT activity against carboxypeptidases and phytochelatin synthase during the degradation of the GSH conjugate. On the other hand, CBZE-CYS-GLY was identified in the media of HR cultures void of endophytic bacteria. Ferretti and coworkers demonstrated the existence of an apoplastic GGT in barley roots, important for the recovery of extracellular GSH (Ferretti et al., 2009). An apoplastic route for the degradation of GSH conjugates could explain the low content of the CBZE-CYS-GLY detected in the growth media of HRs. In samples involving bacterial metabolism it was present at higher levels, revealing an important role of bacterial partners for the degradation of GSH conjugates. The trends of this TP and the final metabolite in the GSH degradation pathway (CBZE-CYS) showed phases at different time points during the incubation where concentrations decreased significantly. In the case of *D. nitroreducens*, CBZE-CYS-GLY decreased from day 1 to day 8 of incubation, accumulating again until the last day. Contrastingly, CBZE-CYS decreased between days 8 and 14. In the case of *R. radiobacter*, CBZE-CYS decreased

from day 4 to 8, after a maximum on the fourth day, suggesting further degradation of the cysteine conjugate when plants were inoculated by endophytic bacteria. The TPs derived from this further catabolic route were not identified in this study.

#### 5.3.2.4. The acridine pathway

Cleavage of the carbamoyl group and rearrangement of the central ring of CBZ initiate the acridine sub-pathway. Several TPs with an acridine-related structure were found in the growth media. This pathway has previously been described in fungi under anoxic conditions (Golan-Rozen et al., 2015) and several related TPs have been identified in soil after CBZ exposure and long aerobic incubation (Li et al., 2013b). To our knowledge, no acridine-like metabolite has been identified in plants treated with CBZ so far. The order of reactions involved in this pathway could be predicted from the observation of the trends and absolute amounts exhibited by each of the compounds.

The first TP of this pathway is 9-acridine carboxaldehyde which is formed from CBZ-10,11-epoxide after cleavage of the carbamoyl group and contraction of the seven-membered central ring to a six-membered ring. This compound is known to be reactive and toxic as well (Furst et al., 1995). The aldehyde moiety is then cleaved to form acridine, a compound also known to be reactive and toxic in the aquatic environment (Parkhurst et al., 1981). Acridine can finally be oxidized to acridone (non-toxic) in two steps, with the formation of the intermediate 9-OH-acridine (Mathieu et al., 2011).

HR cultures showed an increase of the first three compounds accumulating at the end of the experiment. The total amount accumulated after 21 days decreased 10-fold in each step of the pathway. These TPs were identified in the growth media of autoclaved HRs with trends and amounts like those exhibited in living roots. Acridone could barely be detected at the beginning of the incubation, disappearing from the media after the fourth day. These results suggest that plants, at least horseradish, are lacking genes for the degradation of CBZ through the acridine pathway.

The inoculation with *R. radiobacter* induced this pathway strongly, leading to a burst in the synthesis of 9-acridine carboxaldehyde, acridine and 9-OH-acridine in the first

days of incubation, reaching a maximum after 4 days. Acridone accumulated in these samples from the fourth day on, but this increase does not explain the decreasing trend of the upstream TPs. Therefore, we think that acridine is further metabolized in samples containing the endophytic strain *R. radiobacter*. Similar trends were observed when HRs were inoculated with *D. nitroreducens*. At the end of the incubation, even the acridone signal decreased, revealing again the existence of further steps in the metabolic pathway of acridine-like TPs.

#### 5.3.2.5. Transformation products in root extracts

The content and composition of TPs identified in the media was investigated in root extracts after 21 days of incubation. The amount of CBZ found in root extracts inoculated with endophytic bacteria was twice as high as in HR extracts. This result confirmed the observations performed in experiments with concentrations of 10 and 25  $\mu\text{M}$ . The distribution of TPs of the diol pathways was similar in HRs and inoculated HRs with a slight higher prevalence for the 2,3-diol pathway in roots inoculated with *R. radiobacter*. Acridine-related TPs were much higher in HRs inoculated with *D. nitroreducens* (10 fold). In absolute numbers, this was the most important metabolic sub-pathway found in root extracts. Metabolites derived from GSH conjugation and related degradation products were present in higher amounts in non-inoculated HRs. Specifically, CBZE-CYS had accumulated in great amounts in root tissues after 21 days of incubation.

All these observations allow dissecting the overall metabolism of CBZ in HRs and the endophytic bacteria used in this study (Fig. 34). However, as indicated previously, there is evidence of further metabolism in the case of GSH and acridine pathways in inoculated HRs for which TPs downstream could not be identified. Even though the relative amounts measured in the extracts after 21 days may slightly change the final picture, the potential applications of the results remain consistent.

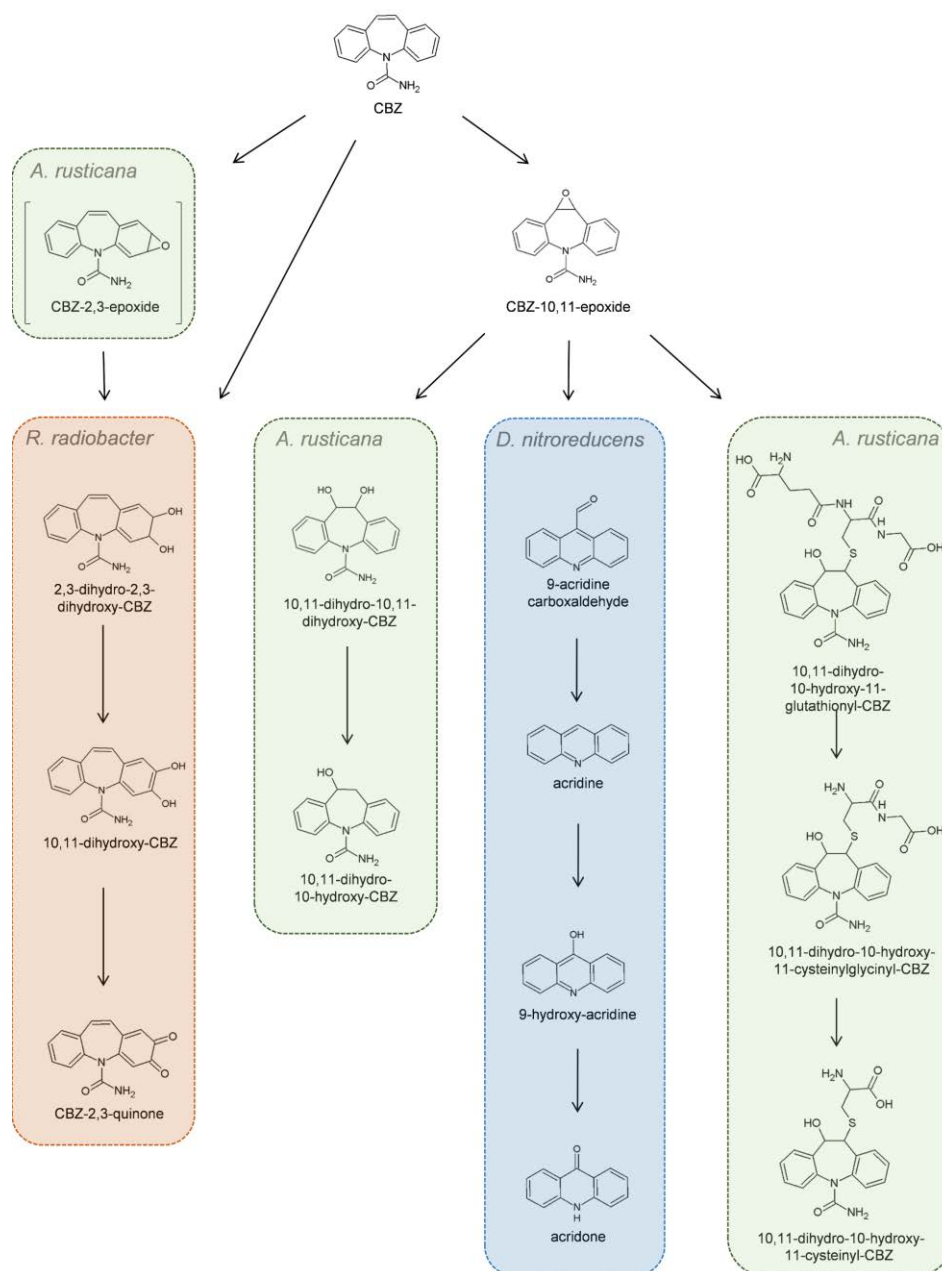


Figure 34: Proposed carbamazepine metabolic pathways in *A. rusticana* hairy roots and hairy roots inoculated with the endophytic bacteria *R. radiobacter* and *D. nitroreducens*.

### 5.3.1. Analyses of proteins and antioxidant enzymatic activities in HRs

Extracellular proteins identified in the media of HR cultures exposed to CBZ revealed metabolic changes occurring in HRs in response to CBZ. Moreover, the inoculation of HRs with endophytic bacteria modulated these changes. Proteins identified when HRs were cultivated in MS medium were classified mainly into three functional groups: biosynthesis of primary metabolites (amino acids, carbohydrates and lipids) and defence response. Other minor functional categories were



identified such as growth, cell wall structure and organization, protein signalling, transport and degradation, signalling, and lipid transport and metabolism.

When CBZ was added to the nutrient medium, the total amount of plant proteins detected increased and the functional composition of the secreted proteome displayed some significant variations depending on treatment. Proteins involved in biosynthesis of primary metabolites and proteins involved in redox homeostasis and oxidative stress decreased in number. On the other hand, identified proteins involved in cell wall structure and organization, signalling and defence increased when HRs were exposed to CBZ. This shows a shift on HRs metabolism from primary metabolism to structural and chemical defence processes.

Among the proteins identified in response to CBZ, several are intrinsically connected to CBZ removal and metabolism. This is the case of peroxidases, cytochrome c and cytochrome b5, involved in oxidation reactions of phase I metabolism, and GSTs involved in phase II metabolism. The group of peroxidases with 18 different isoforms was especially high represented. Other enzymes like carboxypeptidases involved in degradation of glutathione conjugates were as well identified in the growth medium. The production and release in form of root exudates of enzymes like laccases and peroxidases has been observed in HR cultures obtained from several plant species and make them a well suited tool to study removal and degradation of pollutants (Agostini et al., 2013).

When treated HRs were inoculated with *D. nitroreducens* or *R. radiobacter*, a group of 16 proteins remained invariable. On the other hand, big differences were found among the different conditions, and some proteins seemed to be very exclusive for each condition. Roots inoculated with the endophytic strain *R. radiobacter* presented the highest number of exclusive proteins. The application of different endophytic bacteria results in specific responses in the plant root as reveal the fact that only a few proteins are stable in the three biological matrices. In addition to proteins identified HRs in response to CBZ, proteins involved in ROS scavenging and oxidative stress were identified when HRs were inoculated with endophytic bacteria and treated with CBZ. Superoxide dismutase, GR, monodehydroascorbate reductase, APOX, all enzymes from the Halliwell-Asada cycle were indeed identified in the growth media of HRs assisted by endophytic bacteria. Again, the induction of antioxidant responses and the development of responses

against stress was observed in inoculated roots. This hypothesis has been postulated by White and Torres (2010) to explain fungal endophyte protection of plant hosts. By producing ROS compounds, endophytes can enhance the production of antioxidant enzymes and compounds in plants, which in turn protect the plant from pathogen attacks or stress situations.

This hypothesis was confirmed by measuring enzymatic activities in HR extracts. GR and APOX activities were higher in HRs inoculated with both strains than in HRs alone, and POX was higher when HRs were inoculated with *D. nitroreducens*. In non-inoculated HRs, only the activity of GR increased after CBZ treatment. The fact that endophytic bacteria induce other enzymes from the Halliwell-Asada cycle than CBZ alone, may play a complementary role in the improvement of CBZ removal besides a direct implication in degradative pathways. A similar behaviour was observed in the activity of GSTs after inoculation. Activity of GSTs increased significantly when using pNBoC and fluorodifen as substrates after treatment with CBZ. The same effect was observed in HRs inoculated with *D. nitroreducens*. High amounts of CBZE-CYS-GLY and CBZE-CYS were identified in growth media of HRs and HRs inoculated with this strain. This observation led to the conclusion that the glutathione conjugation is enzymatic and that the GST responsible for it may be one or several inducible GST isozymes specific for the substrates pNBoC and/or fluorodifen.

#### **5.4. Practical applications**

The concern about emerging pollutants in our water systems has increased over the last decades in Europe. The scientific community has informed governments about the risk that these compounds pose to the maintenance of natural ecosystems and human health. The necessity to preserve our water resources from this danger has been recognized and resulted in the publication of the “Directive 2000/60/EC of the European Parliament and of the Council establishing a framework for the Community action in the field of water policy”, or, in short, the EU Water Framework Directive (WFD). Emerging pollutants are in continuous change, and new compounds are often joining this group. Consequently, the WFD has been modified and updated in two occasions.

With a growing and more and more urbanized population, forecasts are such that the use of treated wastewater will be unavoidable in the future to alleviate the stress put on the water cycle. Within European Cooperation in Science and Technology (COST) framework a large group of scientists launched in 2015 the action ES1403 “NEREUS, New and emerging challenges and opportunities in wastewater reuse”. The goal of this COST-action is to develop a multi-disciplinary network to determine which of the current challenges related to wastewater reuse are the most concerning in relation to public health and environmental protection, and how these can be overcome. The action should end with general recommendations for practices in wastewater reuse and one of the critical points is the use of reclaimed water for agriculture.

Phytoremediation has been proposed as a tertiary or polishing step of reclaimed wastewater before its use for human activities. This technique represents a cheap and environmentally friendly solution for wastewater treatment and CWs have been used since more than 60 years (Vymazal, 2011). As recommended in all cases of phytoremediation, harvested biomass should be collected and might be used for bioenergy purposes to avoid leaching of unmetabolized compounds or even more toxic transformation products from decaying plant material (Chen et al., 2017). Some compounds like CBZ are still recalcitrant, and its removal in CWs is incomplete (Verlicchi and Zambello, 2014).

Phytoremediation has been traditionally studied from a plant-based point of view. Many scientists and companies have advertised and promoted certain plant species or cultivation systems. However, the role of the microbiome in plant health and metabolic functions has been recognized in the last years. To date, the closely meshed relationship between a plant and its adhering or inhabiting microbes is defined as holobiont. An improvement in the removal of recalcitrant compounds can be achieved by increasing the performance of the plant holobiont, and there, plant-associated microbial communities play an essential role. The study of these communities, their ecology and their behaviour during plant inoculation at laboratory and field scales is necessary to improve the removal of recalcitrant compounds such as CBZ.

The metabolism of CBZ in HRs led to the formation of 13 TPs, some of them with assumed toxicity for humans. It is important that this multiplication effect takes place in a system used as a filter like a CW and not in the final product, entering ground water recharge or the food chain.

Under these conditions it becomes clear that the application of endophytic bacteria may improve the removal of recalcitrant compounds in CWs.

While the endophytes generally seem to provide a convincing solution for the removal of organic xenobiotics and PPCP at first sight, unexpected problems might arise from the large numbers of genera/isolates found in exposed plants. While most of them contribute to the functioning of the holobiont, some specialists can also have unexpected and unwanted traits, at least for practical application. This might be the case when antibiotic resistant bacteria (ARB) are present within the community. In fact, among our isolated communities few ARB were found, although plants had not been exposed to antibiotics. Such a finding may be of special relevance in WWTPs and CWs treating contaminated water with antibiotics because resistant organisms can become dominant, resulting in a transfer of antibiotic resistant genes (ARG) and ARB from one level to the other of the trophic chain ending finally in our dietary products. Moreover, human pathogenic bacteria in plants have been previously identified and isolated, the most significant case being the outspread of *Escherichia coli* O104:H4 in Germany and France in 2011 (reviewed by van Overbeek et al., 2014). Thus, the spread of these genes and bacteria should be kept under strict surveillance especially when using treated wastewater for crop irrigation. In this sense, a winner strategy for phytoremediation would be to stimulate exclusively bacteria carrying genes for the detoxification of pollutants but not ARG, increasing their abundance in the plant-associated bacterial community in detriment of ARB.

## 6. Conclusions

From the observations in this study, it can be concluded that the use of *Phragmites australis* in concert with its associated bacteria represents a good solution to polish treated wastewater before using it for irrigation purposes. The specific conclusions derived from our work are:

- *P. australis* removed up to 90% of the initial CBZ amount after 9 days. Plant health was not compromised and no visual symptoms of stress were observed.
- Twenty-two endophytic strains were isolated and characterized. Several strains exhibit plant growth promoting traits and can remove CBZ in liquid culture. Differences between rhizoplane and endophytic bacteria were observed.
- HR cultures are a well-suited model to study interactions between plants and endophytic bacteria. Axenic HR cultures permitted to dissect the metabolism of CBZ in plants assisted by the endophytic strains *Rhizobium radiobacter* and *Diaphorobacter nitroreducens*. We could unravel different metabolic pathways in the plant holobiont, discerning between microbial and plant part.
- The metabolism of CBZ in HRs led to the formation of 13 TPs, some of them with assumed toxicity. CBZ metabolism in horseradish roots alone undergoes preferentially the 10,11-diol and GSH pathways. *R. radiobacter* favours the 2,3-diol pathway, whereas *D. nitroreducens* strongly induces the acridine pathway.
- Proteomics analyses in HRs inoculated with the endophytic bacteria *R. radiobacter* and *D. nitroreducens* revealed an essential role for endophytic bacteria in plant health and stress resilience, by enhancing their antioxidative defence systems as well as prominent enzymes involved in phase II metabolism of CBZ in horseradish.

## 7. References

- Afzal M, Khan QM, Sessitsch A** (2014) Endophytic bacteria: prospects and applications for the phytoremediation of organic pollutants. *Chemosphere* **117C**: 232–242
- Afzal M, Yousaf S, Reichenauer TG, Kuffner M, Sessitsch A** (2011) Soil type affects plant colonization, activity and catabolic gene expression of inoculated bacterial strains during phytoremediation of diesel. *J Hazard Mater* **186**: 1568–1575
- Agostini E, Talano MA, González PS, Oller ALW, Medina MI** (2013) Application of hairy roots for phytoremediation: what makes them an interesting tool for this purpose? *Appl Microbiol Biotechnol* **97**: 1017–1030
- Aken B Van, Yoon JM, Schnoor JL** (2004) Biodegradation of nitro-substituted explosives 2, 4, 6-Trinitrotoluene, by a phytosymbiotic *methylobacterium* sp. associated with poplar tissues (*Populus deltoides* x *nigra* DN34). *Appl Environ Microbiol* **70**: 508–517
- Alexander DB, Zuberer DA** (1991) Use of chrome azurol S reagents to evaluate siderophore production by rhizosphere bacteria. *Biol Fertil Soils* **12**: 39–45
- Boxall AB, Johnson P, Smith EJ, Sinclair CJ, Stutt E, Levy LS** (2006) Uptake of Veterinary Medicines from Soils into Plants. *J Agric Food Chem* **54**: 2288–2297
- Allen F, Greiner R, Wishart D** (2015) Competitive fragmentation modeling of ESI-MS/MS spectra for putative metabolite identification. *Metabolomics* **11**: 98–110
- Altschul SF, Madden TL, Schäffer AA, Zhang J, Zhang Z, Miller W, Lipman DJ** (1997) Gapped BLAST and PSI-BLAST: a new generation of protein database search programs. *Nucleic Acids Res* **25**: 3389–3402
- Andria V, Reichenauer TG, Sessitsch A** (2009) Expression of alkane monooxygenase (alkB) genes by plant-associated bacteria in the rhizosphere and endosphere of Italian ryegrass (*Lolium multiflorum* L.) grown in diesel contaminated soil. *Environ Pollut* **157**: 3347–3350
- Auger R** (1995) Effect of nonionic surfactant addition on bacterial metabolism of naphthalene: assessment of toxicity and overflow metabolism potential. *J Hazard Mater* **43**: 263–272
- Bahlmann A, Brack W, Schneider RJ, Krauss M** (2014) Carbamazepine and its metabolites in wastewater: analytical pitfalls and occurrence in Germany and Portugal. *Water Res* **57**: 104–114

- Bano N, Musarrat J** (2003) Isolation and characterization of phorate degrading soil bacteria of environmental and agronomic significance. *Lett Appl Microbiol* **36**: 349–353
- Barac T, Taghavi S, Borremans B, Provoost A, Oeyen L, Colpaert J V, Vangronsveld J, van der Lelie D** (2004) Engineered endophytic bacteria improve phytoremediation of water-soluble, volatile, organic pollutants. *Nat Biotechnol* **22**: 583–588
- Bartha B** (2012) Uptake and metabolism of human pharmaceuticals in plants. Identification of metabolites and specification of the defense enzyme systems under pharmaceutical exposure. Doctoral dissertation. Technische Universität München. Retrieved from <http://mediatum.ub.tum.de/doc/1099038/1099038.pdf>
- Beck A, Lenzian K, Oven M, Christmann A, Grill E** (2003) Phytochelatin synthase catalyzes key step in turnover of glutathione conjugates. *Phytochemistry* **62**: 423–431
- Beijerinck M** (1888) Cultur des *Bacillus radicola* aus den Knöllchen. *Bot Ztg* **46**: 740–750
- Berg G, Grube M, Schloter M, Smalla K** (2014) Unraveling the plant microbiome: looking back and future perspectives. *Front Microbiol* **5**: 148
- Bradford MM** (1976) A rapid and sensitive method for the quantitation of microgram quantities of protein utilizing the principle of protein-dye binding. *Anal Biochem* **72**: 248–254
- Brisson J, Chazarenc F** (2009) Maximizing pollutant removal in constructed wetlands: should we pay more attention to macrophyte species selection? *Sci Total Environ* **407**: 3923–3930
- Bu H, Kang P, Deese A, Zhao P, Pool W** (2005) Human in vitro glutathionyl and protein adducts of carbamazepine-10, 11-epoxide, a stable and pharmacologically active metabolite of carbamazepine. *Drug Metab Dispos* **33**: 1920–1924
- Carson R** (2002) *Silent spring* - 40th Anniversary Edition. Boston: Mariner
- Carvalho PN, Basto MCP, Almeida CMR** (2012) Potential of *Phragmites australis* for the removal of veterinary pharmaceuticals from aquatic media. *Bioresour Technol* **116**: 497–501
- Chandra S** (2012) Natural plant genetic engineer *Agrobacterium rhizogenes*: role of T-DNA in plant secondary metabolism. *Biotechnol Lett* **34**: 407–415
- Chazarenc F, Naylor S, Comeau Y, Merlin G, Brisson J** (2010) Modeling the effect of plants and peat on evapotranspiration in constructed wetlands. *Int J Chem Eng* **2010**: 1–6

- Chen F, Huber C, May R, Schröder P** (2016) Metabolism of oxybenzone in a hairy root culture: perspectives for phytoremediation of a widely used sunscreen agent. *J Hazard Mater* **306**: 230–236
- Chen F, Huber C, Schröder P** (2017) Fate of the sunscreen compound oxybenzone in *Cyperus alternifolius* based hydroponic culture: uptake, biotransformation and phytotoxicity. *Chemosphere* **182**: 638–646
- Chilton MD** (2001) *Agrobacterium*. A Memoir. *Plant Physiol* **125**: 9–14
- Chilton MD, Tepfer DA, Petit A, David C, Casse-Delbart F, Tempé J** (1982) *Agrobacterium rhizogenes* inserts T-DNA into the genomes of the host plant root cells. *Nature* **295**: 432–434
- Compant S, Clément C, Sessitsch A** (2010) Plant growth-promoting bacteria in the rhizo- and endosphere of plants: their role, colonization, mechanisms involved and prospects for utilization. *Soil Biol Biochem* **42**: 669–678
- Conkle JL, White JR, Metcalfe CD** (2008) Reduction of pharmaceutically active compounds by a lagoon wetland wastewater treatment system in Southeast Louisiana. *Chemosphere* **73**: 1741–1748
- Daughton CG, Ternes TA** (1999) Pharmaceuticals and personal care products in the environment: agents of subtle change? *Environ Health Perspect* **107**: 907–938
- Delorme S, Lemanceau P, Christen R** (2002) *Pseudomonas lini* sp. nov., a novel species from bulk and rhizospheric soils. *Int J Syst Evol Microbiol*. **52**: 513–523
- Dixon DP, Cummins I, Cole DJ, Edwards R** (1998) Glutathione-mediated detoxification systems in plants. *Curr Opin Plant Biol* **1**: 258–266
- Dordio AV, Belo M, Martins Teixeira D, Palace Carvalho AJ, Dias CMB, Picó Y, Pinto AP** (2011) Evaluation of carbamazepine uptake and metabolization by *Typha* spp., a plant with potential use in phytotreatment. *Bioresour Technol* **102**: 7827–7834
- Drotar A, Phelps P, Fall R** (1985) Evidence for glutathione peroxidase activities in cultured plant cells. *Plant Sci* **42**: 35–40
- Duffy BK, Défago G** (1999) Environmental factors modulating antibiotic and siderophore biosynthesis by *Pseudomonas fluorescens* biocontrol strains. *Appl Environ Microbiol* **65**: 2429–2438
- Edwards R, Dixon DP** (2005) Plant glutathione transferases. *Methods Enzymol* **401**: 169–186



- Edwards R, Dixon DP, Cummins I, Brazier-Hicks M, Skipsey M** (2011) New perspectives on the metabolism and detoxification of synthetic compounds in plants. In Schröder P, and Collins CD (Eds.) *Organic xenobiotics and plants: from mode of action to ecophysiology* (pp 125–148). Dordrecht: Springer Netherlands
- Eevers N, Beckers B, Op de Beeck M, White JC, Vangronsveld J, Weyens N** (2015) Comparison between cultivated and total bacterial communities associated with *Cucurbita pepo* using cultivation-dependent techniques and 454 pyrosequencing. *Syst Appl Microbiol* **39**: 1–9
- Eevers N, Gielen M, Sánchez-López A, Jaspers S, White JC, Vangronsveld J, Weyens N** (2015) Optimization of isolation and cultivation of bacterial endophytes through addition of plant extract to nutrient media. *Microb Biotechnol* **8**: 707–715
- Elomari M, Coroler L, Hoste B, Gillis M, Izard D, Leclercq H** (1996) DNA Relatedness among *Pseudomonas* strains isolated from natural mineral waters and proposal of *Pseudomonas veronii* sp. nov. *Int J Syst Bacteriol.* **46**: 1138–1144
- European Commission (EC)**, 2000. Directive 2000/60/EC of the European Parliament and of the Council of 23 October 2000 establishing a framework for Community action in the field of water policy. Official Journal of the European Union L 327/1 22/12/2000
- European Commission (EC)**, 2008. Directive 2008/105/EC of the European Parliament and of the Council of 16 December 2008 on environmental quality standards in the field of water policy, amending and subsequently repealing Council Directives 82/176/EEC, 83/513/EEC, 84/156/EEC, 84/491/EEC, 86/280/EEC and amending Directive 2000/60/EC of the European Parliament and of the Council
- European Commission (EC)**, 2013. Directive 2013/39/EU of the European Parliament and of the Council of 12 August 2013 amending Directives 2000/60/EC and 2008/105/EC as regards priority substances in the field of water policy
- European Commission (EC)**, 2015. Commission implementing decision (EU) 2015/495 of 20 March 2015 establishing a watch list of substances for Union-wide monitoring in the field of water policy pursuant to Directive 2008/105/EC of the European Parliament and of the Council
- Fatta-Kassinos D, Meric S, Nikolaou A** (2011) Pharmaceutical residues in environmental waters and wastewater: current state of knowledge and future research. *Anal Bioanal Chem* **399**: 251–275

- Felsenstein J** (2009) Confidence Limits on phylogenies: an approach using the bootstrap. *Evolution* **39**: 783–791
- Ferretti M, Destro T, Tosatto SCE, La Rocca N, Rascio N, Masi A** (2009) Gamma-glutamyl transferase in the cell wall participates in extracellular glutathione salvage from the root apoplast. *New Phytol* **181**: 115–126
- Furst M, McClelland RA, Uetrecht P, Science H** (1995) Binding of carbamazepine neutrophils. *Drug Metab Dispos.* **23**: 590–594
- Gaiero JR, McCall CA, Thompson KA, Day NJ, Best AS, Dunfield KE** (2013) Inside the root microbiome: bacterial root endophytes and plant growth promotion. *Am J Bot* **100**: 1738–1750
- Galippe V.** (1887) Note sur la présence de micro-organismes dans les tissus végétaux. *C R Seances Soc Biol Fil* **39**: 410–416
- Gelvin SB** (1990) Crown gall disease and hairy root disease: a sledgehammer and a tackhammer. *Plant Physiol* **92**: 281–285
- Georgiev MI, Ludwig-Müller J, Alipieva K, Lippert A** (2011) Sonication-assisted *Agrobacterium rhizogenes*-mediated transformation of *Verbascum xanthophoeniceum* Griseb. for bioactive metabolite accumulation. *Plant Cell Rep* **30**: 859–866
- Georgiev MI, Pavlov AI, Bley T** (2007) Hairy root type plant in vitro systems as sources of bioactive substances. *Appl Microbiol Biotechnol* **74**: 1175–1185
- Germaine KJ, Keogh E, Ryan D, Dowling DN** (2009) Bacterial endophyte-mediated naphthalene phytoprotection and phytoremediation. *FEMS Microbiol Lett* **296**: 226–234
- Germaine KJ, Liu X, Cabellos GG, Hogan JP, Ryan D, Dowling DN** (2006) Bacterial endophyte-enhanced phytoremediation of the organochlorine herbicide 2,4-dichlorophenoxyacetic acid. *FEMS Microbiol Ecol* **57**: 302–310
- Ghosal D, Ghosh S, Dutta TK, Ahn Y** (2016) Current state of knowledge in microbial degradation of polycyclic aromatic hydrocarbons (PAHs): a review. *Front Microbiol* **7**: 1369
- Gleeson T, Wada Y, Bierkens MFP, van Beek LPH** (2012) Water balance of global aquifers revealed by groundwater footprint. *Nature* **488**: 197–200

- Golan-Rozen N, Chefetz B, Ben-Ari J, Geva J, Hadar Y** (2011) Transformation of the recalcitrant pharmaceutical compound carbamazepine by *pleurotus ostreatus*: role of cytochrome P450 monooxygenase and manganese peroxidase. *Environ Sci Technol* **45**: 6800–6805
- Golan-Rozen N, Seiwert B, Riemenschneider C, Reemtsma T, Chefetz B, Hadar Y** (2015) Transformation pathways of the recalcitrant pharmaceutical compound carbamazepine by the white-rot fungus *Pleurotus ostreatus*: effects of growth conditions. *Environ Sci Technol* **49**: 12351–12362
- Goldstein M, Shenker M, Chefetz B** (2014) Insights into the uptake processes of wastewater-borne pharmaceuticals by vegetables. *Environ Sci Technol* **48**: 5593–5600
- González PS, Agostini E, Milrad SR** (2008) Comparison of the removal of 2,4-dichlorophenol and phenol from polluted water, by peroxidases from tomato hairy roots, and protective effect of polyethylene glycol. *Chemosphere* **70**: 982–989
- Guo W, Li D, Tao Y, Gao P, Hu J** (2008) Isolation and description of a stable carbazole-degrading microbial consortium consisting of *Chryseobacterium* sp. NCY and *Achromobacter* sp. NCW. *Curr Microbiol* **57**: 251–257
- Hallmann J** (2001) Plant interactions with endophytic bacteria. In Jeger MJ and Spence NJ (Eds.) *Biotic interactions in plant-pathogen associations* (pp 87–119). Wallingford, CABI
- Hallmann J, Quadt-Hallmann A, Mahaffee WF, Kloepper JW** (1997) Bacterial endophytes in agricultural crops. *Can J Microbiol* **43**: 895–914
- Hardoim PR, van Overbeek LS, Berg G, Pirttilä AM, Compant S, Campisano A, Döring M, Sessitsch A** (2015) The hidden world within plants: ecological and evolutionary considerations for defining functioning of microbial endophytes. *Microbiol Mol Biol Rev* **79**: 293–320
- Hartmann A, Rothballer M, Schmid M** (2008) Lorenz Hiltner, a pioneer in rhizosphere microbial ecology and soil bacteriology research. *Plant Soil* **312**: 7–14
- Hay AG, Dees PM, Sayler GS** (2001) Growth of a bacterial consortium on triclosan. *FEMS Microbiol Ecol* **36**: 105–112
- He Y, Langenhoff AAM, Sutton NB, Rijnaarts HHM, Blokland MH, Chen F, Huber C, Schröder P** (2017) Metabolism of ibuprofen by *Phragmites australis*: uptake and phytodegradation. *Environ Sci Technol* **51**: 4576–4584

- Heberer T, Reddersen K, Mechlinski A** (2002) From municipal sewage to drinking water: fate and removal of pharmaceutical residues in the aquatic environment in urban areas. *Water Sci Technol* **46**: 81–88
- Hellriegel H, Wilfarth H** (1888) Untersuchungen über die Stickstoffnahrung der Gramineen und Leguminosen. Berlin Buchdruckerei der “Post” Kayssler Co.
- Herklotz PA, Gurung P, Vanden Heuvel B, Kinney CA** (2010) Uptake of human pharmaceuticals by plants grown under hydroponic conditions. *Chemosphere* **78**: 1416–1421
- Hijosa-Valsero M, Matamoros V, Sidrach-Cardona R, Martín-Villacorta J, Bécares E, Bayona JM** (2010) Comprehensive assessment of the design configuration of constructed wetlands for the removal of pharmaceuticals and personal care products from urban wastewaters. *Water Res* **44**: 3669–3678
- Ho YN, Mathew DC, Hsiao SC, Shih CH, Chien MF, Chiang HM, Huang CC** (2012) Selection and application of endophytic bacterium *Achromobacter xylosoxidans* strain F3B for improving phytoremediation of phenolic pollutants. *J Hazard Mater* **219–220**: 43–49
- Huber C, Bartha B, Harpaintner R, Schröder P** (2009) Metabolism of acetaminophen (paracetamol) in plants—two independent pathways result in the formation of a glutathione and a glucose conjugate. *Environ Sci Pollut Res Int* **16**: 206–213
- Huerta-Fontela M, Galceran MT, Ventura F** (2011) Occurrence and removal of pharmaceuticals and hormones through drinking water treatment. *Water Res* **45**: 1432–1442
- Hurtado C, Domínguez C, Pérez-Babace L, Cañameras N, Comas J, Bayona JM** (2016) Estimate of uptake and translocation of emerging organic contaminants from irrigation water concentration in lettuce grown under controlled conditions. *J Hazard Mater* **305**: 139–148
- Kang JW, Khan Z, Doty SL** (2012) Biodegradation of trichloroethylene by an endophyte of hybrid poplar. *Appl Environ Microbiol* **78**: 3504–3507
- Khan ST, Hiraishi A** (2002) *Diaphorobacter nitroreducens* gen nov, sp nov, a poly(3-hydroxybutyrate)-degrading denitrifying bacterium isolated from activated sludge. *J Gen Appl Microbiol* **48**: 299–308

- Kim OS, Cho YJ, Lee K, Yoon S-H, Kim M, Na H, Park S-C, Jeon YS, Lee JH, Yi H, et al** (2012) Introducing EzTaxon-e: a prokaryotic 16S rRNA gene sequence database with phylotypes that represent uncultured species. *Int J Syst Evol Microbiol* **62**: 716–721
- Kinney CA, Furlong ET, Werner SL, Cahill JD** (2006) Presence and distribution of wastewater-derived pharmaceuticals in soil irrigated with reclaimed water. *Environ Toxicol Chem* **25**: 317–326
- Knaak JB, Stahman MA, Casida LE** (1962) Peroxidase and ethylenediaminetetraacetic acid-ferrous iron-catalyzed oxidation and hydrolysis of parathion. *J Agric Food Chem* **10**: 154–158
- Labrou NE, Papageorgiou AC, Pavli O, Fliemetakis E** (2015) Plant GSTome: structure and functional role in xenome network and plant stress response. *Curr Opin Biotechnol* **32**: 186–194
- Lane DJ** (1991) 16S/23S rRNA sequencing. In Stackebrandt E., Goodfellow M. (Eds.) *Nucleic acid techniques in bacterial systematics* (pp 115–175). New York, NY: John Wiley Sons
- Lane DJ, Pace B, Olsen GJ, Stahl DA, Sogin ML, Pace NR** (1985) Rapid determination of 16S ribosomal RNA sequences for phylogenetic analyses. *Proc Natl Acad Sci U S A* **82**: 6955–6959
- Lapworth DJ, Baran N, Stuart ME, Ward RS** (2012) Emerging organic contaminants in groundwater: a review of sources, fate and occurrence. *Environ Pollut* **163**: 287–303
- Leclercq M, Mathieu O, Gomez E, Casellas C, Fenet H, Hillaire-Buys D** (2009) Presence and fate of carbamazepine, oxcarbazepine, and seven of their metabolites at wastewater treatment plants. *Arch Environ Contam Toxicol* **56**: 408–415
- Lertratanangkoon K, Horning M** (1982) Metabolism of carbamazepine. *Drug Metab. Dispos* **10**: 1-10
- Li A, Cai R, Di C, Qiu T, Pang C, Yang J, Ma F, Ren N** (2013) Characterization and biodegradation kinetics of a new cold-adapted carbamazepine-degrading bacterium, *Pseudomonas* sp. CBZ-4. *J Environ Sci (China)* **25**: 2281–2290
- Li J, Dodgen L, Ye Q, Gan J** (2013) Degradation kinetics and metabolites of carbamazepine in soil. *Environ Sci Technol* **47**: 3678–3684
- Li YH, Zhu JN, Zhai ZH, Zhang Q** (2010) Endophytic bacterial diversity in roots of *Phragmites australis* in constructed Beijing Cuihu Wetland (China). *FEMS Microbiol Lett* **309**: 84–93

- Link H** (1809) *Observationes in ordines plantarum naturales, dissertatio prima, complectens anandrarum ordines Epiphytas, Mucedines, Gastromycos et Fungos*. Der Gesellschaft Naturforschender Freunde zu Berlin, Berlin, Ger.
- Maggs J, Pirmohamed M, Kitteringham N, Park B** (1997) Characterization of the metabolites of carbamazepine in patient urine by liquid chromatography/mass spectrometry. *Drug Metab Dispos* **25**: 275-280
- Malchi T, Maor Y, Tadmor G, Shenker M, Chefetz B** (2014) Irrigation of root vegetables with treated wastewater: evaluating uptake of pharmaceuticals and the associated human health risks. *Environ Sci Technol* **48**: 9325–9333
- Mander U, Jenssen PD** (2002) *Natural wetlands for wastewater treatment in cold climates*. WIT Press
- Matamoros V, Arias C, Brix H, Bayona JM** (2009) Preliminary screening of small-scale domestic wastewater treatment systems for removal of pharmaceutical and personal care products. *Water Res* **43**: 55–62
- Matamoros V, García J, Bayona JM** (2008) Organic micropollutant removal in a full-scale surface flow constructed wetland fed with secondary effluent. *Water Res* **42**: 653–660
- Matamoros V, García J, Bayona JM** (2005) Behavior of selected pharmaceuticals in subsurface flow constructed wetlands: a pilot-scale study. *Environ Sci Technol* **39**: 5449–5454
- Mathieu O, Dereure O, Hillaire-Buys D** (2011) Presence and *ex vivo* formation of acridone in blood of patients routinely treated with carbamazepine: exploration of the 9-acridinecarboxaldehyde pathway. *Xenobiotica* **41**: 91–100
- Mayer AM** (2006) Polyphenol oxidases in plants and fungi: going places? A review. *Phytochemistry* **67**: 2318–2331
- Mendes R, Garbeva P, Raaijmakers JM** (2013) The rhizosphere microbiome: significance of plant beneficial, plant pathogenic, and human pathogenic microorganisms. *FEMS Microbiol Rev* **37**: 634–663
- Miège C, Choubert JM, Ribeiro L, Eusèbe M, Coquery M** (2009) Fate of pharmaceuticals and personal care products in wastewater treatment plants--conception of a database and first results. *Environ Pollut* **157**: 1721–1726
- Mompelat S, Le Bot B, Thomas O** (2009) Occurrence and fate of pharmaceutical products and by-products, from resource to drinking water. *Environ Int* **35**: 803–814
- Myers EW, Miller W** (1988) Optimal alignments in linear space. *Comput Appl Biosci* **4**: 11–17

- Nepovím A, Podlipná R, Soudek P, Schröder P, Vaněk T** (2004) Effects of heavy metals and nitroaromatic compounds on horseradish glutathione S-transferase and peroxidase. *Chemosphere* **57**: 1007–1015
- Neustifter JE** (2007) Phytoremediation organischer Schadstoffe mit Hilfe von *Phragmites australis*. Doctoral dissertation. Technische Universität München. Retrieved from <http://mediatum.ub.tum.de/doc/620857/620857.pdf>
- Onesios KM, Yu JT, Bouwer EJ** (2009) Biodegradation and removal of pharmaceuticals and personal care products in treatment systems: a review. *Biodegradation* **20**: 441–466
- Oulton RL, Kohn T, Cwiertny DM** (2010) Pharmaceuticals and personal care products in effluent matrices: a survey of transformation and removal during wastewater treatment and implications for wastewater management. *J Environ Monit* **12**: 1956–1978
- van Overbeek LS, van Doorn J, Wichers JH, van Amerongen A, van Roermund HJW, Willemsen PTJ** (2014) The arable ecosystem as battleground for emergence of new human pathogens. *Front Microbiol* **5**: 104
- Păcurar DI, Thordal-Christensen H, Păcurar ML, Pamfil D, Botez ML, Bellini C** (2011) *Agrobacterium tumefaciens*: from crown gall tumors to genetic transformation. *Physiol Mol Plant Pathol* **76**: 76–81
- Park N, Vanderford BJ, Snyder SA, Sarp S, Kim SD, Cho J** (2009) Effective controls of micropollutants included in wastewater effluent using constructed wetlands under anoxic condition. *Ecol Eng* **35**: 418–423
- Parkhurst BR, Bradshaw AS, Forte JL, Wright GP** (1981) The chronic toxicity to *Daphnia magna* of acridine, a representative azaarene present in synthetic fossil fuel products and wastewaters. *Environ Pollut Ser A, Ecol Biol* **24**: 21–30
- Peng A, Liu J, Gao Y, Chen Z** (2013) Distribution of endophytic bacteria in *Alopecurus aequalis* Sobol and *Oxalis corniculata* L. from soils contaminated by polycyclic aromatic hydrocarbons. *PLoS One* **8**: e83054
- Pikovskaya R.** (1948) Mobilization of phosphorus in soil in connection with vital activity of some microbial species. *Mikrobiologiya* **17**: 362–370
- Qu J, Xu Y, Ai GM, Liu Y, Liu ZP** (2015) Novel *Chryseobacterium* sp. PYR2 degrades various organochlorine pesticides (OCPs) and achieves enhancing removal and complete degradation of DDT in highly contaminated soil. *J Environ Manage* **161**: 350–357

- Quan ZX, Bae HS, Baek JH, Chen WF, Im WT, Lee ST** (2005) *Rhizobium daejeonense* sp. nov. isolated from a cyanide treatment bioreactor. *Int J Syst Evol Microbiol* **55**: 2543–2549
- Ramírez-Elías MA, Ferrera-Cerrato R, Alarcón A, Almaraz JJ, Ramírez-Valverde G, de-Bashan LE, Esparza-García FJ, García-Barradas O** (2014) Identification of culturable microbial functional groups isolated from the rhizosphere of four species of mangroves and their biotechnological potential. *Appl Soil Ecol* **82**: 1–10
- Ridley HN** (1930) The dispersal of plants throughout the world. London L. Reeve
- Riker AJ, Banfield WM, Wright WH, Keitt GW, Sagen HE** (1930) Studies on infectious hairy root of nursery apple trees. *J Agric Res* **41**: 507–540 .
- Rivera-Utrilla J, Sánchez-Polo M, Ferro-García MÁ, Prados-Joya G, Ocampo-Pérez R** (2013) Pharmaceuticals as emerging contaminants and their removal from water. A review. *Chemosphere* **93**: 1268–1287
- Rosenblueth M, Martínez-Romero E** (2006) Bacterial endophytes and their interactions with hosts. *Mol Plant Microbe Interact* **19**: 827–837
- Ryšlavá H, Pomeislová A, Pšondrová Š, Hýsková V, Smrček S** (2015) Phytoremediation of carbamazepine and its metabolite 10,11-epoxycarbamazepine by C3 and C4 plants. *Environ Sci Pollut Res* **22**: 20271–20282
- Saitou N, Nei M** (1987) The neighbor-joining method: a new method for reconstructing phylogenetic trees. *Mol Biol Evol* **4**: 406–425
- Sandermann H** (1994) Higher plant metabolism of xenobiotics: the “green liver” concept. *Pharmacogenetics* **4**: 225–41
- Santos IJS, Grossman MJ, Sartoratto A, Alexandre N, Durrant LR** (2012) Degradation of the recalcitrant pharmaceuticals carbamazepine and 17 alpha -Ethinylestradiol by ligninolytic fungi. **27**: 169–174
- Sasaki K, Iwai T, Hiraga S, Kuroda K, Seo S, Mitsuhashi I, Miyasaka A, Iwano M, Ito H, Matsui H, et al** (2004) Ten rice peroxidases redundantly respond to multiple stresses including infection with rice blast fungus. *Plant Cell Physiol* **45**: 1442–1452
- Sauvêtre A, Schröder P** (2015) Uptake of carbamazepine by rhizomes and endophytic bacteria of *Phragmites australis*. *Front Plant Sci* **6**: 83
- Schröder P, Collins CD** (2011) Organic xenobiotics and plants: from mode of action to ecophysiology. Dordrecht, Springer Netherlands



- Schröder P, Daubner D, Maier H, Neustifter J, Debus R** (2008) Phytoremediation of organic xenobiotics - Glutathione dependent detoxification in *Phragmites* plants from european treatment sites. *Bioresour Technol* **99**: 7183–7191
- Schröder P, Grosse W, Woermann D** (1986) Localization of thermo-osmotically active partitions in young leaves of *Nuphar lutea*. *J Exp Bot* **37**: 1450–1461
- Schröder P, Harvey PJ, Schwitzguébel JP** (2002) Prospects for the phytoremediation of organic pollutants in Europe. *Environ Sci Pollut Res Int* **9**: 1–3
- Schröder P, Maier H, Debus R** (2005) Detoxification of herbicides in *Phragmites australis*. *Zeitschrift fur Naturforsch. - Sect. C J. Biosci.* pp 317–324
- Schröder P, Navarro-Aviñó J, Azaizeh H, Goldhirsh AG, DiGregorio S, Komives T, Langergraber G, Lenz A, Maestri E, Memon AR, et al** (2007) Using phytoremediation technologies to upgrade waste water treatment in Europe. *Environ Sci Pollut Res - Int* **14**: 490–497
- Segura A, Ramos JL** (2013) Plant-bacteria interactions in the removal of pollutants. *Curr Opin Biotechnol* **24**: 467–473
- Seiwert B, Golan-Rozen N, Weidauer C, Riemenschneider C, Chefetz B, Hadar Y, Reemtsma T** (2015) Electrochemistry combined with LC-HRMS: elucidating transformation products of the recalcitrant pharmaceutical compound carbamazepine generated by the white-rot fungus *Pleurotus ostreatus*. *Environ Sci Technol* **49**: 12342–12350
- Seo JS, Keum YS, Li Q** (2009) Bacterial degradation of aromatic compounds. *Int J Environ Res Public Health* **6**: 278–309
- Sevón N, Oksman-Caldentey KM** (2002) *Agrobacterium rhizogenes*-mediated transformation: root cultures as a source of alkaloids. *Planta Med* **68**: 859–868
- Sheng X, Chen X, He L** (2008) Characteristics of an endophytic pyrene-degrading bacterium of *Enterobacter* sp. 12J1 from *Allium macrostemon* Bunge. *Int Biodeterior Biodegrad* **62**: 88–95
- Shenker M, Harush D, Ben-Ari J, Chefetz B** (2011) Uptake of carbamazepine by cucumber plants--a case study related to irrigation with reclaimed wastewater. *Chemosphere* **82**: 905–10
- Shimabukuro RH** (1976) Glutathione conjugation of herbicides in plants and animals and its role in herbicidal selectivity. *Asian-Pacific Weed Sci Soc* 183–186

- Siciliano SD, Fortin N, Mihoc A, Wisse G, Labelle S, Beaumier D, Ouellette D, Roy R, Whyte LG, Banks MK, et al** (2001) Selection of specific endophytic bacterial genotypes by plants in response to soil contamination. *Appl Environ Microbiol* **67**: 2469–2475
- Silby MW, Winstanley C, Godfrey SAC, Levy SB, Jackson RW** (2011) *Pseudomonas* genomes: diverse and adaptable. *FEMS Microbiol Rev* **35**: 652–680
- Sitaraman R** (2015) *Pseudomonas* spp. as models for plant-microbe interactions. *Front Plant Sci* **6**: 1–4
- Strauch G, Möder M, Wennrich R** (2008) Indicators for assessing anthropogenic impact on urban surface and groundwater. *J. Soils Sediments* **8**: 23–33
- Tamura K, Nei M, Kumar S** (2004) Prospects for inferring very large phylogenies by using the neighbor-joining method. *Proc Natl Acad Sci U S A* **101**: 11030–11035
- Tamura K, Stecher G, Peterson D, Filipski A, Kumar S** (2013) MEGA6: Molecular evolutionary genetics analysis version 6.0. *Mol Biol Evol* **30**: 2725–2729
- Telke AA, Kagalkar AN, Jagtap UB, Desai NS, Bapat VA, Govindwar SP** (2011) Biochemical characterization of laccase from hairy root culture of *Brassica juncea* L. and role of redox mediators to enhance its potential for the decolorization of textile dyes. *Planta* **234**: 1137–1149
- Teng Y, Shen Y, Luo Y, Sun X, Sun M, Fu D, Li Z, Christie P** (2011) Influence of *Rhizobium meliloti* on phytoremediation of polycyclic aromatic hydrocarbons by alfalfa in an aged contaminated soil. *J Hazard Mater* **186**: 1271–1276
- Ternes TA** (1998) Occurrence of drugs in German sewage treatment plants and rivers. *Water Res* **32**: 3245–3260
- Ternes TA, Bonerz M, Herrmann N, Teiser B, Andersen HR** (2007) Irrigation of treated wastewater in Braunschweig, Germany: an option to remove pharmaceuticals and musk fragrances. *Chemosphere* **66**: 894–904
- Thijs S, Sillen W, Weyens N, Vangronsveld J** (2017) Phytoremediation: state-of-the-art and a key role for the plant microbiome in future trends and research prospects. *Int J Phytoremediation* **19**: 23–38
- Tixier C, Singer HP, Oellers S, Müller SR** (2003) Occurrence and fate of carbamazepine, clofibrac acid, diclofenac, ibuprofen, ketoprofen, and naproxen in surface waters. *Environ Sci Technol* **37**: 1061–1068

- Tolou-Ghamari Z, Zare M, Habibabadi JM, Najafi MR** (2013) A quick review of carbamazepine pharmacokinetics in epilepsy from 1953 to 2012. *J Res Med Sci* **18**: S81-85
- Trchounian A, Petrosyan M, Sahakyan N** (2016) Plant cell redox homeostasis and reactive oxygen species. In DK Gupta, JM Palma, FJ Corpas (Eds.) *Redox state as a Cent. Regul. plant-cell Stress responses*. (pp 25–50) Springer (Switzerland)
- Turner TR, James EK, Poole PS** (2013) The plant microbiome. *Genome Biol* **14**: 1–10
- Tybring G, von Bahr C, Bertilsson L, Collste H, Glaumann H, Solbrand M** (1981) Metabolism of carbamazepine and its epoxide metabolite in human and rat liver in vitro. *Drug Metab Dispos* **9**: 561-564
- Vanacker H, Carver TLW, Foyer CH** (1998) Pathogen-induced changes in the antioxidant status of the apoplast in barley leaves. *Plant Physiol* **117**: 1103–1114
- Vandamme P, Moore ERB, Cnockaert M, De Brandt E, Svensson-Stadler L, Houf K, Spilker T, Lipuma JJ** (2013) *Achromobacter animicus* sp. nov., *Achromobacter mucicolens* sp. nov., *Achromobacter pulmonis* sp. nov. and *Achromobacter spiritinus* sp. nov., from human clinical samples. *Syst Appl Microbiol* **36**: 1–10
- Vandenkoornhuysen P, Quaiser A, Duhamel M, Le Van A, Dufresne A** (2015) The importance of the microbiome of the plant holobiont. *New Phytol* **206**: 1196–1206
- Verlicchi P, Zambello E** (2014) How efficient are constructed wetlands in removing pharmaceuticals from untreated and treated urban wastewaters? A review. *Sci Total Environ* **470–471**: 1281–1306
- Vila J, Nieto JM, Mertens J, Springael D, Grifoll M** (2010) Microbial community structure of a heavy fuel oil-degrading marine consortium: linking microbial dynamics with polycyclic aromatic hydrocarbon utilization. *FEMS Microbiol Ecol* **73**: 349–362
- Vymazal J** (2011) Constructed wetlands for wastewater treatment: five decades of experience. *Environ Sci Technol* **45**: 61–69
- Weyens N, Croes S, Dupae J, Newman L, van der Lelie D, Carleer R, Vangronsveld J** (2010) Endophytic bacteria improve phytoremediation of Ni and TCE co-contamination. *Environ Pollut* **158**: 2422–2427
- Weyens N, Schellingen K, Beckers B, Janssen J, Ceulemans R, van der Lelie D, Taghavi S, Carleer R, Vangronsveld J** (2012) Potential of willow and its genetically engineered associated bacteria to remediate mixed Cd and toluene contamination. *J Soils Sediments* **13**: 176–188

- Weyens N, Taghavi S, Barac T, van der Lelie D, Boulet J, Artois T, Carleer R, Vangronsveld J** (2009) Bacteria associated with oak and ash on a TCE-contaminated site: characterization of isolates with potential to avoid evapotranspiration of TCE. *Environ Sci Pollut Res Int* **16**: 830–843
- White JF, Torres MS** (2010) Is plant endophyte-mediated defensive mutualism the result of oxidative stress protection? *Physiol Plant* **138**: 440–446
- Wiegel S, Aulinger A, Brockmeyer R, Harms H, Löffler J, Reincke H, Schmidt R, Stachel B, von Tümpling W, Wanke A** (2004) Pharmaceuticals in the river Elbe and its tributaries. *Chemosphere* **57**: 107–126
- Wolf AE, Dietz KJ, Schröder P** (1996) Degradation of glutathione S-conjugates by a carboxypeptidase in the plant vacuole. *FEBS Lett* **384**: 31–34
- Yousaf S, Afzal M, Reichenauer TG, Brady CL, Sessitsch A** (2011) Hydrocarbon degradation, plant colonization and gene expression of alkane degradation genes by endophytic *Enterobacter ludwigii* strains. *Environ Pollut* **159**: 2675–2683
- Zambryski P, Tempe J, Schell J** (1989) Transfer and function of T-DNA genes from agrobacterium Ti and Ri plasmids in plants. *Cell* **56**: 193–201
- Zhang D, Gersberg RM, Ng WJ, Tan SK** (2014) Removal of pharmaceuticals and personal care products in aquatic plant-based systems: A review. *Environ Pollut* **184**: 620–639
- Zhang J, Kirkham MB** (1996) Antioxidant responses to drought in sunflower and sorghum seedlings. *New Phytol* **132**: 361–373
- Zhang Y, Geissen SU, Gal C** (2008) Carbamazepine and diclofenac: removal in wastewater treatment plants and occurrence in water bodies. *Chemosphere* **73**: 1151–1161